

## REFERNCES

- Bar-Cohen Y., 2004, Electroactive Polymer (EAP) Actuators as Artificial Muscles Reality, Bellingham, Washington, USA.
- Bar-Cohen, Y., 2004, Dielectric elastomers as electromechanical transducers (fundamentals, materials, devices, models and applications of an emerging electroactive polymer technology), 1<sup>st</sup> Edition, Elsevier.
- Behl M., Lendlein A., 2007, Materialstoday, Elsevier, 10, 4-17.
- Bishai A.M., Ghoneim A.M., Ward A.A.M., 2002, Inter. J. Poly. Mat. 51, 793-812.
- Cannon L.A., Pehtrick R.A., 2002, Polymer 43, 1249-1257.
- Carpi F., Chiarelli P., Mazzoldi A., and De Rosii D., 2003, Sensors and Actuators A, 107(85), 29-32.
- Chandrasekhar, P., 1999, Conducting Polymers. Fundamentals and Application, London, Britain.
- Choi Y.H., Skliar M., 2002, Proceeding of American Control Conference, Anchorage, AK, May 8-10, 5 4285-4290.
- Chotpattananont D., Sirivat A., Jamieson A.M., 2004, Colloid Polymer Science 282, 357-365.
- Della Santa A., Rossi D.D., Mazzoldi A., 1997, Synthetic Metals. 90, 93-101.
- Diaconu I., Dorohoi D.O., Topoliceanu F. 2006, IEEE Sensors J. 6, 876-884.
- Evans W.V., Pearson R., Braithwaite D., 1994, J. of American Chemistry Society 63, 1024-1030.
- Feher J., Filipcsei G., Szalma J., Zrinyi M., 2001, Colloid Surface A 183, 505-515.
- Geetha S., Trivedi D.C., 2005, Synthetic Metals 148, 891-900.
- Gharavi, N., Razzaghi Kashani, M., Moradi, A., 2009, Proceedings of SPIE - The International Society for Optical Engineering 7287, art. no. 72871W.
- Gunzler H., Gremlich H.U., IR Spectroscopy, Wiley-VCH.
- Hiamtup P., Sirivat S., Jamieson A.M., 2007, Mat. Sci. Eng. C-Bio S. 15, 771-779.
- Hotta A., Clarke S.M., Terentjev E. M., 2002, Macromolecules 35, 271-277.
- Kim H.S., Li Y. and Kim J., 2008, Sensors and Actuators A, 147(1), 304-309.
- Kim J., Kang K., Yun S., 2007, Sensor Actuat. A-Phy. 133, 401-407.
- Kofod G., Larsen P.S., 2005, Sens. Actuator A-Phys. 122, 273-281.

- Kornbluh R., Pelrine R., Pei Q., Chiba S., Joseph J., 2000, Materials Science Engineering C 11, 89-100.
- Kovacic P., and Kyriakis A., 1961, Journal of American Chemistry Society 85(454), 2238-2242.
- Krause S., Bohon K., 2001, Macromolecules 34, 7179-7189.
- Ku C.C., Liepins R., 1987, Electrical Properties of Polymers, Hanser Publisher, New York, USA.
- Kunanuruksapong R., Sirivat A., 2007, Materials Science and Engineering A 454–455, 453–460.
- Kunanuruksapong R., Sirivat A., 2008, Appl. Phys. A. 96, 2, 313-320.
- Liu B., Shaw T.M., 2001, J. of Rheology 45, 641-657.
- Lu C. Tan, J. Xu, He C., 2003, Synth. Met. 138, 429-438.
- Ma W., Cross L.E., 2004, Apply Physics A. 78(5), 1201-1208.
- Madbouly S.A., Mansour A.A., Abdou N.Y., 2007, Euro. Polym. J. 43, 1892-1898
- Mazzoldi A., Tesconi M., Tognetti A., Rocchia W., Vozzi G., Pioggia G., Ahluwalia A., Rossi D.D., 2007, Mat. Sci. Eng. C-Bio S.  
doi:10.1016/j.msec.2007.04.032.
- Metz P., Alici G., Spinks G.M., 2006, Sensor Actuat. A-Phy. 130-131, 1-11.
- Nagata Y., Masuda J., Noro A., Cho D., Takano A. Matsushita Y., 2005,  
Macromolecules 38, 10220-10225.
- Narita, F., Shindo, Y., Mikami, M., 2005, ActaMaterialia, 53, 4523–4529.
- Newnham, R.E., Sundar, V., Yimnirun, R., Su, J., Zhang, Q.M., 1997,  
J.Phys.Chem.B, 101, 10141-10150.
- Niamlang S., Sirivat A., 2007, Macromol. Symp. 264, 176-186.
- Oguma J., Akagi K., Shirakawa H., 1999, Synthetic Metals 101, 86-103.
- Palakodeti R., Kessler M.R., 2006, Mater. Lett. 60, 3437-3439.
- Pelrine R., Kornbluh R., Joseph J., 1998, Sens. Actuator A-Phys. 64, 77-83.
- Pelrine, R., Kornbluh, R., Pei, Q., and Joseph, J.G., 2000, Science, 287, 836-83.
- Puvanatvattana T., Chotpattananont D., Hiamtup P., Niamlang S., Kunanuruksapong R., Sirivat A., Jamieson A.M., 2008, Materials Science and Engineering C 28(1), 119-128

- Raju G.G., 2003, Dielectrics in Electric Fields, University of Windsor, Windsor, Ontario, Canada.
- Riad A.J., Korayem M.T., Abdul Malik T.G., 1999, Physica B 270, 140-147.
- Rubinstein M., Colby R.H., 2003, Polymer Physics 298-300.
- Sato T., Watanabe H., Osaki K., 1996, Macromolecules 29, 6231-6238.
- Shiga T., 1993, Advances in Polymer Science 134, 133-163.
- Shiga T., Hirose, Y., Okada, A., Kurauchi, T., 1994, Journal of Materials Science 29, 5715-5718.
- Shirakawa H., Louis E.J., MacDiarmid A.G., Chiang C.K., Heeger A.J., 1997, J. of Chemistry Society 578, 911-923.
- Soares B.G., Leyva M.E., Barra G.M.O., Khastgir D., 2006, Euro. Polym. J. 42, 676-684.
- Study report by the University of Pisa, University of Rome& Kayser Italia. EAP based artificial muscle as an alternative to space mechanisms, 1-31.
- Thuau, D., Koutsos, V., Cheung, R., 2009, J. Vac. Sci. Technol. B 27(6), 3139-3144.
- Thipdech P., Kunanuruksapong R., Sirivat A., 2008, Express Polymer Letters 2(12), 866-877.
- Timoshenko S.P., Gere J.M., Mechanics of Materials, 3<sup>rd</sup> Edition, Chapman & Hall, New York, USA.
- Uddin Z., Watanabe M., Shirai H., Hirai T., 2003, J. Polym. Sci. B 41, 2119-2138.
- Ueda T., Kasazaki T., Kunitake N., Hirai T., Kyokane J., Yoshino K., 1997, Synt. Metals 85, 1415-1420.
- Von Hippel A., Wesson L.G., 1946, Ind. Eng. Chem. 38, 1121 -1130.
- Wang Y., Shen J.S., Long C.F., 2001, Polymer 42, 8443-8446.
- Watanabe M., Hirai T., 2004, J. Polym. Sci. B 42, 523-531.
- Watanabe M., Kato T., Suzuki M., Hirako Y., Shirai H., Hirai T., 2001, J. Polym. Sci. B 39, 1061-1068.
- Wichiansee W., Sirivat A., 2009, Materials Science and Engineering C 29(1), 78-84.
- Wissler M., Mazza E., 2005, Sensor Actuat. A-Phy. 120, 184-192.
- Yamauchi T., Tansuriyavong S., Doi K., Oshima K., Shimomura M., Tsubukawa N., Vincent J.F.V., 2005, Synthetic Metals 152, 45-51.
- Yang W., Zen H., Hamman J., 1999, Synthetic rubber 10, 184-195.

Yun S., Kim J., Song C., 2007, Sensor Actuat. A-Phy. 133, 225-237.

Zrínyi M., Fehér J., and Filipcsei G., 2000, Macromolecules, 33, 5751-5753.

## APPENDICES

### Appendix A Identification of Characteristic Peaks in FT-IR Spectrum of Undoped Poly(p-phynylene)

The undoped poly(p-phynylene) (PPP) was characterized by FT-IR spectroscopy in order to identify functional groups. The FT-IR spectrometer (Thermo Nicolet, Nexus 670) operated in the absorption mode with 32 scans and a resolution of  $\pm 4 \text{ cm}^{-1}$ , covering a wavenumber range of 4000-400  $\text{cm}^{-1}$  using a deuterated triglycine sulfate detector. Optical grade KBr (Carlo Erba Reagent) was used as the background material. The synthesized PPP was intimately mixed with dried KBr at a ratio of PPP:KBr = 1:20

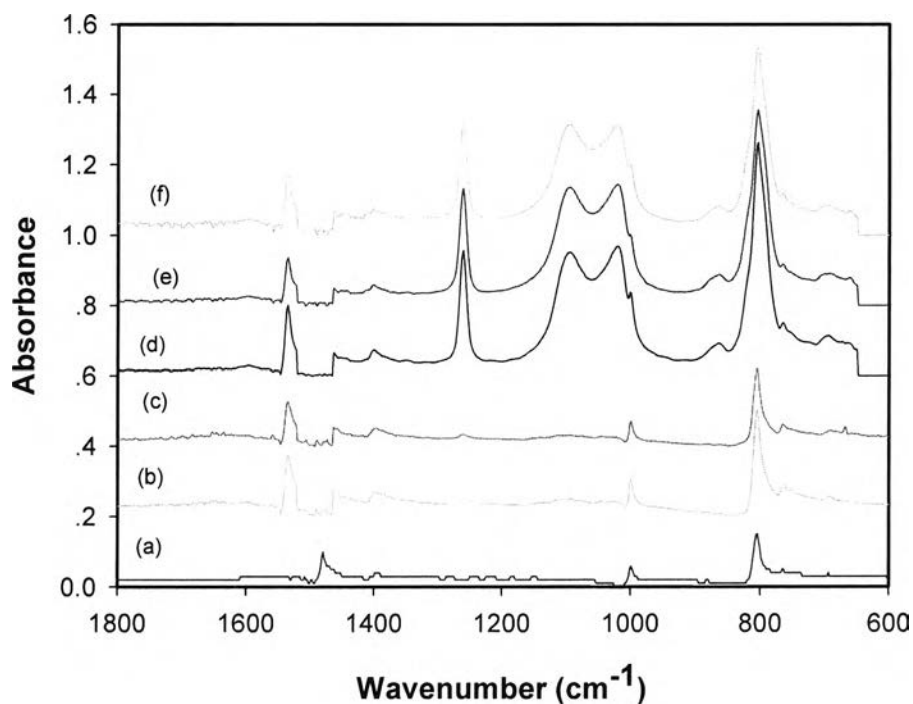


**Figure A1** The FT-IR spectra of: a) undoped poly(p-phenylene); and poly(p-phenylene) doped with  $\text{H}_2\text{SO}_4$  at various mole ratios of acid to monomer unit ( $N_{\text{acid}} : N_{\text{monomer}}$ ); b) 1:100; c) 1:10; d) 1:1; (e) 10:1 and (f) 100:1

The assignments of peaks in the spectrum are shown in Table A1. The characteristic peaks of PPP were found at 3025-3020 cm<sup>-1</sup> and can be assigned to the stretching vibration of the C-H bond on the benzene ring; peak at 1477 and 805 cm<sup>-1</sup> represents the double sides p-substituted stretching vibration; peak at 1000 cm<sup>-1</sup> represents the C-C stretching vibration of benzene ring; and peaks at 757 and 693 cm<sup>-1</sup> represent the single side p-substituted stretching vibration (Kovacic *et al.*, 1962). After the neutral poly(p-phenylene) was doped with sulfuric acid, some characteristic peaks of acid appeared on FT-IR spectra: the double sides p-substituted stretching vibration will be shifted to higher wavenumbers at 1530 and 810 cm<sup>-1</sup>. The shift of the C-C stretching vibration of benzene ring from 1000 to 1080 cm<sup>-1</sup> is present (Geetha *et al.*, 2004).

**Table A1** The FT-IR absorption spectrum of undoped and doped PPP with H<sub>2</sub>SO<sub>4</sub>

Wavenumber (cm <sup>-1</sup> )	Assignments	References
3025 - 3020	C-H stretching of benzene ring	Kovacic <i>et al.</i> (1962)
1530 and 810	Double sides p-substitute stretching after doping	Geetha <i>et al.</i> (2004)
1477 and 805	Double sides p-substitute stretching	Kovacic <i>et al.</i> (1962)
1080	C-C stretching of benzene ring after doping	Geetha <i>et al.</i> (2004)
1000	C-C stretching of benzene ring	Kovacic <i>et al.</i> (1962)
757 and 693	Single side p-substitute stretching	Kovacic <i>et al.</i> (1962)

## Appendix B Identification of Characteristic Peaks of Undoped and Doped Poly(p-phynylene) from UV-Visible Spectroscopy

The UV-Visible spectra of undoped and doped Poly(p-phynylene) recorded with a UV-Vis absorption spectrometer (Perkin-Elmer, Lambda 10). Measurements were taken in the reflectance mode in the wavelength range of 200-900 nm. Synthesized PPP was grinded into a fine powder and put into a sample holder. Scan speed was 100 mm/min, and a slit width of 5.0 nm using a deuterium lamp as the light source.

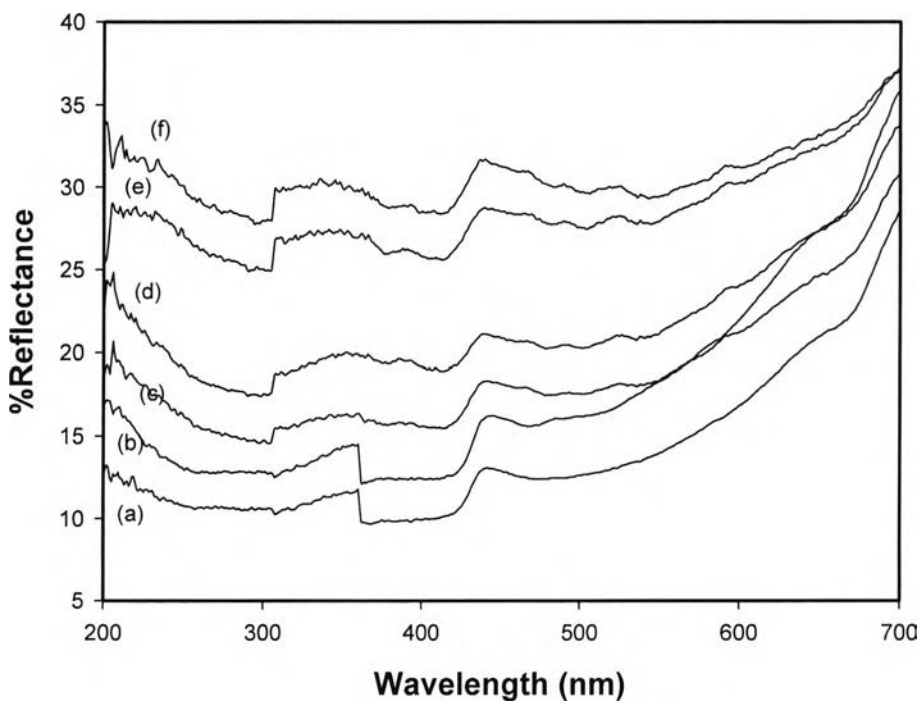


**Figure B1** The UV-Visible spectra of : a) undoped Poly(p-phynylene); and Poly(p-phynylene) doped with  $\text{H}_2\text{SO}_4$  at various mole ratios of acid to monomer unit ( $N_{\text{acid}} : N_{\text{monomer}}$ ) ; b) 1:100 ; c) 1:10; d) 1:1 ; e) 10:1 ; and f) 100:1.

The UV-Visible spectra of undoped and doped Poly(p-phynylene) from the references are shown in Table B1. The wavelength in [ ] refers to the results of the assignments cited from references.

**Table B1** Assignment peaks of UV-Visible peaks of undoped and doped Poly(p-phynylene)

Wavelength (nm)	Assignments	References
350±10 [359]	$\pi-\pi^*$ transitions of the benzoid ring	Geetha <i>et al.</i> (2004)
300-400 [320-370]	$\pi-\pi^*$ transitions of the conjugated polymer chains after doping	Demanze <i>et al.</i> (1996)
400-600 [870]	Charge carriers	Geetha <i>et al.</i> (2004)

### Appendix C Determination of Particle Sizes of Undoped and Doped PPP

**Table C1** Summary of the particles diameter of undoped PPP\_U), N<sub>acid</sub> : N<sub>monomer</sub> 1:100 (PPP\_1:100), N<sub>acid</sub> : N<sub>monomer</sub> 1:10 (PPP\_1:10), N<sub>acid</sub> : N<sub>monomer</sub> 1:1 (PPP\_1:1), N<sub>acid</sub> : N<sub>monomer</sub> 10:1 (PPP\_10:1), and N<sub>acid</sub> : N<sub>monomer</sub> 100:1 (PPP\_100:1)

<b>Samples</b>	<b>Particle diameter (<math>\mu\text{m}</math>)</b>				
	1	2	3	Avg.	STD
PPP_U	44.73	42.18	40.97	42.62	1.19
PPP_1:100	50.15	49.7	46.67	48.84	0.96
PPP_1:10	54.04	46.47	50.52	46.34	4.24
PPP_1:1	51.46	43.33	48.13	47.64	4.08
PPP_10:1	45.49	46.42	48.37	46.76	1.47
PPP_100:1	47.75	45.56	45.92	46.41	1.17

**Table C2** The raw data from particle size analysis of undoped PPP

Size		Undoped poly(p-phenylene)					
Low (μm)	High (μm)	In%	Under%	In%	Under%	In%	Under%
0.50	1.32	0.17	0.17	0.07	0.07	0.20	0.20
1.32	1.60	0.54	0.71	0.71	0.78	0.13	0.33
1.60	1.95	0.79	1.50	0.62	1.40	0.73	1.06
1.95	2.38	0.90	2.39	0.55	1.95	0.78	1.84
2.38	2.90	0.91	3.30	0.57	2.52	0.69	2.53
2.90	3.53	0.94	4.24	0.88	3.40	0.84	3.37
3.53	4.30	1.06	5.30	1.54	4.94	1.25	4.62
4.30	5.24	1.33	6.63	1.23	6.17	1.13	5.75
5.24	6.39	1.74	8.37	1.80	7.97	1.68	7.43
6.39	7.78	2.21	10.58	2.51	10.48	2.34	9.77
7.78	9.48	2.69	13.27	2.11	12.59	3.99	13.76
9.48	11.55	3.25	16.51	2.88	15.47	2.97	16.73
11.55	14.08	3.98	20.50	4.53	20.00	4.04	20.77
14.08	17.15	4.94	25.44	4.51	24.51	3.98	24.75
17.15	20.90	6.08	31.51	4.89	29.40	5.39	30.14
20.90	25.46	7.15	38.66	8.54	37.94	6.57	36.71
25.46	31.01	7.78	46.44	9.78	47.72	8.79	45.50
31.01	37.79	7.77	54.21	7.08	54.80	7.42	52.92
37.79	46.03	7.24	61.45	6.97	61.77	6.81	59.73
46.03	56.09	6.29	67.74	4.03	65.08	9.22	68.95
56.09	68.33	5.03	72.77	5.54	71.34	4.39	73.34
68.33	83.26	3.48	76.20	7.51	78.85	5.30	78.64
83.26	101.44	2.22	78.43	10.10	88.95	3.48	82.12
101.44	123.59	1.96	80.39	1.02	89.97	0.88	83.00
123.59	150.57	2.82	83.22	0.09	92.01	1.24	84.24
150.57	183.44	3.89	87.10	2.51	94.52	2.57	86.81
183.44	223.51	4.33	91.43	0.88	95.40	6.75	93.56
223.51	272.31	3.38	94.81	2.99	98.39	3.34	96.90
272.31	331.77	1.84	96.65	0.17	98.47	0.22	97.12
331.77	404.21	0.87	97.52	1.11	99.58	1.69	98.81
404.21	492.47	0.75	98.28	0.26	99.84	0.83	99.64
492.47	600.00	1.73	100.00	0.16	100.00	0.36	100.00

**Table C3** The raw data from particle size analysis of N<sub>acid</sub> : N<sub>monomer</sub> about 1:100

Size		N <sub>acid</sub> : N <sub>monomer</sub> about 1:100					
Low (μm)	High (μm)	In%	Under%	In%	Under%	In%	Under%
0.50	1.32	0.06	0.06	0.06	0.07	0.06	0.06
1.32	1.60	0.30	0.37	0.31	0.38	0.28	0.34
1.60	1.95	0.50	0.86	0.51	0.89	0.46	0.80
1.95	2.38	0.64	1.51	0.66	1.55	0.60	1.40
2.38	2.90	0.77	2.28	0.79	2.35	0.73	2.13
2.90	3.53	0.91	3.19	0.94	3.28	0.87	3.00
3.53	4.30	10.9	4.28	1.12	4.41	1.06	4.06
4.30	5.24	1.33	5.61	1.36	5.77	1.29	5.35
5.24	6.39	1.58	7.19	1.61	7.38	1.54	6.89
6.39	7.78	1.81	9.00	1.85	9.23	1.76	8.65
7.78	9.48	2.07	11.07	2.11	11.34	1.99	10.64
9.48	11.55	2.54	13.61	2.60	13.93	2.44	13.08
11.55	14.08	3.38	16.99	3.46	17.40	3.23	16.32
14.08	17.15	4.59	21.58	4.71	22.11	4.41	20.72
17.15	20.90	5.93	27.50	6.07	28.17	5.74	26.45
20.90	25.46	6.82	34.32	6.96	35.13	6.69	33.14
25.46	31.01	6.61	40.93	6.68	41.81	6.60	39.74
31.01	37.79	5.32	46.26	5.29	47.11	5.47	45.20
37.79	46.03	4.15	50.41	4.06	51.17	4.41	49.61
46.03	56.09	4.43	54.84	4.32	55.49	4.74	54.36
56.09	68.33	6.59	61.44	6.50	61.99	6.94	61.30
68.33	83.26	10.00	71.44	9.96	71.95	10.34	71.64
83.26	101.44	11.50	82.93	11.52	83.45	11.66	83.28
101.44	123.59	7.99	90.92	8.00	91.45	7.85	91.13
123.59	150.57	3.84	94.76	3.74	95.19	3.70	94.83
150.57	183.44	2.11	96.88	1.86	97.06	2.19	97.03
183.44	223.51	1.30	98.18	0.97	98.03	1.53	98.55
223.51	272.31	0.86	99.04	0.62	98.65	0.99	99.54
272.31	331.77	0.59	99.63	0.62	99.27	0.46	100.00
331.77	404.21	0.32	99.95	0.73	99.99	0.00	100.00
404.21	492.47	0.05	100.00	0.00	100.00	0.00	100.00
492.47	600.00	0.00	100.00	0.00	100.00	0.00	100.00

**Table C4** The raw data from particle size analysis of N<sub>acid</sub> : N<sub>monomer</sub> about 1:10

Size		N <sub>acid</sub> : N <sub>monomer</sub> about 1:10					
Low (μm)	High (μm)	In%	Under%	In%	Under%	In%	Under%
0.50	1.32	0.11	0.12	0.13	0.13	0.10	0.10
1.32	1.60	0.45	0.57	0.51	0.64	0.40	0.49
1.60	1.95	0.71	1.28	0.80	1.45	0.62	1.12
1.95	2.38	0.87	2.15	0.98	2.43	0.76	1.88
2.38	2.90	0.97	3.12	1.09	3.52	0.86	2.74
2.90	3.53	1.08	4.21	1.21	4.73	0.97	3.71
3.53	4.30	1.26	5.46	1.39	6.12	1.15	4.86
4.30	5.24	1.52	6.98	1.66	7.78	1.41	6.26
5.24	6.39	1.85	8.84	2.02	9.80	1.74	8.00
6.39	7.78	2.20	11.04	2.38	12.18	2.08	10.09
7.78	9.48	2.54	13.58	2.74	14.92	2.42	12.51
9.48	11.55	3.03	16.61	3.26	18.19	2.88	15.40
11.55	14.08	3.76	20.37	4.07	22.26	3.57	18.97
14.08	17.15	4.75	24.12	5.15	27.41	4.49	23.45
17.15	20.90	5.82	30.94	6.31	33.72	5.50	28.95
20.90	25.46	6.56	37.49	7.07	40.79	6.26	35.20
25.46	31.01	6.51	43.99	6.91	47.70	6.39	41.59
31.01	37.79	5.66	49.66	5.85	53.56	5.90	47.50
37.79	46.03	4.80	54.46	4.79	58.35	5.44	52.94
46.03	56.09	4.92	59.39	4.80	63.16	5.86	58.80
56.09	68.33	6.39	65.79	6.26	69.43	7.45	66.26
68.33	83.26	8.58	74.36	8.45	77.87	9.54	75.80
83.26	101.44	9.17	83.53	8.96	86.82	9.75	85.54
101.44	123.59	6.38	89.90	6.08	92.90	6.48	92.02
123.59	150.57	3.25	93.16	2.92	95.82	3.09	95.11
150.57	183.44	2.00	95.17	1.58	97.41	1.75	96.87
183.44	223.51	1.51	96.68	1.05	98.46	1.31	98.18
223.51	272.31	1.21	97.89	0.77	99.23	1.03	99.21
272.31	331.77	0.96	98.85	0.53	99.76	0.65	99.86
331.77	404.21	0.67	99.52	0.24	100.00	0.14	100.00
404.21	492.47	0.38	99.90	0.00	100.00	0.00	100.00
492.47	600.00	0.10	100.00	0.00	100.00	0.00	100.00

**Table C5** The raw data from particle size analysis of N<sub>acid</sub> : N<sub>monomer</sub> about 1:1

Size		N <sub>acid</sub> : N <sub>monomer</sub> about 1:1					
Low (μm)	High (μm)	In%	Under%	In%	Under%	In%	Under%
0.50	1.32	0.07	0.07	0.07	0.07	0.07	0.07
1.32	1.60	0.30	0.37	0.33	0.40	0.29	0.36
1.60	1.95	0.49	0.85	0.54	0.95	0.51	0.87
1.95	2.38	0.64	1.50	0.71	1.66	0.66	1.53
2.38	2.90	0.81	2.30	0.88	2.54	0.85	2.38
2.90	3.53	1.02	3.33	1.11	3.65	1.08	3.46
3.53	4.30	1.34	4.67	1.44	5.09	1.33	4.79
4.30	5.24	1.77	6.44	1.88	6.97	1.95	6.74
5.24	6.39	2.27	8.71	2.40	9.37	2.38	9.12
6.39	7.78	2.75	11.46	2.89	12.25	2.84	11.96
7.78	9.48	3.14	14.60	3.28	15.53	3.09	15.05
9.48	11.55	3.54	18.14	3.67	19.20	3.88	18.93
11.55	14.08	4.05	22.19	4.16	23.36	4.09	23.02
14.08	17.15	4.67	26.87	4.76	28.13	4.66	27.68
17.15	20.90	5.31	32.17	5.37	33.49	5.32	33.00
20.90	25.46	5.73	37.90	5.73	39.23	5.77	38.77
25.46	31.01	5.75	43.65	5.67	44.90	5.71	44.48
31.01	37.79	5.84	49.12	5.30	50.19	5.46	49.94
37.79	46.03	5.38	54.51	5.09	55.29	5.29	55.23
46.03	56.09	5.92	60.43	5.55	60.84	5.77	61.00
56.09	68.33	7.18	67.61	6.78	67.62	7.13	68.13
68.33	83.26	8.55	76.16	8.17	75.78	8.64	76.77
83.26	101.44	8.49	84.64	8.21	83.98	8.34	85.11
101.44	123.59	6.05	90.69	5.92	89.90	5.97	91.08
123.59	150.57	3.25	93.94	3.26	93.17	3.27	94.35
150.57	183.44	1.78	95.72	1.88	95.05	1.82	96.17
183.44	223.51	1.06	96.78	1.19	96.24	1.15	97.32
223.51	272.31	0.76	97.54	0.89	97.12	0.84	98.16
272.31	331.77	0.68	98.23	0.81	97.94	0.71	98.87
331.77	404.21	0.66	98.89	0.79	98.73	0.54	99.41
404.21	492.47	0.60	99.49	0.70	99.43	0.12	99.53
492.47	600.00	0.51	100.00	0.57	100.00	0.47	100.00

**Table C6** The raw data from particle size analysis of N<sub>acid</sub> : N<sub>monomer</sub> about 10:1

Size		N <sub>acid</sub> : N <sub>monomer</sub> about 10:1					
Low ( $\mu\text{m}$ )	High ( $\mu\text{m}$ )	In%	Under%	In%	Under%	In%	Under%
0.50	1.32	0.08	0.08	0.10	0.10	0.07	0.07
1.32	1.60	0.33	0.41	0.31	0.41	0.36	0.43
1.60	1.95	0.52	0.93	0.54	0.95	0.99	1.42
1.95	2.38	0.64	1.57	0.66	1.61	0.61	2.03
2.38	2.90	0.72	2.29	0.75	2.36	0.80	2.83
2.90	3.53	0.85	3.10	0.78	3.14	0.65	4.43
3.53	4.30	0.97	4.07	0.95	4.09	0.92	5.35
4.30	5.24	1.19	5.26	1.28	5.37	1.24	6.59
5.24	6.39	1.47	6.73	1.56	6.93	1.55	8.14
6.39	7.78	1.75	8.48	1.80	8.73	1.71	9.85
7.78	9.48	1.99	10.47	1.85	10.58	1.97	11.82
9.48	11.55	2.30	12.77	2.44	13.02	2.51	14.33
11.55	14.08	2.76	15.54	2.85	15.87	2.72	17.05
14.08	17.15	3.43	18.97	3.41	19.28	3.45	20.50
17.15	20.90	4.29	23.26	4.27	23.55	4.16	24.66
20.90	25.49	5.16	28.42	5.11	28.66	5.39	30.05
25.46	31.01	5.83	34.25	5.23	33.89	5.22	35.27
31.01	37.79	6.19	40.44	6.78	40.67	6.67	41.94
37.79	46.03	6.40	46.84	6.44	47.11	6.39	48.33
46.03	56.09	6.88	53.73	6.69	53.80	6.84	55.17
56.09	68.33	7.85	61.58	7.86	61.66	7.88	63.05
68.33	83.26	8.92	70.50	8.94	70.60	8.99	72.04
83.26	101.44	8.77	79.26	8.42	79.02	8.69	80.73
101.44	123.59	6.49	85.75	6.49	85.51	6.41	87.14
123.59	150.57	3.94	89.69	3.64	89.15	3.65	90.79
150.57	183.44	2.79	92.49	2.88	92.03	2.84	93.63
183.44	223.51	2.26	94.75	2.34	94.37	2.26	95.89
223.51	272.31	1.93	96.68	1.94	96.31	1.90	97.79
272.31	331.77	1.60	98.28	1.55	97.86	1.59	99.38
331.77	404.21	1.16	99.44	1.21	99.07	0.50	99.88
404.21	600.00	0.56	100.00	0.93	100.00	0.12	100.00

**Table C7** The raw data from particle size analysis of N<sub>acid</sub> : N<sub>monomer</sub> about 100:1

Size		N <sub>acid</sub> : N <sub>monomer</sub> about 100:1					
Low ( $\mu\text{m}$ )	High ( $\mu\text{m}$ )	In%	Under%	In%	Under%	In%	Under%
0.50	1.32	0.08	0.08	0.08	0.09	0.09	0.09
1.32	1.60	0.26	0.34	0.28	0.37	0.29	0.38
1.60	1.95	0.39	0.73	0.42	0.79	0.44	0.82
1.95	2.38	0.46	1.18	0.50	1.29	0.52	1.34
2.38	2.90	0.50	1.68	0.55	1.84	0.56	1.90
2.90	3.53	0.57	2.26	0.63	2.47	0.64	2.54
3.53	4.30	0.72	2.98	0.78	3.26	0.79	4.38
4.30	5.24	0.97	3.95	1.04	4.29	1.05	5.76
5.24	6.39	1.30	5.25	1.37	5.66	1.38	7.49
6.39	7.78	1.64	6.89	1.72	7.38	1.73	9.53
7.78	9.48	1.95	8.84	2.03	9.42	2.04	11.89
9.48	11.55	2.26	11.10	2.36	11.78	2.36	14.66
11.55	14.08	2.64	13.74	2.76	14.54	2.76	18.00
14.08	17.15	3.16	16.90	3.34	17.88	3.34	22.14
17.15	20.90	3.90	20.80	4.14	22.02	4.15	27.31
20.90	25.49	4.85	25.65	5.14	27.16	5.16	33.61
25.46	31.01	5.94	31.59	6.25	33.41	6.30	41.01
31.01	37.79	7.08	38.67	7.36	40.77	7.40	49.40
37.79	46.03	8.20	46.87	8.40	49.17	8.39	58.64
46.03	56.09	9.28	56.15	9.33	58.50	9.24	68.50
56.09	68.33	10.20	66.35	10.06	68.56	9.87	78.38
68.33	83.26	10.50	76.84	10.12	78.67	9.88	86.99
83.26	101.44	9.30	86.14	8.77	87.43	8.61	92.99
101.44	123.59	6.49	92.63	5.99	93.42	6.01	96.42
123.59	150.57	3.68	96.31	3.29	96.72	3.43	98.30
150.57	183.44	2.01	98.33	1.74	98.47	1.87	99.33
183.44	223.51	1.07	99.40	0.95	99.41	1.03	99.85
223.51	272.31	0.49	99.89	0.47	99.88	0.52	100.00
272.31	331.77	0.11	100.00	0.12	100.00	0.15	100.00
331.77	404.21	0.00	100.00	0.00	100.00	0.00	100.00
404.21	600.00	0.00	100.00	0.00	100.00	0.00	100.00

## Appendix D Properties of the Polymer Blend Matrix.

The matrix used in research is acrylic elastomers from Nipon Zeon Advance Polymix Co.,LTD. There are two types: Nipol AR71 and Nipol AR72HF. Their different properties are tabulated in Table D1.

**Table D1** The properties of Nipol AR71 and Nipol AR72HF from Nipon Zeon Advance Polymix Co.,LTD.

Properties	AR71	AR72HF
Elongation (%)	400	230
Volatile matter (%)	0.32	0.56
Tensile Strength (MPa)	11.8	11.2
100% Modulus (MPa)	4.1	6
Ash (%)	0.22	0.16
Moony Viscosity at 100C	50	48
Glass Transition C	-15	-28
Specific Gravity	1.11	1.11
Type	Heat resistance	Low Temperature resistance

\* Note: 100<sup>^</sup> modulus is Young's modulus at strain equal 100%.

## Appendix E Determination of the Correction Factor (K)

The electrical conductivity of undoped and doped PPP was measured by a two-point probe meter. The meter consists of two probes, making contact on the surface of film sample. These probes were connected to a source meter (Keithley, Model 6517A) for a constant voltage source and reading the resultant current.

The geometrical correction factor was taken into account of geometric effects, depending on the configuration and probe tip spacing.

$$K = \frac{w}{l}$$

(E.1)

K is geometrical correction factor, w is width of probe tip spacing (cm), l is the length between probes (cm).

In this measurement, the constant K value was determined by using standard materials whose specific resistivity values were known; we used silicon wafer chips ( $\text{SiO}_2$ ). In our case, the sheet resistivity was measured by using our custom made two-point probe and then the geometric correction factor was calculated by equation (E.2) as follows:

$$K = \frac{\rho}{R \times t} = \frac{I \times \rho}{V \times t}$$

(E.2)

K is geometric correction factor,  $\rho$  is resistivity of standard silicon wafer which has been calibrated by using a four point probe at King Mongkut's Institute Technology of Lad Krabang ( $\Omega \cdot \text{cm}$ ), t is the film thickness (cm), R is the film resistance ( $\Omega$ ), I is the measured current (A), and V is the voltage drop (V).

Standard Si wafer were cleaned to remove organic impurities prior to be used according to the standard RCA method (Kern, 1993).

## Materials

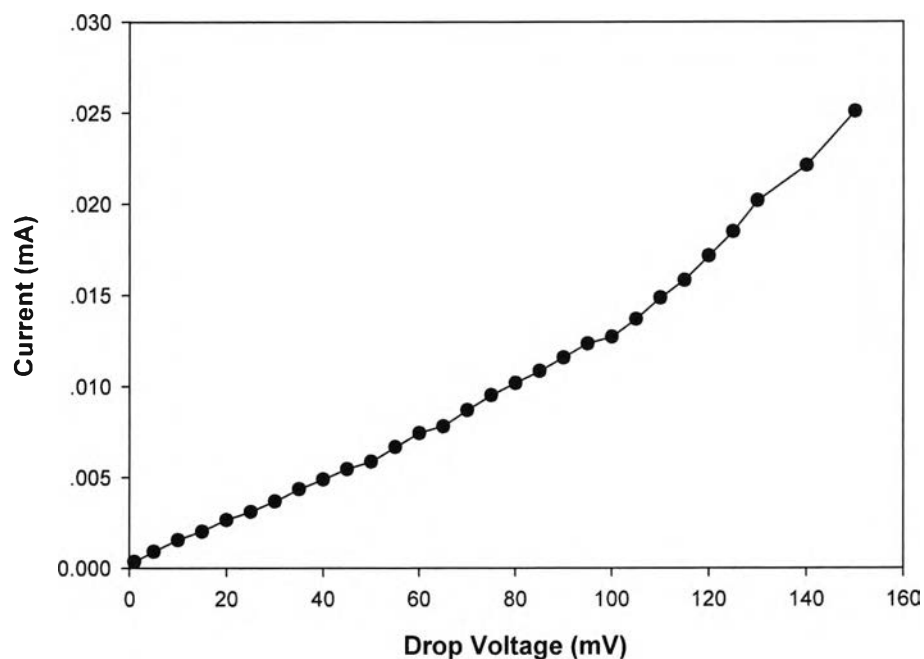
Acetones (Scharlau, 99.5%), Methanol (CARLO ERBA, 99.9%), Ammonium hydroxide (Merk, 99.9%), Hydrogen peroxide (CARLO ERBA, 30% in water), and dilute (2%) Hydrofuranic acid

## Experiment

The cleaning procedure contains 3 steps: the solvent clean, the RCA01 and the HF dip. The first step is the solvent clean step, employed to remove oils and organic residues that appeared on Si wafer surface. The Si wafer was placed into the acetone at 55°C for 10 min, removed and placed in methanol for 2-5 min, subsequently rinsed with deionized water and blown dried with nitrogen gas. Second step is the RCA clean, to remove organic residues from silicon wafers. This process oxidized the silicon wafer and left a thin oxide on the surface of the wafer. RCA solution was prepared with 5 parts of water ( $H_2O$ ), 1 part of 27% ammonium hydroxide ( $NH_4OH$ ), and 1 part of 30% hydrogen peroxide ( $H_2O_2$ ). 65 ml of  $NH_4OH$  (27%) was added into 325 ml of deionized water in a beaker and then heated to  $70 \pm 5^\circ C$ . The mixture would bubble vigorously after 1-2 min, indicated that it was ready to use. Silicon wafer was soaked in the solution for 15 min, consequently overflowed with deionized water in order to rinse and remove the solution. The third step is the HF dip, which was carried out to remove native silicon dioxide from wafer. 480 ml of deionised water was added to the polypropylene bottle and then added to 20 ml HF. Wafer was soaked in this solution for 2 min, removed and checked for hydrophobicity by performing the wetting test. Deionized water was poured onto the surface wafer; the clean silicon surface would show that the beads of water would roll off. Clean Si wafer was further blown dried with nitrogen and stored in a clean and dry environment.

**Table E1** Determination the geometrical factor of probe A

Probe	K (correction factor)				
	1	2	3	Average	STD
A	2.75E-05	2.84E-05	2.80E-05	2.80E-05	4.59E-07

**Figure E1** The calibration data of Si-wafer: K tay which specific resistivity ( $\rho$ ) 0.014265  $\Omega \cdot \text{cm}$ , thickness 0.0724 cm, 24-25°C, 55-59 %R.H.

**Table E2** Determination the correction factor of probe A with standard Si wafer  
(specific resistivity 0.014265 Ω.cm, thickness 0.0724 cm, 24-25°C, 55-59% R.H)

Volt Applied (mV)			Current (mA)		
1	2	3	1	2	3
1	1	1	0.00034	0.00031	0.00037
5	5	5	0.00091	0.00085	0.00088
10	10	10	0.00154	0.00158	0.00155
15	15	15	0.00214	0.00213	0.00217
20	20	20	0.00265	0.00264	0.00265
25	25	25	0.00311	0.00312	0.00309
30	30	30	0.00370	0.00368	0.00364
35	35	35	0.00439	0.00435	0.00431
40	40	40	0.00488	0.00491	0.00489
45	45	45	0.0054	0.00548	0.0055
50	50	50	0.00587	0.00584	0.00588
55	55	55	0.00673	0.00665	0.00662
60	60	60	0.00741	0.00746	0.00744
65	65	65	0.00784	0.00782	0.00768
70	70	70	0.00872	0.00860	0.00875
75	75	75	0.00947	0.00952	0.00955
80	80	80	0.0104	0.0102	0.01
85	85	85	0.0108	0.0109	0.0108
90	90	90	0.0115	0.0117	0.0115
95	95	95	0.0124	0.0122	0.0122
100	100	100	0.0125	0.0129	0.0127
105	105	105	0.0138	0.0135	0.0137
110	110	110	0.0149	0.0148	0.0151
115	115	115	0.0158	0.0159	0.0158
120	120	120	0.0171	0.0171	0.0174
125	125	125	0.0184	0.0185	0.0185
130	130	130	0.0202	0.0204	0.0203
140	140	140	0.0222	0.0223	0.0228
150	150	150	0.0251	0.0255	0.0252

## Appendix F Conductivity Measurement

The specific conductivity, which is the inversion of specific resistivity ( $\rho$ ) of undoped and doped PPP pellets were measured by using the two-point probe connected to a source meter (Keithley, Model 6517A) for a constant voltage source and reading resultant current under the atmospheric pressure, 54-60% relative humidity and at 24-25°C. The geometric correction factor (K) of probe A is  $2.8 \times 10^{-5}$ . The thickness of pellets was measured by a thickness gauge. The applied voltage was plotted versus the current to determine the linear ohmic regime of each sample. The applied voltage and the current change in the linear ohmic regime were converted to the electrical conductivity of the polymer by using equation (F.1) as follows:

$$\sigma = \frac{1}{\rho} = \frac{1}{R_s \times t} = \frac{I}{K \times V \times t} \quad (\text{F.1})$$

where  $\sigma$  is specific conductivity (S/cm),  $\rho$  is specific resistivity ( $\Omega \cdot \text{cm}$ ),  $R_s$  is the sheet resistivity ( $\Omega$ ),  $I$  is the measured current (A),  $K$  is the geometric correction factor,  $V$  is the applied voltage (voltage drop) (V),  $t$  is the pellet thickness (cm).

In addition, the conductivity of matrixes can be measured by using the resistivity testing fixture (Keithley, Model 8009) connected to a source meter (Keithley, Model 6517A) for a constant voltage source and reading resultant current under the atmospheric pressure, 54-60% relative humidity and 24-25°C. The conductivity of matrixes can calculate by using equation (F.2 – F.3) as follows:

$$K_v = \frac{\pi \times (D + [\beta \times g])^2}{4} \quad (\text{F.2})$$

where  $K_v$  is effective area of the guarded electrode for the particular electrode arrangement employed ( $\text{cm}^2$ ),  $D$  is diameter of the guarded electrode (cm),  $\beta$  is effective area coefficient ( $\text{cm}^2$ ) ( $\beta$  is always zero),  $g$  is distance between the guarded electrode and the ring electrode (cm).

$$\sigma = \frac{1}{\rho} = \frac{t \times I}{22.9 \times V} \quad (\text{F.3})$$

where  $\sigma$  is the specific conductivity (S/cm),  $\rho$  is the specific resistivity ( $\Omega \cdot \text{cm}$ ),  $I$  is the measured current (A),  $V$  is the applied voltage (voltage drop) (V),  $t$  is the sheet thickness (cm).

**Table F1** Determination the specific conductivity (S/cm) of matrixes, undoped and doped poly(p-phenylene) at various mole ratios of acid to monomer unit

Code	Specific conductivity (S/cm)	STD
AR71	5.16E-12	1.38E-13
AR72HF	1.03E-12	1.24E-14
PPP_U	5.28E-06	4.86E-07
PPP_1:100	1.07E-05	1.66E-07
PPP_1:10	1.56E-05	7.24E-07
PPP_1:1	3.48E-05	2.86E-06
PPP_10:1	3.31E-04	4.78E-05
PPP_100:1	1.30E-03	2.26E-05

**Table F2** The raw data of the determination of linear regime of AR72HF at 24-25°C, 54-60% R.H

Sample	Thickness (cm)	Applied voltage (V)			Mesuered Current (A)			Conductivity (S/cm)		
		1	2	3	1	2	3	1	2	3
AR72HF	1) 0.0157	5	5	5	6.88E-09	6.91E-09	6.89E-09	9.43E-13	9.47E-13	9.45E-13
	2) 0.0155	10	10	10	1.44E-08	1.44E-08	1.43E-08	9.87E-13	9.87E-13	9.80E-13
	3) 0.0158	15	15	15	2.19E-08	2.18E-08	2.20E-08	1.00E-12	9.96E-13	1.01E-12
		20	20	20	2.96E-08	2.96E-08	2.97E-08	1.01E-12	1.01E-12	1.02E-12
		25	25	25	3.68E-08	3.67E-08	3.66E-08	1.01E-12	1.01E-12	1.00E-12
		30	30	30	4.51E-08	4.50E-08	4.55E-08	1.03E-12	1.03E-12	1.04E-12
		35	35	35	5.30E-08	5.30E-08	5.31E-08	1.04E-12	1.04E-12	1.04E-12
		40	40	40	6.08E-08	6.08E-08	6.08E-08	1.04E-12	1.04E-12	1.04E-12
		45	45	45	6.87E-08	6.87E-08	6.68E-08	1.05E-12	1.05E-12	1.02E-12
		50	50	50	7.48E-08	7.44E-08	7.45E-08	1.03E-12	1.02E-12	1.02E-12
		55	55	55	8.46E-08	8.46E-08	8.44E-08	1.05E-12	1.05E-12	1.05E-12
		60	60	60	9.19E-08	9.20E-08	9.22E-08	1.05E-12	1.05E-12	1.05E-12
		65	65	65	9.94E-08	9.95E-08	9.98E-08	1.05E-12	1.05E-12	1.05E-12
		70	70	70	1.07E-07	1.07E-07	1.07E-07	1.05E-12	1.05E-12	1.05E-12
		75	75	75	1.14E-07	1.14E-07	1.14E-07	1.04E-12	1.04E-12	1.04E-12
		80	80	80	1.21E-07	1.22E-07	1.22E-07	1.04E-12	1.05E-12	1.05E-12
		85	85	85	1.29E-07	1.29E-07	1.28E-07	1.04E-12	1.04E-12	1.03E-12
		90	90	90	1.35E-07	1.36E-07	1.36E-07	1.03E-12	1.04E-12	1.04E-12
		95	95	95	1.43E-07	1.43E-07	1.44E-07	1.03E-12	1.03E-12	1.04E-12
		100	100	100	1.51E-07	1.52E-07	1.55E-07	1.04E-12	1.04E-12	1.06E-12
		105	105	105	1.61E-07	1.64E-07	1.62E-07	1.05E-12	1.07E-12	1.06E-12
		110	110	110	1.70E-07	1.71E-07	1.70E-07	1.06E-12	1.07E-12	1.06E-12
		115	115	115	1.84E-07	1.84E-07	1.88E-07	1.10E-12	1.10E-12	1.12E-12
		120	120	120	1.98E-07	1.96E-07	1.94E-07	1.13E-12	1.12E-12	1.11E-12

**Table F3** The raw data of the determination conductivity of AR71 at 24-25°C, 54-60% R.H

Sample	Thickness (cm)	Applied voltage (V)			Mesuered Current (A)			Conductivity (S/cm)		
		1	2	3	1	2	3	1	2	3
AR71	1) 0.0235	10	10	10	5.17E-08	5.28E-08	5.39E-08	5.26E-12	5.37E-12	5.48E-12
	2) 0.0222	20	20	20	1.06E-07	1.05E-07	1.06E-07	5.39E-12	5.34E-12	5.39E-12
	3) 0.0241	30	30	30	1.56E-07	1.52E-07	1.59E-07	5.29E-12	5.16E-12	5.39E-12
		40	40	40	2.02E-07	2.01E-07	2.00E-07	5.14E-12	5.11E-12	5.09E-12
		50	50	50	2.46E-07	2.49E-07	2.48E-07	5.01E-12	5.07E-12	5.05E-12
		60	60	60	3.04E-07	3.06E-07	3.10E-07	5.16E-12	5.19E-12	5.26E-12
		70	70	70	3.51E-07	3.50E-07	3.48E-07	5.10E-12	5.09E-12	5.06E-12
		80	80	80	3.98E-07	3.99E-07	3.97E-07	5.06E-12	5.07E-12	5.05E-12
		90	90	90	4.43E-07	4.49E-07	4.45E-07	5.01E-12	5.08E-12	5.03E-12
		100	100	100	4.97E-07	4.92E-07	4.94E-07	5.06E-12	5.01E-12	5.03E-12

**Table F4** The raw data of the determination of linear regime of PPP\_U at 24-25°C, 54-60% R.H

Sample	Thickness (cm)	Applied voltage (V)			Mesuered Current (A)			Conductivity (S/cm)		
		1	2	3	1	2	3	1	2	3
PPP_U	1) 0.0201	0.1	0.1	0.1	1.25E-12	1.20E-12	1.21E-12	2.22E-05	2.13E-05	2.15E-05
	2) 0.0199	0.5	0.5	0.5	1.79E-12	1.85E-12	1.74E-12	6.36E-06	6.57E-06	6.18E-06
	3) 0.0203	1	1	1	2.86E-12	2.83E-12	2.88E-12	5.08E-06	5.03E-06	5.12E-06
		1.5	1.5	1.5	4.26E-12	4.25E-12	4.26E-12	5.05E-06	5.03E-06	5.05E-06
	2	2	2	2	5.32E-12	5.31E-12	5.35E-12	4.73E-06	4.72E-06	4.75E-06
		2.5	2.5	2.5	6.86E-12	6.78E-12	6.85E-12	4.88E-06	4.82E-06	4.87E-06
	3	3	3	3	8.13E-12	8.11E-12	8.14E-12	4.82E-06	4.80E-06	4.82E-06
		3.5	3.5	3.5	1.01E-11	1.05E-11	1.00E-11	5.13E-06	5.33E-06	5.08E-06
	4	4	4	4	1.16E-11	1.15E-11	1.19E-11	5.15E-06	5.11E-06	5.29E-06
		4.5	4.5	4.5	1.40E-11	1.34E-11	1.38E-11	5.53E-06	5.29E-06	5.45E-06
	5	5	5	5	1.58E-11	1.55E-11	1.60E-11	5.61E-06	5.51E-06	5.69E-06
		5.5	5.5	5.5	1.79E-11	1.78E-11	1.78E-11	5.78E-06	5.75E-06	5.75E-06
	6	6	6	6	5.98E-11	5.94E-11	5.99E-11	1.77E-05	1.76E-05	1.77E-05
		6.5	6.5	6.5	6.38E-11	6.34E-11	6.40E-11	1.74E-05	1.73E-05	1.75E-05
	7	7	7	7	6.87E-11	6.89E-11	6.88E-11	1.74E-05	1.75E-05	1.75E-05
		7.5	7.5	7.5	7.44E-11	7.40E-11	7.43E-11	1.76E-05	1.75E-05	1.76E-05
	8	8	8	8	7.83E-11	7.77E-11	7.75E-11	1.74E-05	1.73E-05	1.72E-05
		8.5	8.5	8.5	8.30E-11	8.36E-11	8.32E-11	1.74E-05	1.75E-05	1.74E-05
	9	9	9	9	8.91E-11	8.91E-11	8.95E-11	1.76E-05	1.76E-05	1.77E-05
		9.5	9.5	9.5	9.42E-11	9.40E-11	9.44E-11	1.76E-05	1.76E-05	1.77E-05
	10	10	10	10	9.93E-11	9.95E-11	9.98E-11	1.76E-05	1.77E-05	1.77E-05
		10.5	10.5	10.5	1.05E-10	1.04E-10	1.03E-10	1.78E-05	1.76E-05	1.74E-05
	11	11	11	11	1.09E-10	1.09E-10	1.05E-10	1.76E-05	1.76E-05	1.70E-05
		11.5	11.5	11.5	1.16E-10	1.17E-10	1.16E-10	1.79E-05	1.81E-05	1.79E-05
	12	12	12	12	1.22E-10	1.23E-10	1.20E-10	1.81E-05	1.82E-05	1.78E-05
		12.5	12.5	12.5	1.28E-10	1.29E-10	1.27E-10	1.82E-05	1.83E-05	1.81E-05
	13	13	13	13	1.34E-10	1.33E-10	1.39E-10	1.83E-05	1.82E-05	1.90E-05
		13.5	13.5	13.5	1.38E-10	1.38E-10	1.39E-10	1.82E-05	1.82E-05	1.83E-05
	14	14	14	14	1.41E-10	1.43E-10	1.41E-10	1.79E-05	1.81E-05	1.79E-05
		14.5	14.5	14.5	1.44E-10	1.44E-10	1.43E-10	1.76E-05	1.76E-05	1.75E-05
	15	15	15	15	1.49E-10	1.50E-10	1.55E-10	1.76E-05	1.78E-05	1.84E-05
		15.5	15.5	15.5	1.58E-10	1.57E-10	1.59E-10	1.81E-05	1.80E-05	1.82E-05
	16	16	16	16	1.61E-10	1.62E-10	1.59E-10	1.79E-05	1.80E-05	1.77E-05
		16.5	16.5	16.5	1.64E-10	1.65E-10	1.61E-10	1.77E-05	1.78E-05	1.73E-05
	17	17	17	17	1.69E-10	1.68E-10	1.65E-10	1.77E-05	1.76E-05	1.72E-05

**Table F5** The raw data of the determination conductivity of N<sub>acid</sub>:N<sub>monomer</sub> (PPP\_1:100) at 24-25°C, 54-60% R.H

Sample	Thickness (cm)	Applied voltage (V)			Mesuered Current (A)			Conductivity (S/cm)		
		1	2	3	1	2	3	1	2	3
PPP_1:100	1) 0.0225	0.1	0.1	0.1	5.56E-13	5.53E-13	5.60E-13	6.69E-06	6.65E-06	6.73E-06
	2) 0.0240	0.5	0.5	0.5	1.30E-12	1.43E-12	1.44E-12	3.13E-06	3.44E-06	3.46E-06
	3) 0.0236	1	1	1	2.19E-12	2.37E-12	2.11E-12	2.63E-06	2.85E-06	2.54E-06
		1.5	1.5	1.5	3.18E-12	3.12E-12	3.14E-12	2.55E-06	2.50E-06	2.52E-06
		2	2	2	4.11E-12	4.16E-12	4.12E-12	2.47E-06	2.50E-06	2.48E-06
		2.5	2.5	2.5	5.24E-12	5.33E-12	5.38E-12	2.52E-06	2.56E-06	2.59E-06
		3	3	3	6.40E-12	6.28E-12	6.51E-12	2.57E-06	2.52E-06	2.61E-06
		3.5	3.5	3.5	7.49E-12	7.54E-12	7.51E-12	2.57E-06	2.59E-06	2.58E-06
		4	4	4	8.83E-12	8.93E-12	8.99E-12	2.65E-06	2.68E-06	2.70E-06
		4.5	4.5	4.5	1.05E-11	1.04E-11	1.06E-11	2.81E-06	2.78E-06	2.83E-06
		5	5	5	1.22E-11	1.23E-11	1.19E-11	2.93E-06	2.96E-06	2.86E-06
		5.5	5.5	5.5	1.60E-11	1.58E-11	1.64E-11	3.50E-06	3.45E-06	3.59E-06
		6	6	6	1.92E-11	1.91E-11	1.91E-11	3.85E-06	3.83E-06	3.83E-06
		7	7	7	2.01E-11	2.05E-11	2.04E-11	3.45E-06	3.52E-06	3.50E-06
		8	8	8	6.90E-11	6.95E-11	6.94E-11	1.04E-05	1.04E-05	1.04E-05
		9	9	9	7.82E-11	7.80E-11	7.85E-11	1.04E-05	1.04E-05	1.05E-05
		10	10	10	8.87E-11	8.89E-11	8.79E-11	1.07E-05	1.07E-05	1.06E-05
		11	11	11	9.67E-11	9.65E-11	9.70E-11	1.06E-05	1.05E-05	1.06E-05
		12	12	12	1.06E-10	1.06E-10	1.06E-10	1.06E-05	1.06E-05	1.06E-05
		13	13	13	1.16E-10	1.15E-10	1.16E-10	1.07E-05	1.06E-05	1.07E-05
		14	14	14	1.25E-10	1.24E-10	1.28E-10	1.07E-05	1.07E-05	1.10E-05
		15	15	15	1.34E-10	1.35E-10	1.33E-10	1.07E-05	1.08E-05	1.07E-05
		16	16	16	1.42E-10	1.43E-10	1.47E-10	1.07E-05	1.07E-05	1.10E-05
		17	17	17	1.58E-10	1.52E-10	1.55E-10	1.12E-05	1.08E-05	1.10E-05
		18	18	18	1.61E-10	1.62E-10	1.62E-10	1.08E-05	1.08E-05	1.08E-05
		19	19	19	1.72E-10	1.71E-10	1.74E-10	1.09E-05	1.08E-05	1.10E-05
		20	20	20	1.80E-10	1.80E-10	1.81E-10	1.08E-05	1.08E-05	1.09E-05

**Table F6** The raw data of the determination conductivity of N<sub>acid</sub>:N<sub>monomer</sub> (PPP\_1:10) at 24-25°C, 54-60% R.H

Sample	Thickness (cm)	Applied voltage (V)			Mesuered Current (A)			Conductivity (S/cm)		
		1	2	3	1	2	3	1	2	3
PPP_1:10	1) 0.0220	1	1	1	2.30E-12	2.13E-12	2.28E-12	3.80E-06	3.52E-06	3.77E-06
	2) 0.0215	2	2	2	4.41E-12	4.40E-12	4.52E-12	3.65E-06	3.64E-06	3.74E-06
	3) 0.0213	3	3	3	6.72E-12	6.84E-12	6.80E-12	3.70E-06	3.77E-06	3.75E-06
		4	4	4	9.39E-12	9.40E-12	9.41E-12	3.88E-06	3.89E-06	3.89E-06
		5	5	5	1.24E-11	1.22E-11	1.25E-11	4.10E-06	4.03E-06	4.13E-06
		6	6	6	1.51E-11	1.53E-11	1.56E-11	4.16E-06	4.22E-06	4.30E-06
		7	7	7	1.92E-11	1.90E-11	1.94E-11	4.54E-06	4.49E-06	4.58E-06
		8	8	8	7.37E-11	7.38E-11	7.41E-11	1.52E-05	1.53E-05	1.53E-05
		9	9	9	8.27E-11	8.17E-11	8.25E-11	1.52E-05	1.50E-05	1.52E-05
		10	10	10	9.11E-11	9.08E-11	9.15E-11	1.51E-05	1.50E-05	1.51E-05
		11	11	11	9.89E-11	9.94E-11	9.97E-11	1.49E-05	1.49E-05	1.50E-05
		12	12	12	1.10E-10	1.11E-10	1.15E-10	1.52E-05	1.53E-05	1.58E-05
		13	13	13	1.22E-10	1.24E-10	1.25E-10	1.55E-05	1.58E-05	1.59E-05
		14	14	14	1.32E-10	1.31E-10	1.37E-10	1.56E-05	1.55E-05	1.62E-05
		15	15	15	1.58E-10	1.57E-10	1.53E-10	1.74E-05	1.73E-05	1.69E-05

**Table F7** The raw data of the determination conductivity of N<sub>acid</sub>:N<sub>monomer</sub> (PPP\_1:1) at 24-25°C, 54-60% R.H

Sample	Thickness (cm)	Applied voltage (V)			Mesuered Current (A)			Conductivity (S/cm)		
		1	2	3	1	2	3	1	2	3
PPP_1:1	1) 0.0187	1	1	1	3.72E-12	3.85E-12	3.82E-12	7.30E-06	7.55E-06	7.50E-06
	2) 0.0179	2	2	2	7.28E-12	7.34E-12	7.41E-12	7.14E-06	7.20E-06	7.27E-06
		3	3	3	1.18E-11	1.19E-11	1.16E-11	7.72E-06	7.78E-06	7.59E-06
		4	4	4	1.86E-11	1.88E-11	1.94E-11	9.12E-06	9.22E-06	9.52E-06
		5	5	5	6.84E-11	6.89E-11	6.91E-11	2.68E-05	2.70E-05	2.71E-05
		6	6	6	8.76E-11	8.74E-11	8.81E-11	2.86E-05	2.86E-05	2.88E-05
		7	7	7	1.02E-10	1.05E-10	1.01E-10	2.86E-05	2.94E-05	2.83E-05
		8	8	8	1.26E-10	1.25E-10	1.25E-10	3.09E-05	3.07E-05	3.07E-05
		9	9	9	1.45E-10	1.44E-10	1.46E-10	3.16E-05	3.14E-05	3.18E-05
		10	10	10	1.68E-10	1.66E-10	1.68E-10	3.30E-05	3.26E-05	3.30E-05
		11	11	11	1.91E-10	1.95E-10	1.93E-10	3.41E-05	3.48E-05	3.44E-05
		12	12	12	2.21E-10	2.23E-10	2.23E-10	3.61E-05	3.65E-05	3.65E-05
		13	13	13	2.45E-10	2.44E-10	2.47E-10	3.70E-05	3.68E-05	3.73E-05
		14	14	14	2.69E-10	2.72E-10	2.70E-10	3.77E-05	3.81E-05	3.78E-05
		15	15	15	2.93E-10	2.89E-10	2.94E-10	3.83E-05	3.78E-05	3.85E-05

**Table F8** The raw data of the determination conductivity of N<sub>acid</sub>:N<sub>monomer</sub> (PPP\_10:1) at 24-25°C, 54-60% R.H

Sample	Thickness (cm)	Applied voltage (V)			Mesuered Current (A)			Conductivity (S/cm)		
		1	2	3	1	2	3	1	2	3
PPP_10:1	1) 0.0180	0.001	0.001	0.001	2.22E-13	2.29E-13	2.19E-13	4.26E-04	4.40E-04	4.21E-04
	2) 0.0215	0.005	0.005	0.005	8.87E-13	8.86E-13	8.91E-13	3.41E-04	3.40E-04	3.42E-04
	3) 0.0168	0.010	0.010	0.010	1.56E-12	1.61E-12	1.68E-12	3.00E-04	3.09E-04	3.23E-04
		0.015	0.015	0.015	2.38E-12	2.44E-12	2.51E-12	3.05E-04	3.12E-04	3.21E-04
		0.020	0.020	0.020	3.33E-12	3.41E-12	3.36E-12	3.20E-04	3.27E-04	3.23E-04
		0.025	0.025	0.025	4.15E-12	4.19E-12	4.18E-12	3.19E-04	3.22E-04	3.21E-04
		0.030	0.030	0.030	5.02E-12	5.11E-12	5.13E-12	3.21E-04	3.27E-04	3.28E-04
		0.035	0.035	0.035	5.94E-12	5.89E-12	5.88E-12	3.26E-04	3.23E-04	3.23E-04
		0.040	0.040	0.040	6.88E-12	6.82E-12	6.91E-12	3.30E-04	3.27E-04	3.32E-04
		0.045	0.045	0.045	7.95E-12	7.90E-12	7.81E-12	3.39E-04	3.37E-04	3.33E-04

**Table F9** The raw data of the determination conductivity of N<sub>acid</sub>:N<sub>monomer</sub> (PPP\_100:1) at 24-25°C, 54-60% R.H

Sample	Thickness (cm)	Applied voltage (V)			Mesuered Current (A)			Conductivity (S/cm)		
		1	2	3	1	2	3	1	2	3
PPP_100:1	1) 0.0202	0.001	0.001	0.001	9.91E-13	9.88E-13	9.78E-13	1.82E-03	1.82E-03	1.79E-03
	2) 0.0195	0.005	0.005	0.005	3.83E-12	3.94E-12	3.89E-12	1.40E-03	1.40E-03	1.42E-03
		0.010	0.010	0.010	7.02E-12	6.89E-12	6.98E-12	1.29E-03	1.29E-03	1.28E-03
		0.015	0.015	0.015	1.08E-11	1.04E-11	1.06E-11	1.32E-03	1.32E-03	1.29E-03
		0.020	0.020	0.020	1.41E-11	1.45E-11	1.44E-11	1.29E-03	1.29E-03	1.32E-03
		0.025	0.025	0.025	1.82E-11	1.83E-11	1.80E-11	1.33E-03	1.33E-03	1.32E-03
		0.030	0.030	0.030	2.09E-11	2.11E-11	2.11E-11	1.28E-03	1.28E-03	1.29E-03
		0.035	0.035	0.035	2.43E-11	2.43E-11	2.45E-11	1.27E-03	1.27E-03	1.28E-03
		0.040	0.040	0.040	2.80E-11	2.79E-11	2.88E-11	1.28E-03	1.28E-03	1.32E-03
		0.045	0.045	0.045	3.13E-11	3.14E-11	3.18E-11	1.27E-03	1.27E-03	1.29E-03

## Appendix G Density Measurement

The specific density ( $\rho_p$ ) of poly(p-phenylene) can be measured by using a pyncometer. In this case we use a pyncometer of size 25 ml. In the first step, we measured the weight of blank pyncometer and added water into the pyncometer and remeasured its weight again. The specific density of water at testing temperature can calculated by equation (G.1).

$$\rho_w = \frac{(a-b)}{25} \quad (G.1)$$

where  $\rho_w$  is the specific density of water ( $\text{g.cm}^{-3}$ ), a is the weight of pyncometer with water (g), and b is the weight of a blank pyncometer (g).

In the second step, we measured the weight of blank pyncometer again and added PPP powders into pynometer, and remeasured the weight change. Then we added water into the pyncometer and remeasured the weight of the pyncometer. The specific density of poly(p-phenylene) at testing temperature can calculated by equation (G2) – (G.3).

$$A = \frac{(e-d)}{\rho_w} \quad (G.2)$$

where A is the volume of water which was added into the pyncometer ( $\text{cm}^3$ ),  $\rho_w$  is specific density of water ( $\text{g.cm}^{-3}$ ), e is the weight of the pyncometer with water and PPP powders (g), and d is the weight of PPP powder and pyncometer (g).

$$\rho_p = \frac{(d-b)}{25-A} \quad (G.3)$$

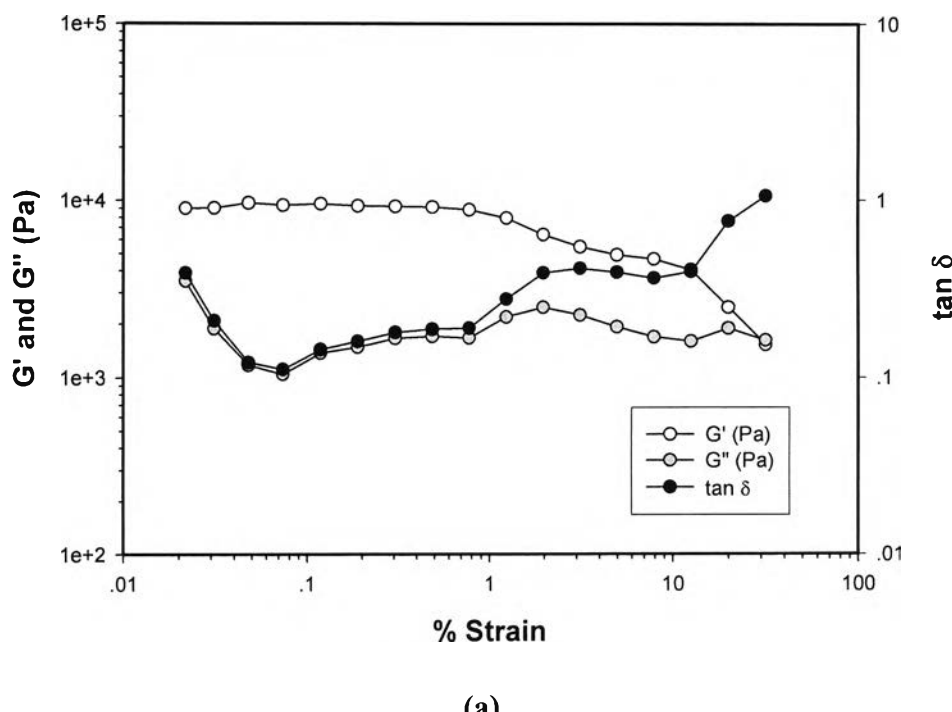
where  $\rho_p$  is the specific density of PPP ( $\text{g.cm}^{-3}$ ), d is the weight of PPP powder and pyncometer (g), b is the weight of a blank pyncometer (g), and A is the volume of water which was added into pyncometer ( $\text{cm}^3$ ).

**Table G1** The data of the determination specific density of water and PPP at 298K.

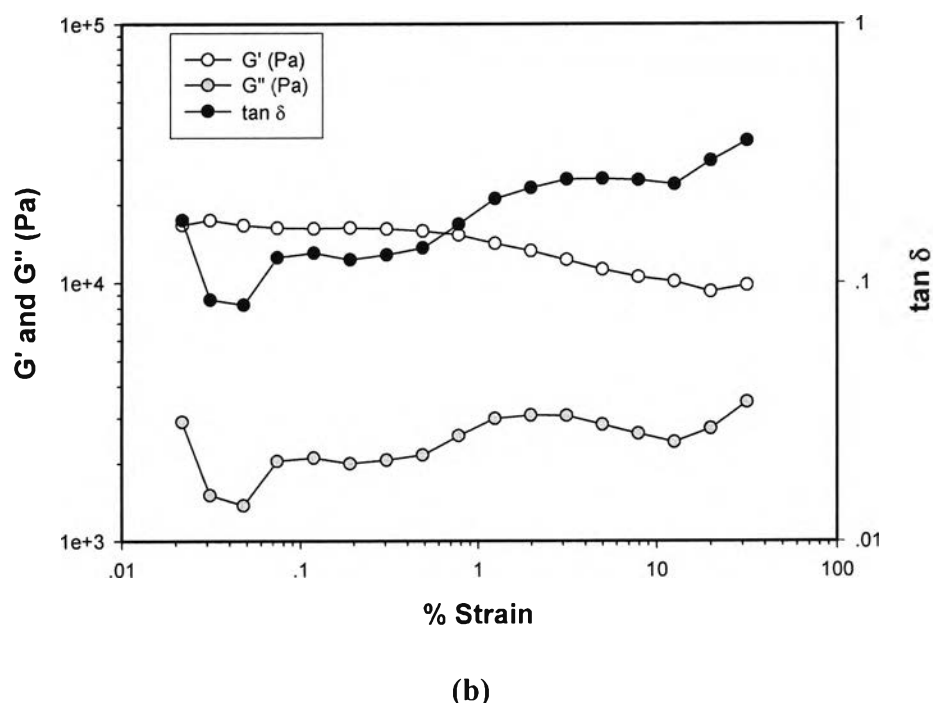
Specific density (g.cm <sup>-3</sup> )	Measurements (g.cm <sup>-3</sup> )			Average (g.cm <sup>-3</sup> )	SD
	1	2	3		
<b>Water</b>	0.9883	0.9815	0.9844	0.9847	0.0034
<b>PPP</b>	1.129	1.122	1.137	1.129	0.008

## **Appendix H Electrorheological Properties Measurement of Pure Acrylic elastomer Nipol AR71 and AR72HF**

The electrorheological properties of pure acrylic elastomer Nipol AR71 and AR72 HF from Zeon Polymix Advance Co.,Ltd were measured by the melt rheometer (Rheometric Scientific, ARES) under oscillatory shear mode and applied electric field strength varying from 0 to 2 kV/mm. In these experiments, the dynamic moduli ( $G'$  and  $G''$ ) were measured as functions of frequency and electric field strength. Strain sweep tests were first carried out to determine the suitable strain to measure  $G'$  and  $G''$  in the linear viscoelastic regime as showed in Figure J1 and J2.

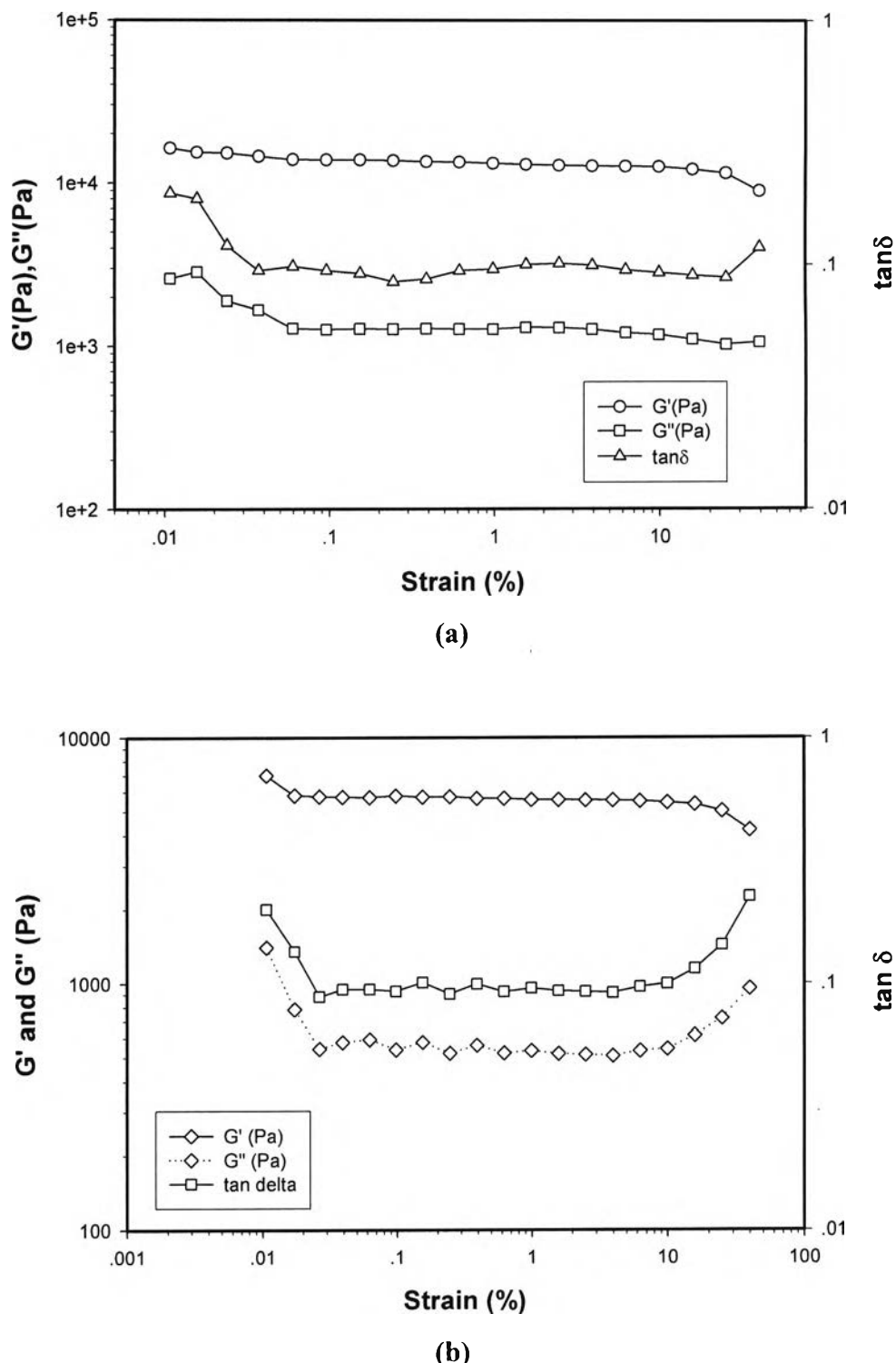


(a)

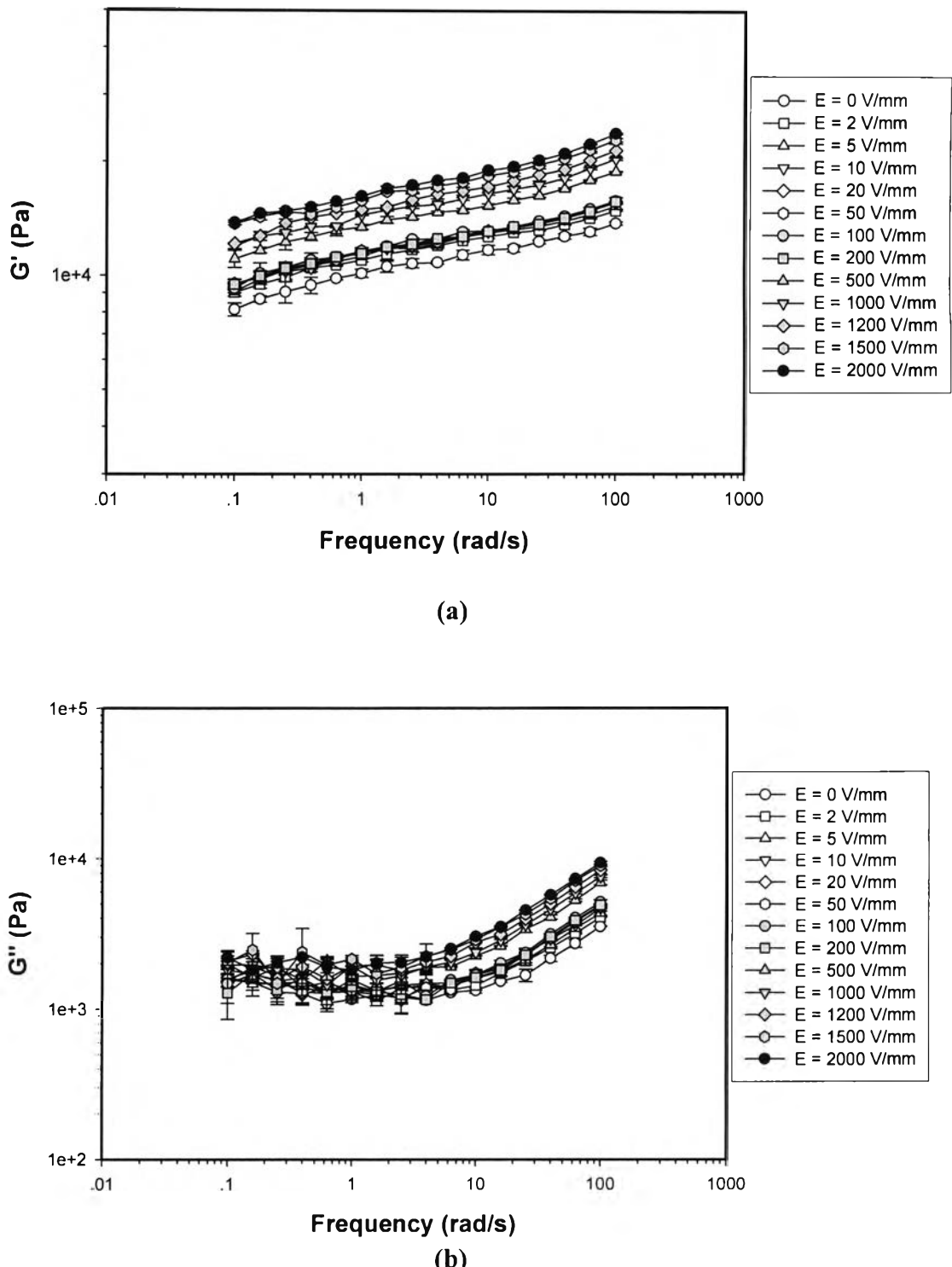


(b)

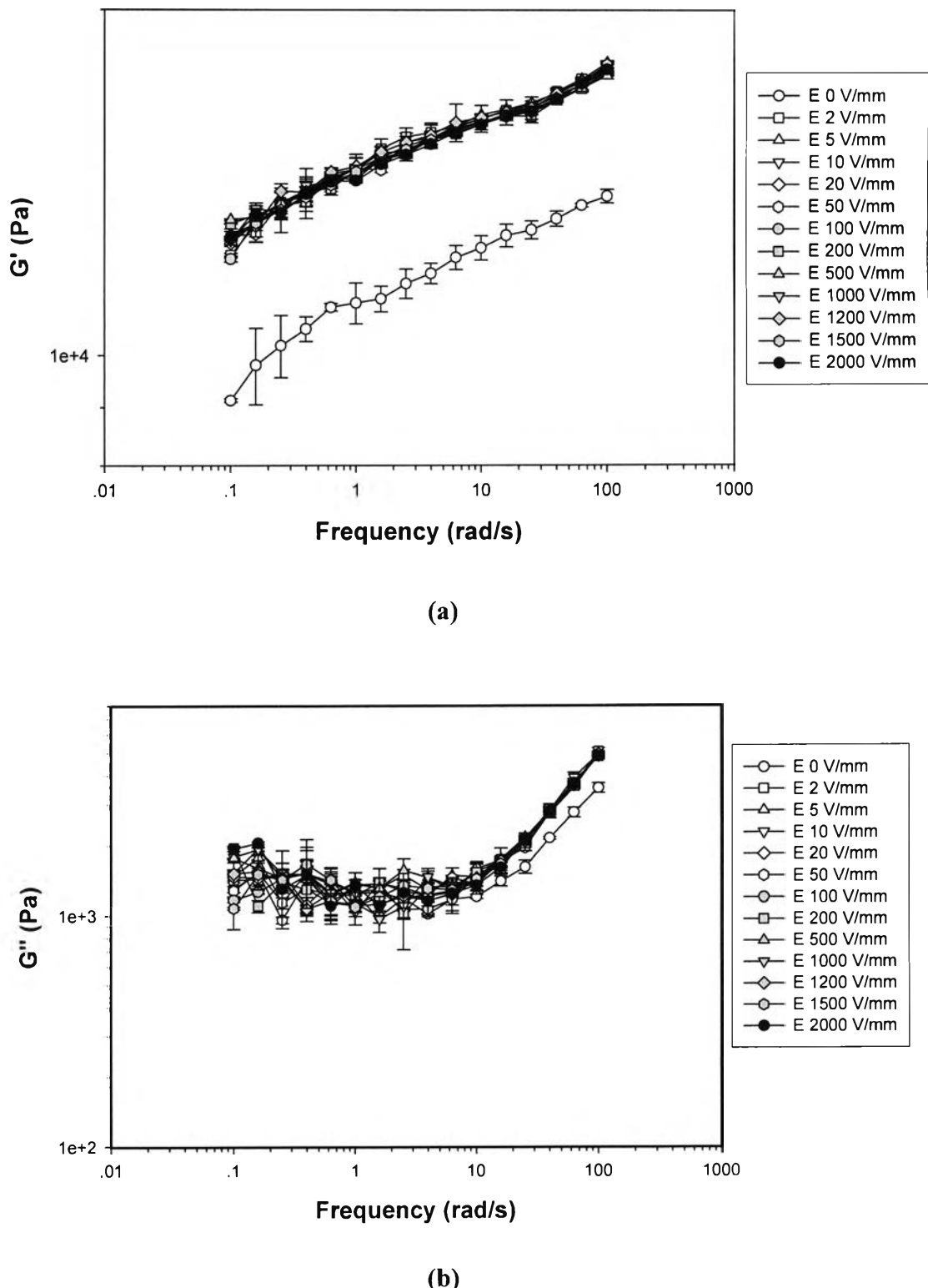
**Figure H1** Strain sweep test of pure acrylic elastomer AR71, frequency 1.0 rad/s,  $27^\circ\text{C}$ , gap 0.780 mm at a)  $E = 0 \text{ V/mm}$ , b)  $E = 2000 \text{ V/mm}$ .



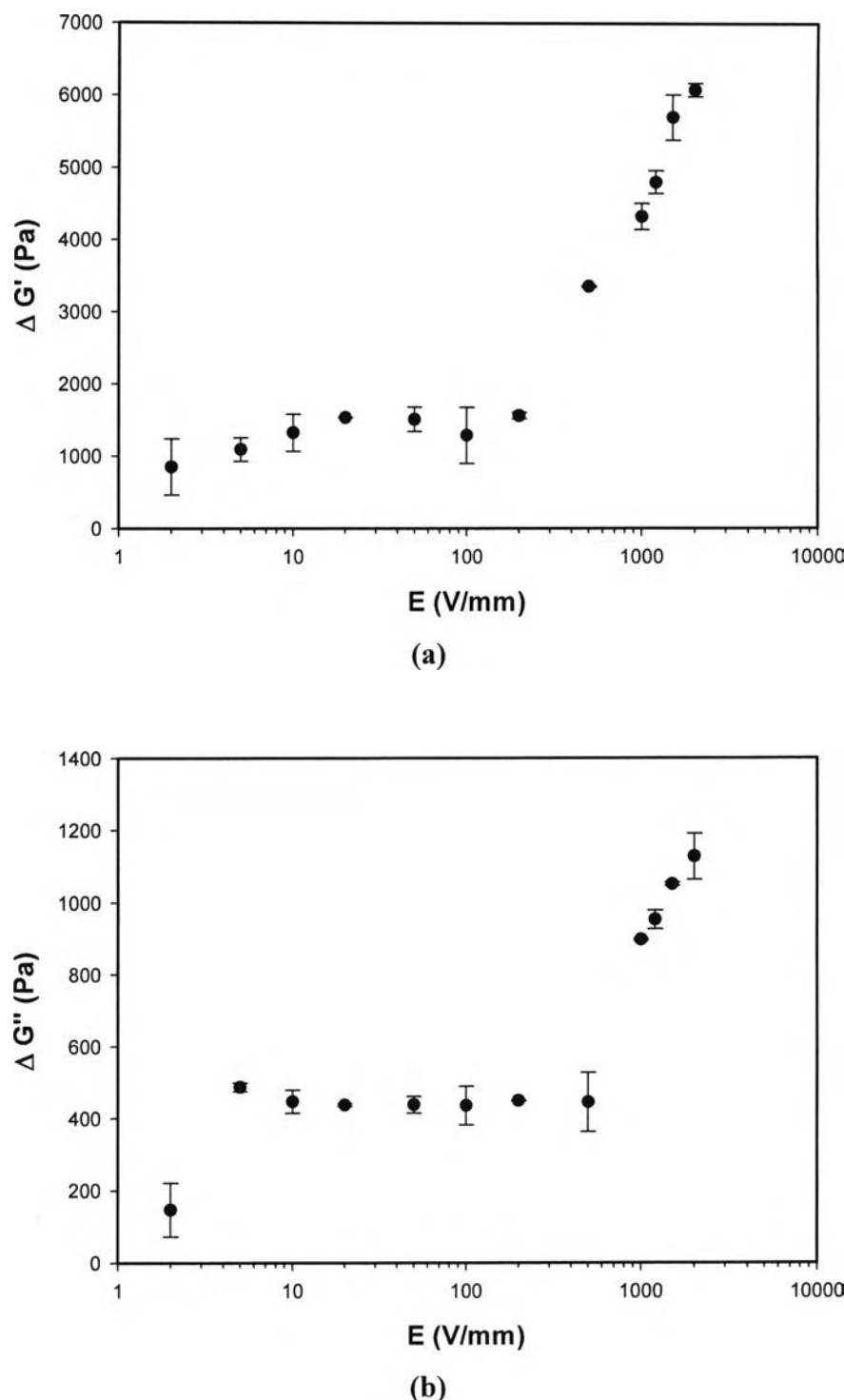
**Figure H2** Strain sweep test of pure acrylic elastomer AR72HF, frequency 1.0 rad/s, 27° C, gap 0.860 mm at a) E = 0 V/mm, b) E = 2000 V/mm.



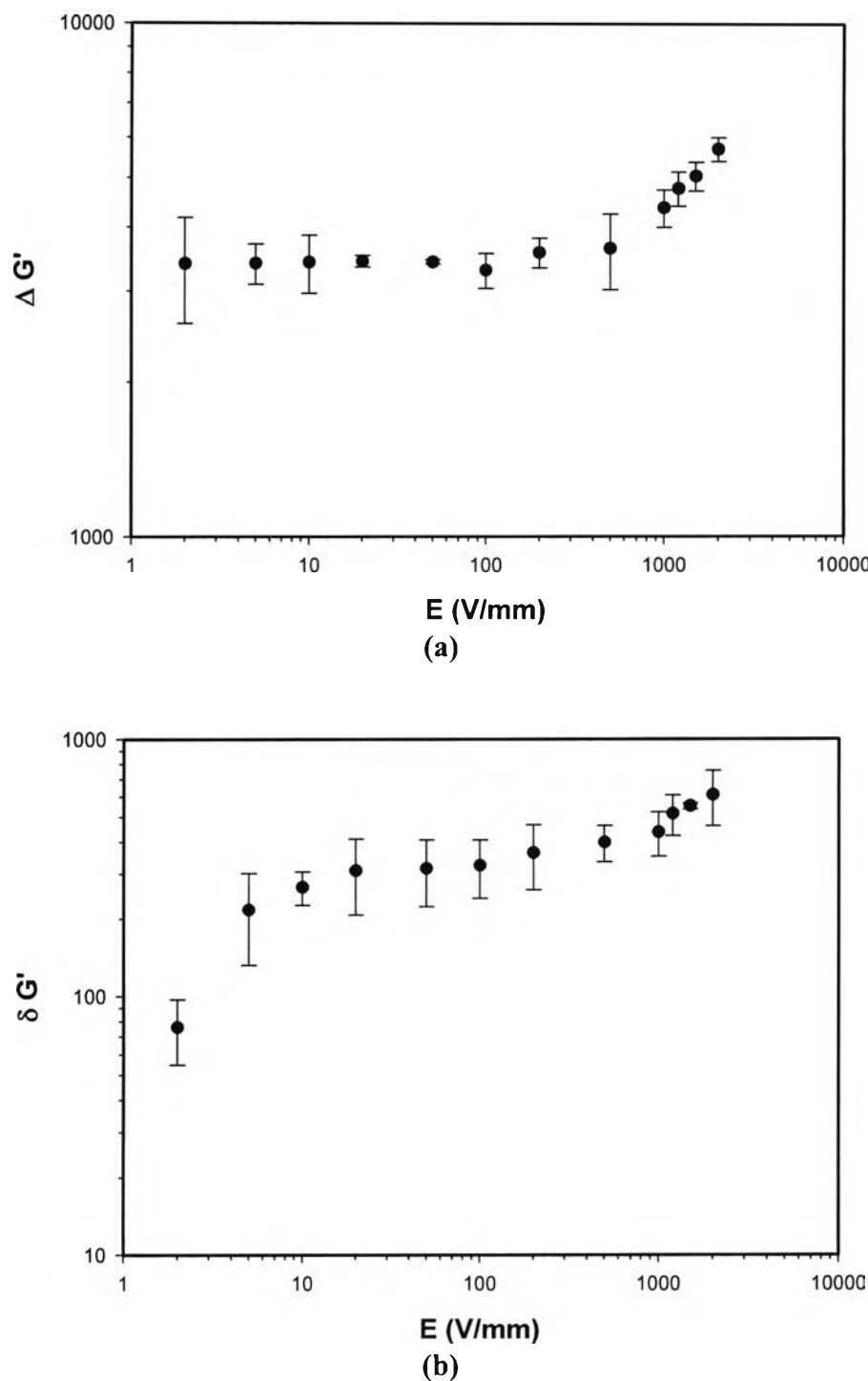
**Figure H3** Frequency sweep test of pure acrylic elastomer AR71, strain 0.1%, 27° C, gap 0.780 mm various electric field strengths: a)  $G'$  (Pa), b)  $G''$  (Pa).



**Figure H4** Frequency sweep test of pure acrylic elastomer AR72HF, strain 0.1%, 27° C, gap 0.860 mm various electric field strengths: a) G'(Pa), b) G'' (Pa).



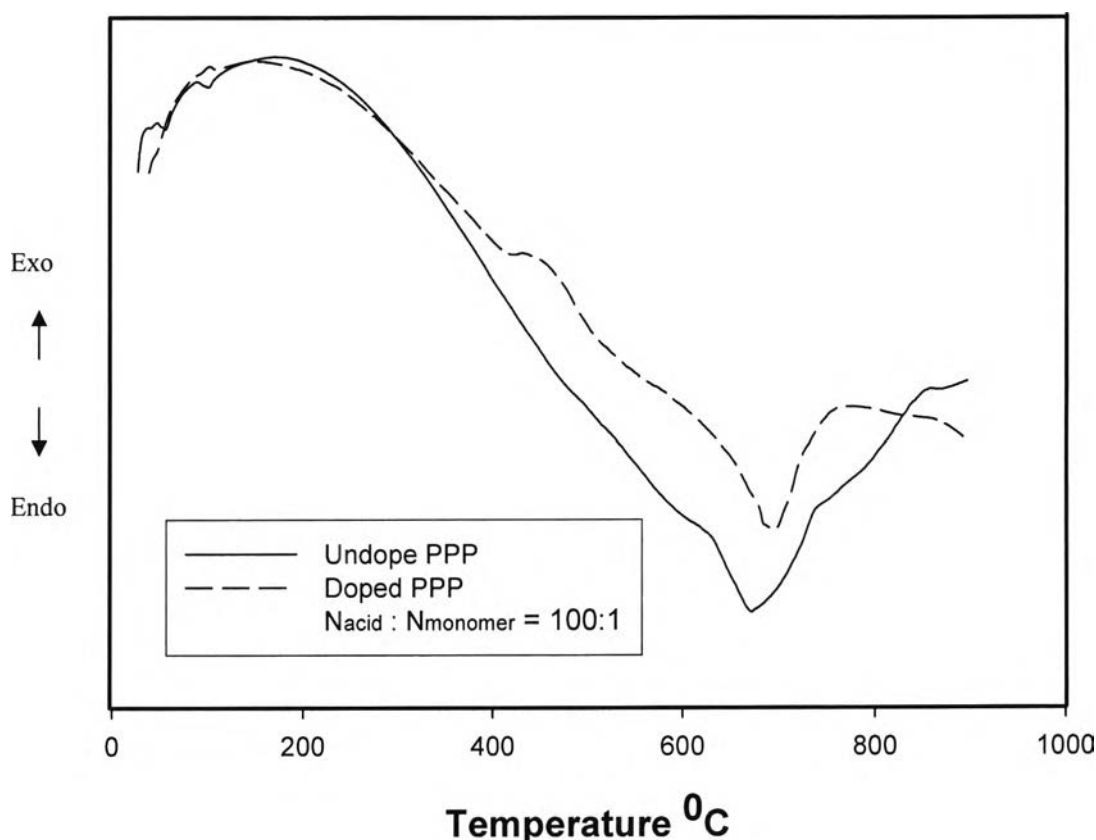
**Figure H5** Responses of the storage and the loss moduli ( $\Delta G'(\omega)$ ) and  $\Delta G''(\omega)$  of the acrylic elastomer AR71 vs. electric field strength, frequency 1.0 rad/s, strain 0.1%, gap 0.780 mm at  $27^{\circ}\text{C}$ : (a)  $\Delta G'(\omega)$ , (b)  $\Delta G''(\omega)$  when  $G'_0 = 10,314 \text{ Pa}$  and  $G''_0 = 1,017 \text{ Pa}$ .



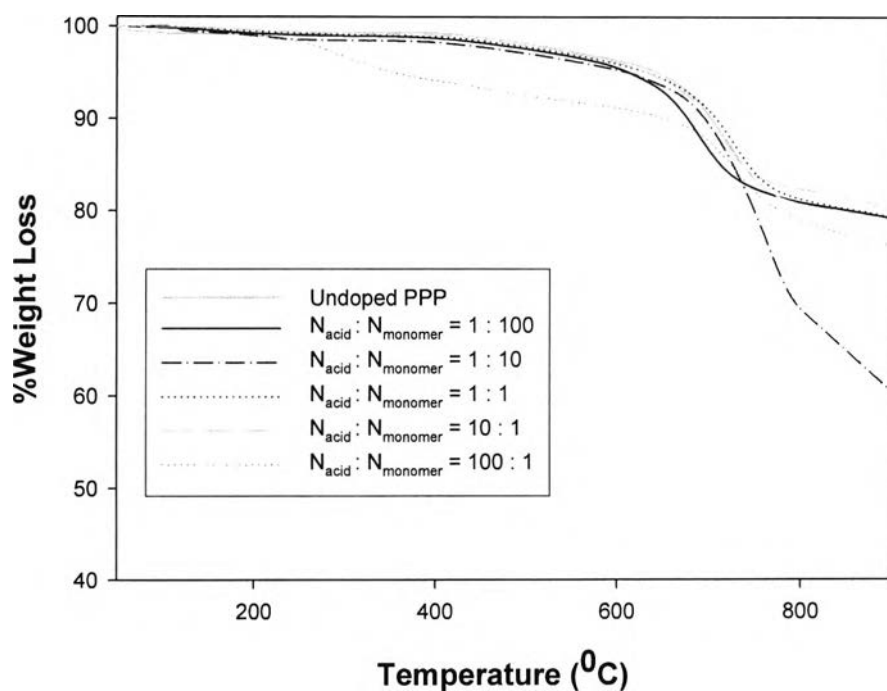
**Figure H6** Responses of the storage and the loss moduli ( $\Delta G'(\omega)$ ) and  $\Delta G''(\omega)$  of the acrylic elastomer AR72HF vs. electric field strength, frequency 1.0 rad/s, strain 0.1%, gap 0.860 mm at  $27^{\circ}\text{C}$ : (a)  $\Delta G'(\omega)$ , (b)  $\Delta G''(\omega)$  when  $G'_0 = 11,427$  Pa and  $G''_0 = 1,190$  Pa.

### Appendix I The Differential Thermal Analysis of Undoped and doped PPP.

A DT-TGA1760 differential thermal- thermal gravity analyzer (DT-TGA) was used to record the degrading exotherms for undoped and doped PPP. Calibration for the temperature scale was carried out with a pure platinium pan and blank pan for obtains zero weight of pan. Then put sample into pan and run under interesting condition ( $40\text{-}900^{\circ}\text{C}$ ). The result was show by Figure L1 and L2. From DT-TGA the depredateing temperature of undoped PPP is lower than doped PPP.



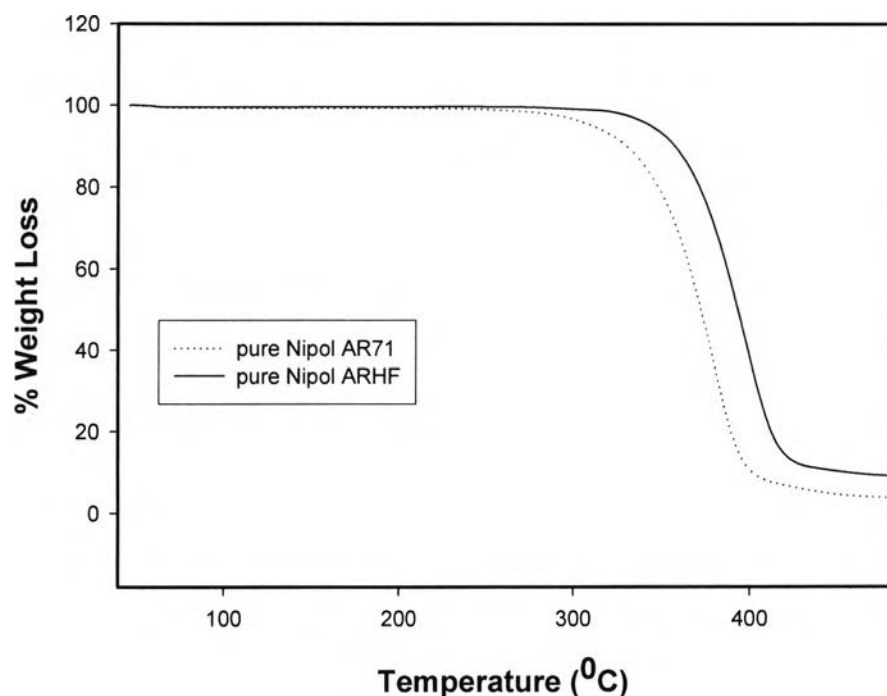
**Figure I1** The DT-TGA thermograms of undoped PPP and doped PPP at  $\text{N}_{\text{acid}}$  :  $\text{N}_{\text{monomer}} = 100:1$  between  $40\text{-}900^{\circ}\text{C}$  at rate of  $10^{\circ}\text{C}/\text{min}$ .



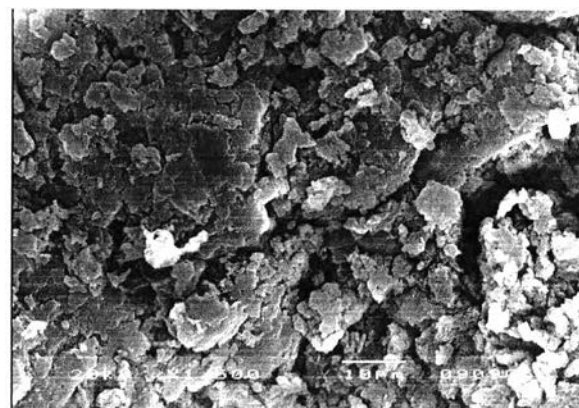
**Figure I2** The DT-TGA thermograms of undoped PPP and doped PPP between 40-900 °C at rate of 10 °C/min.

## Appendix J The Thermal Gravity Analysis of NipolAR71 and AR72HF.

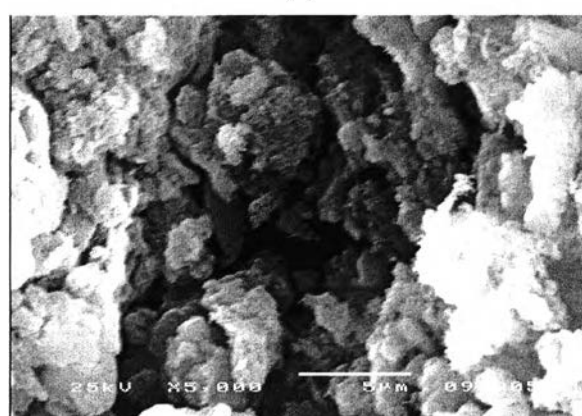
A TGA7 Thermal Gravity Analyzer (TGA) was used to record the degrading exotherms for Nipol AR71 and AR72HF. Calibration for the temperature scale was carried out with a pure platinium pan and blank pan for obtains zero weight of pan. Then put sample into pan and run under interesting condition ( $40\text{-}500^{\circ}\text{C}$ ). The result was show by Figure M1. From DT-TGA the depredating temperature of Nipol AR71 is lower than AR72HF.



**Figure J1** The TGA thermograms of Nipol AR71 and AR72HF between  $40\text{-}500^{\circ}\text{C}$  at rate of  $10^{\circ}\text{C}/\text{min}$ .

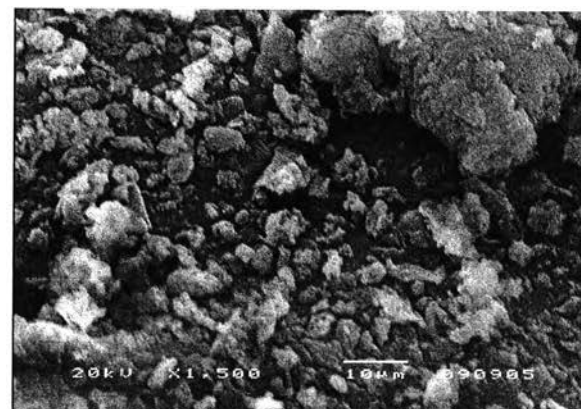
**Appendix K Scanning Electron Micrograph of Undoped PPP, Doped PPP**

(a)

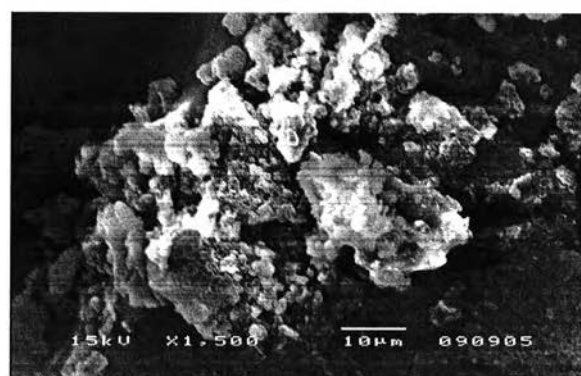


(b)

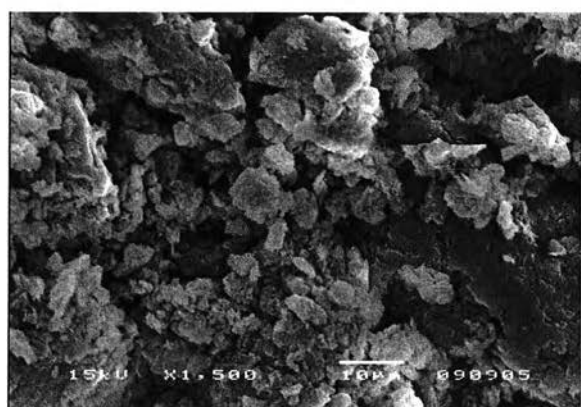
**Figure K1** The morphology of undoped poly(p-phenylene) (PPP) powder at magnification of a) 1,500 and b) 5000.



(a)



(b)



(c)

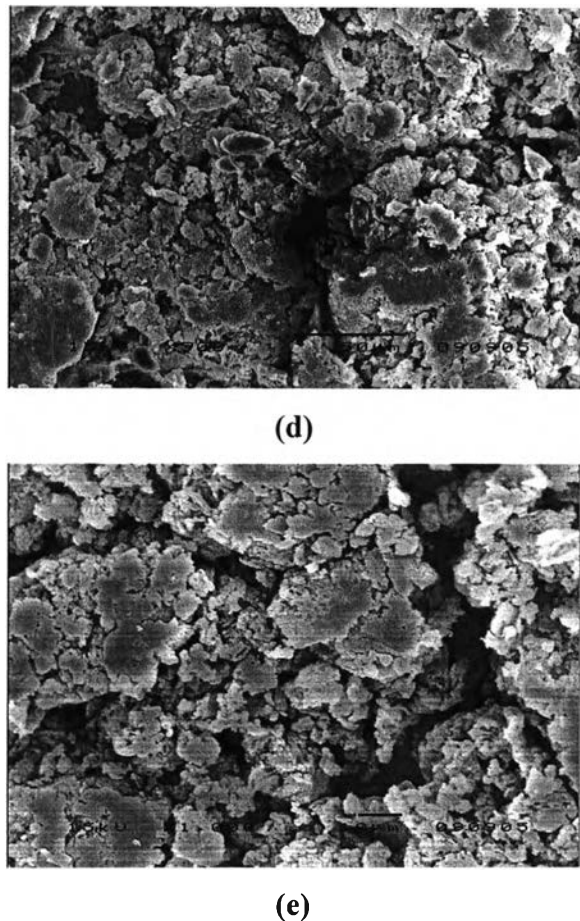


**Figure K2** The morphology of doped PPP powder with  $\text{H}_2\text{SO}_4$  as various doping ratio at magnification of 1,500: a) 100:1; b) 10:1; c) 1:1; d) 1:10; and e) 1:100.

**Appendix L Electrorheological Properties Measurement of Polymer Blends between PPP and Nipol AR71 at Various ratio of PPP.**

The electrorheological properties of polymer blends between PPP and Nipol AR71 at various ratio of PPP were measured by the melt rheometer (Rheometric Scientific, ARES) under oscillatory shear mode and applied electric filed strength varying from 0 to 2 kV/mm. In these experiments, the dynamic moduli ( $G'$  and  $G''$ ) were measured as functions of frequency and electric field strength. Strain sweep tests were first carried out to determine the suitable strain to measure  $G'$  and  $G''$  in the linear viscoelastic regime.

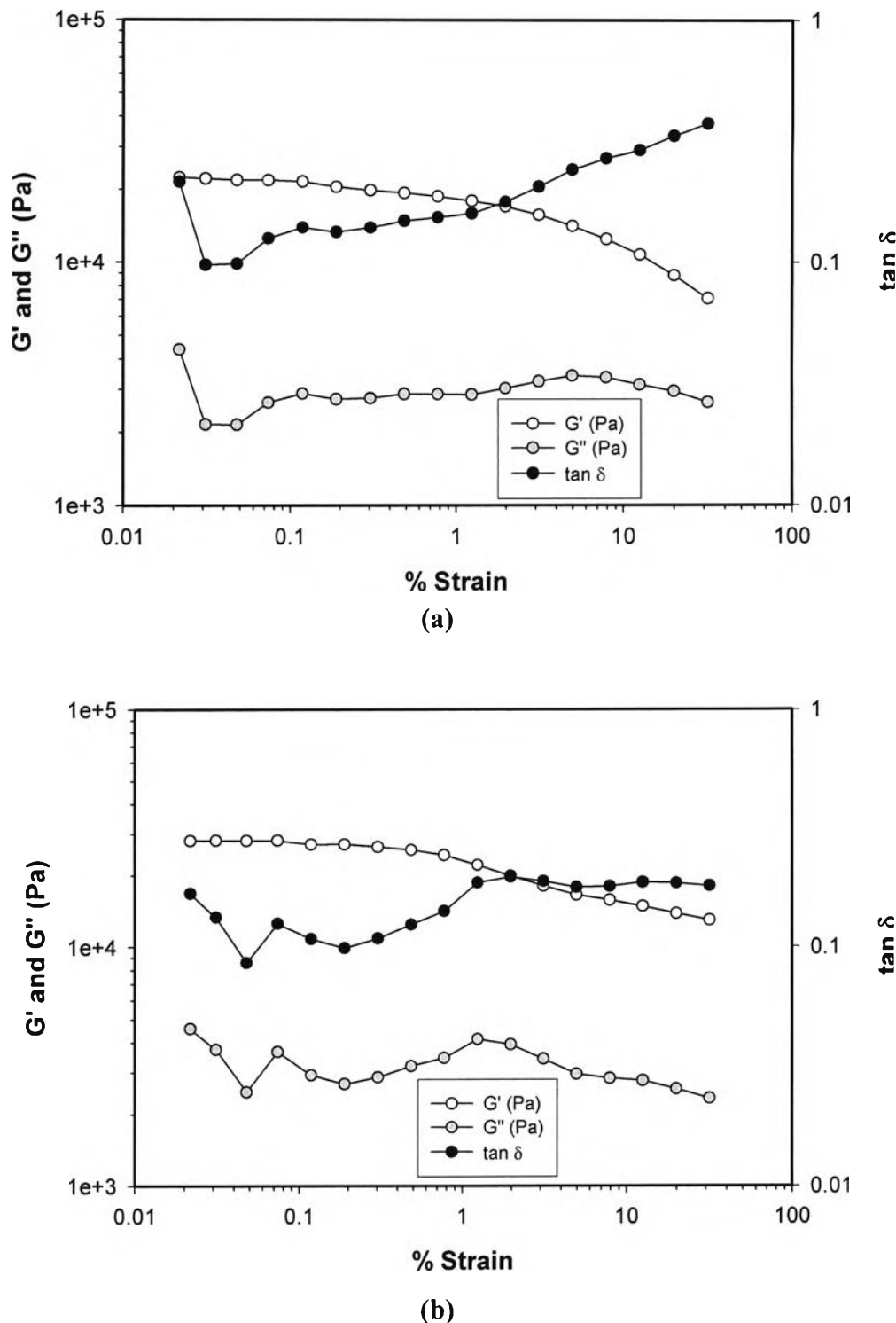


**Figure L1** Strain sweep test of polymer blend between PP and AR71 at 10% v/v of PPP (AR 10%PPP), frequency 1.0 rad/s, 27<sup>0</sup> C, gap 0.530 mm at a) E = 0 V/mm, b) E = 2000 V/mm.

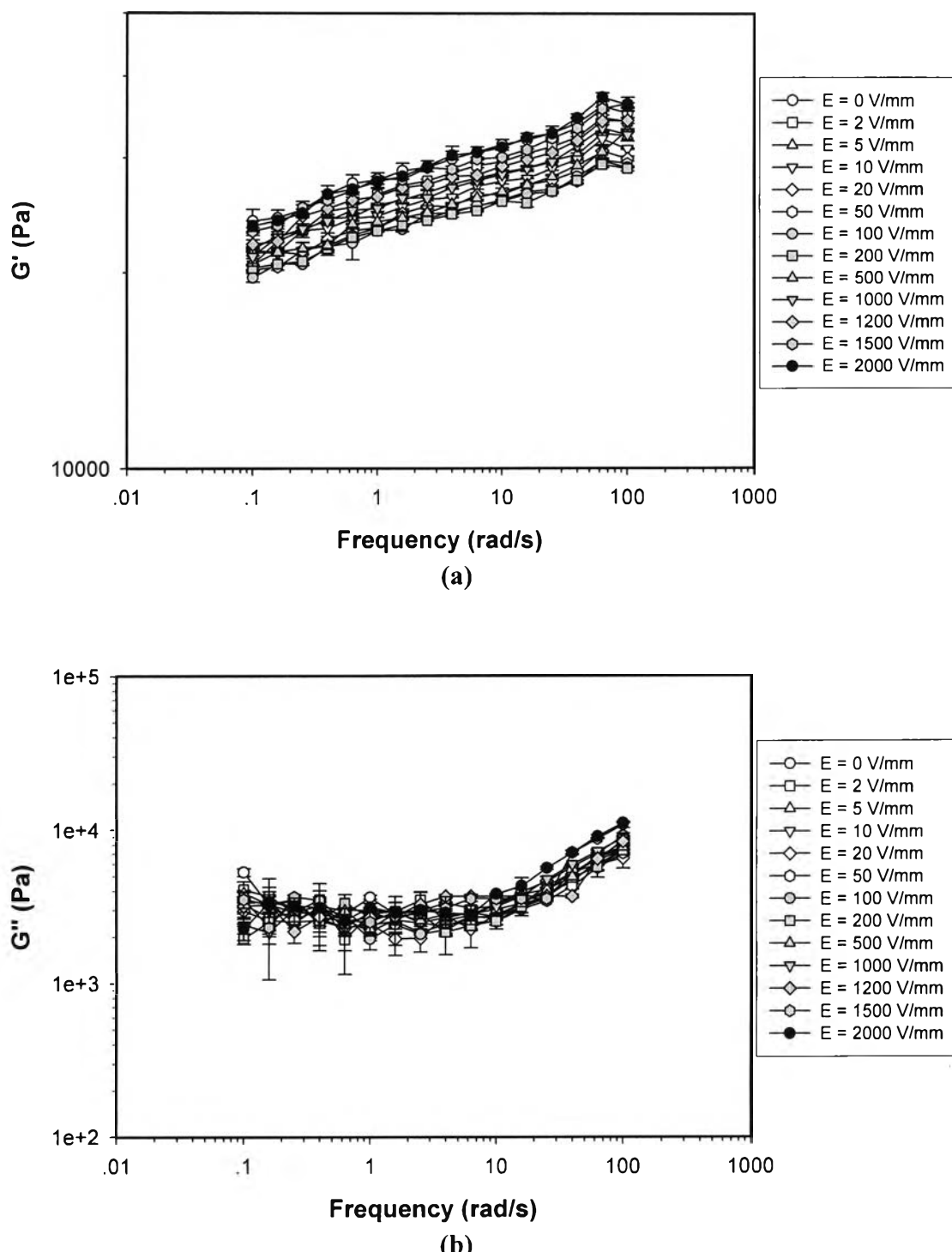
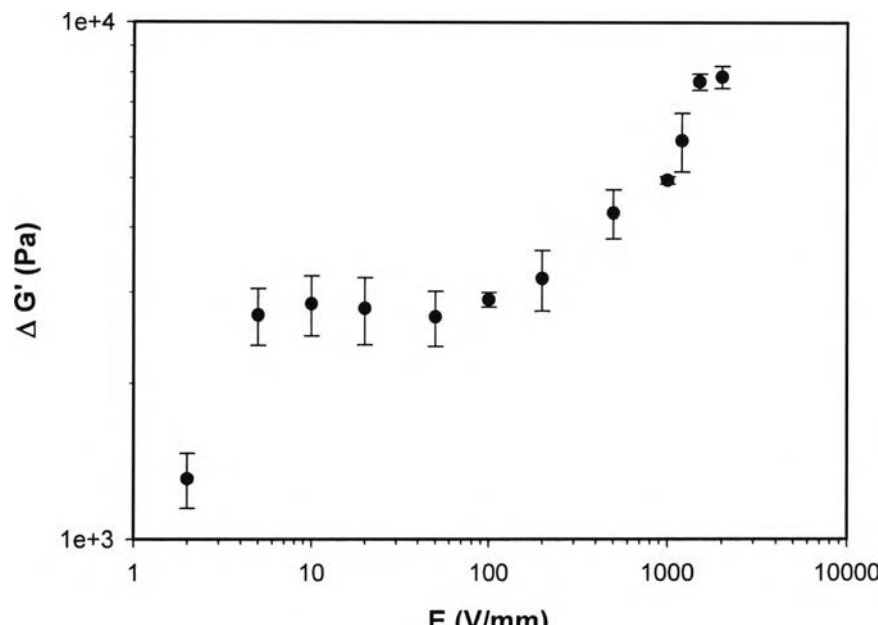
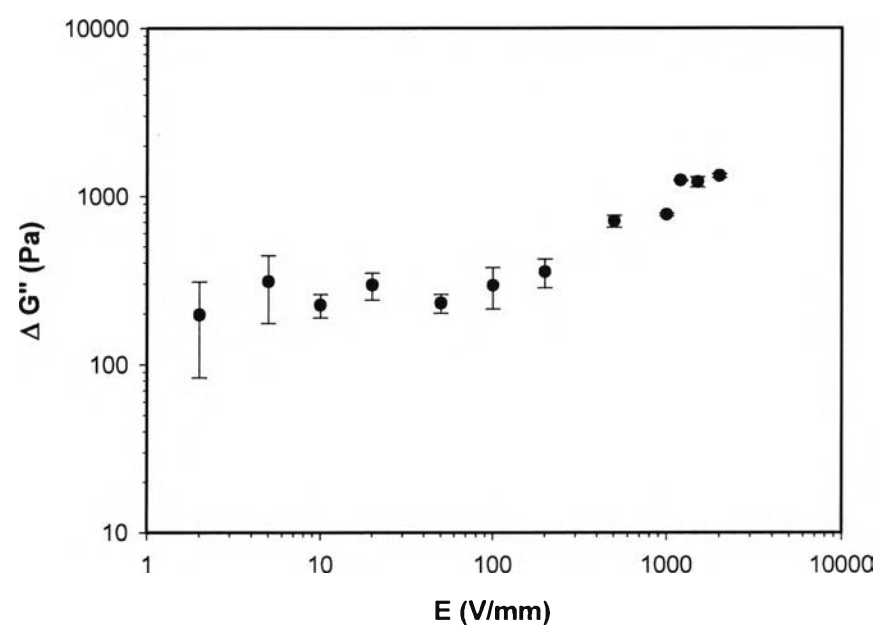


**Figure L2** Frequency sweep test of polymer blend between PP and AR71 at 10% v/v of PPP (AR 10%PPP), strain 0.1%, 27° C, gap 0.530 mm at various electric field strengths: a) G'(Pa), b) G'' (Pa).

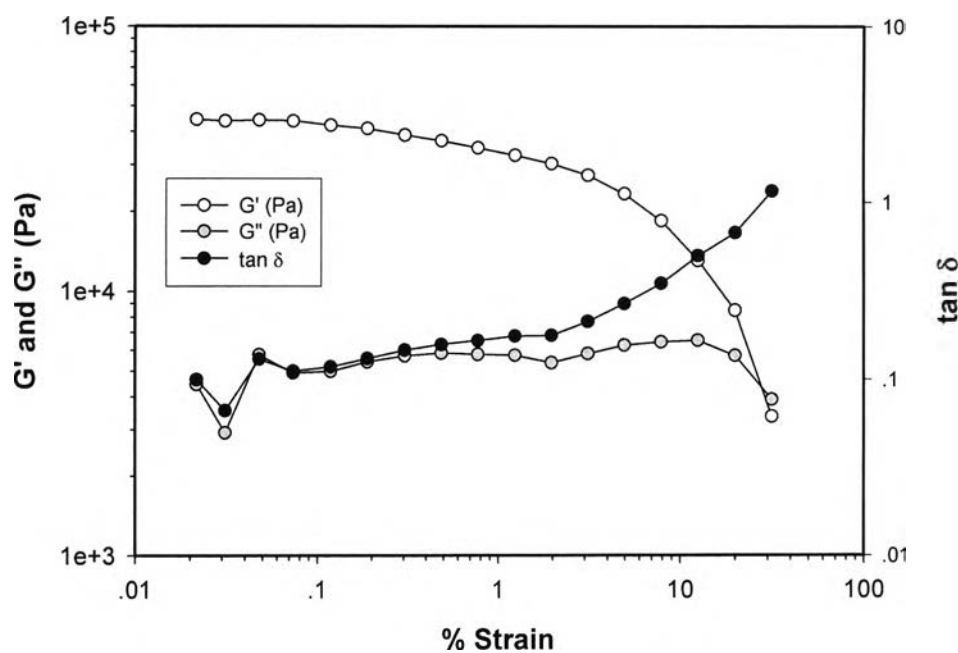


(a)

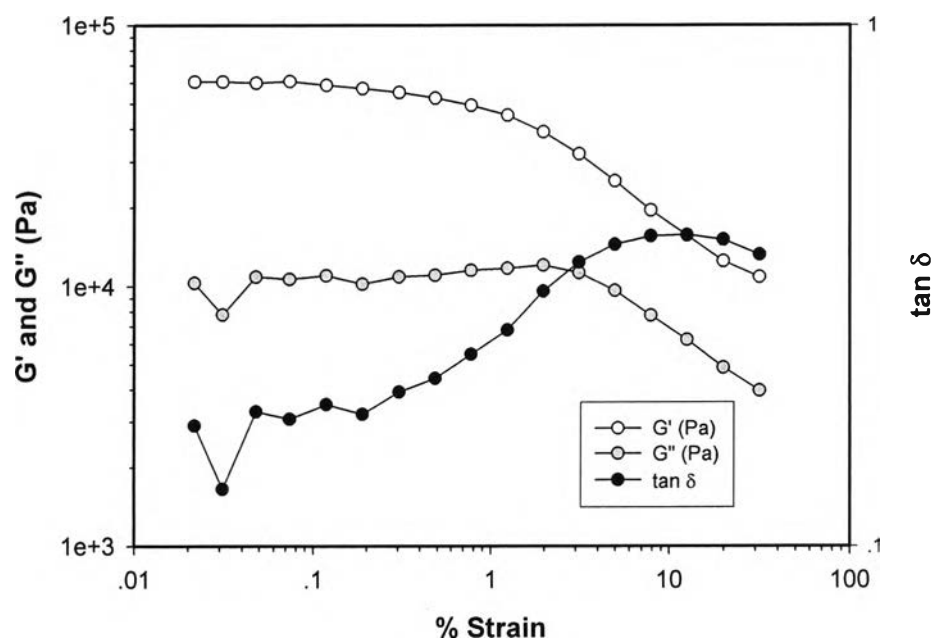


(b)

**Figure L3** Responses of the storage and the loss moduli ( $\Delta G'(\omega)$  and  $\Delta G''(\omega)$ ) of polymer blend between PP and AR71 at 10% v/v of PPP (AR 10%PPP) vs. electric field strength, frequency 1.0 rad/s, strain 0.1%, gap 0.530 mm at 27°C: (a)  $\Delta G'(\omega)$ , (b)  $\Delta G''(\omega)$  when  $G'_0 = 27,250$  Pa and  $G''_0 = 3,565$  Pa.



(a)



(b)

**Figure L4** Strain sweep test of polymer blend between PP and AR71 at 20% v/v of PPP (AR 20%PPP), frequency 1.0 rad/s,  $27^0$  C, gap 0.690 mm at a)  $E = 0$  V/mm, b)  $E = 2000$  V/mm.

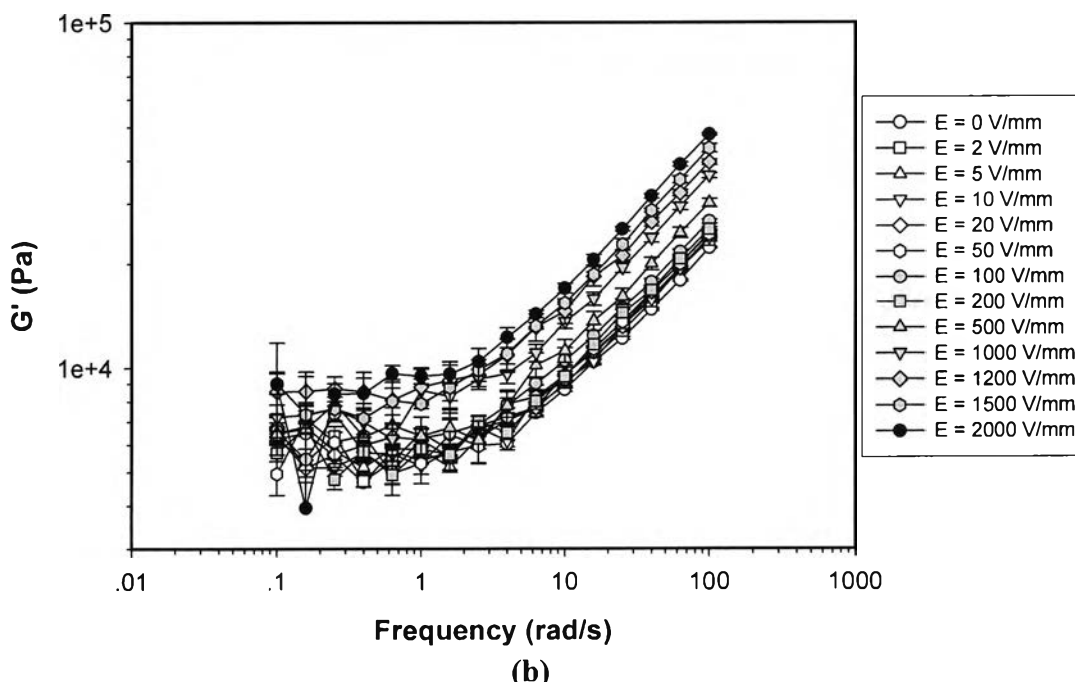
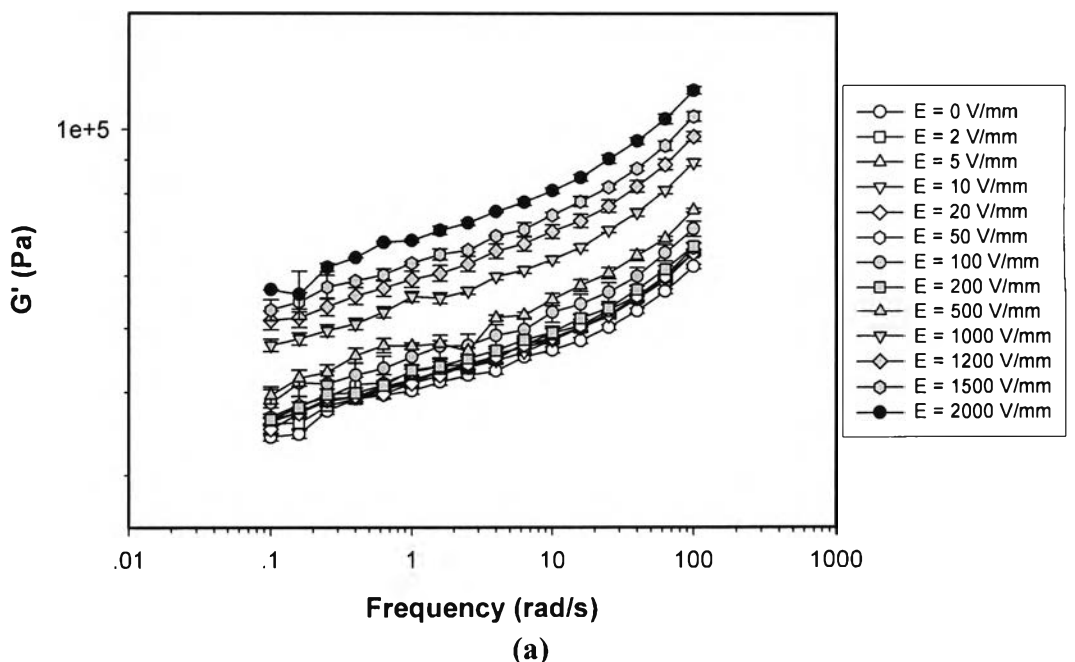
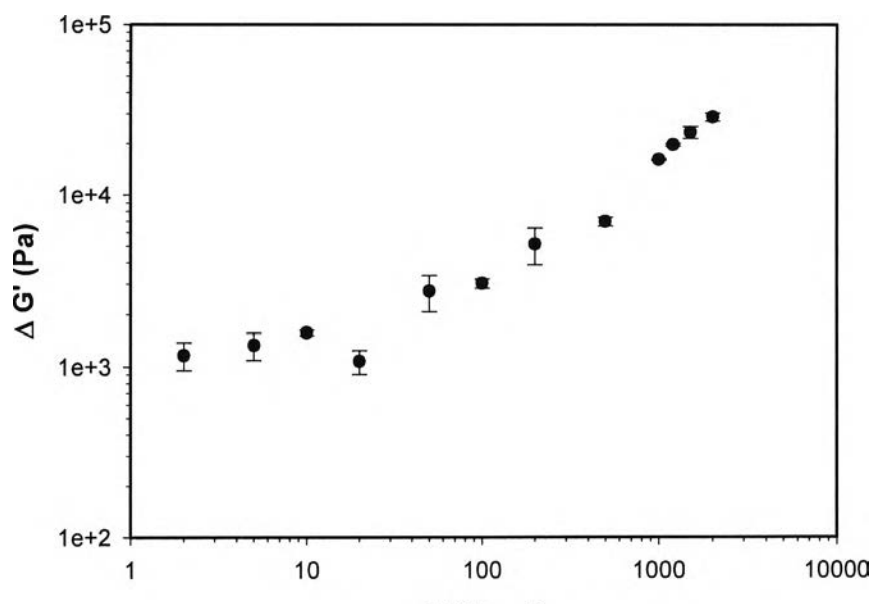
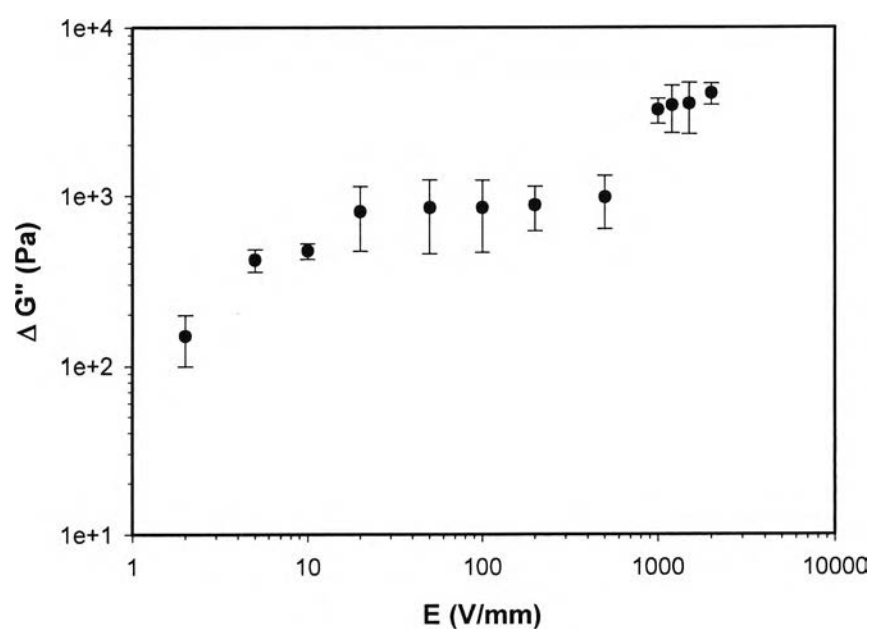


**Figure L5** Frequency sweep test of polymer blend between PP and AR71 at 20% v/v of PPP (AR 20%PPP), strain 0.1%, 27° C, gap 0.690 mm at various electric field strengths: a) G'(Pa), b) G'' (Pa).

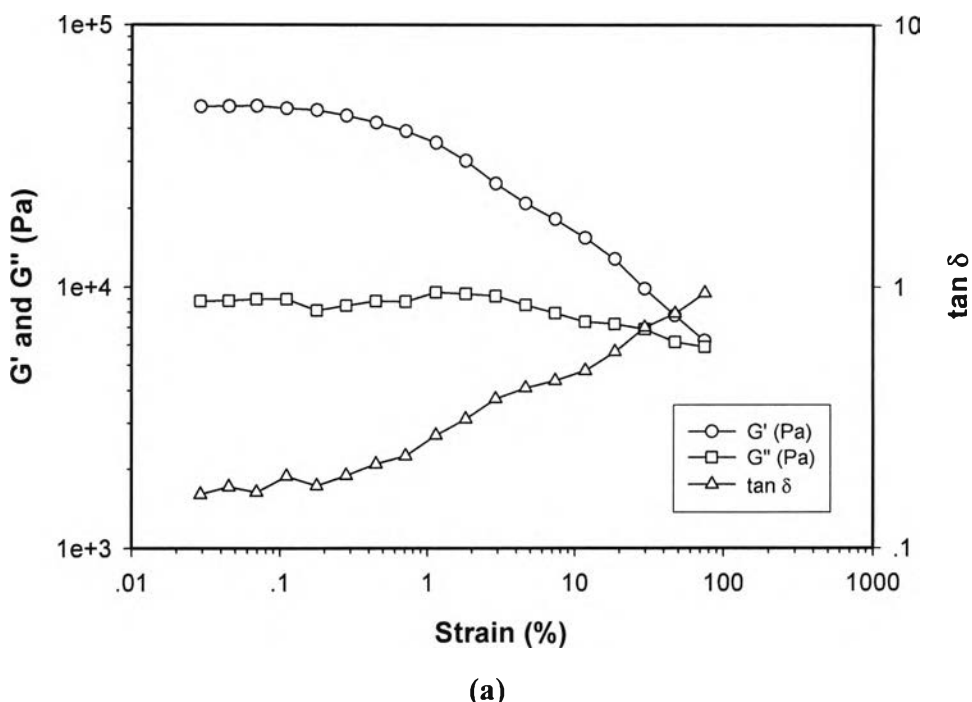


(a)

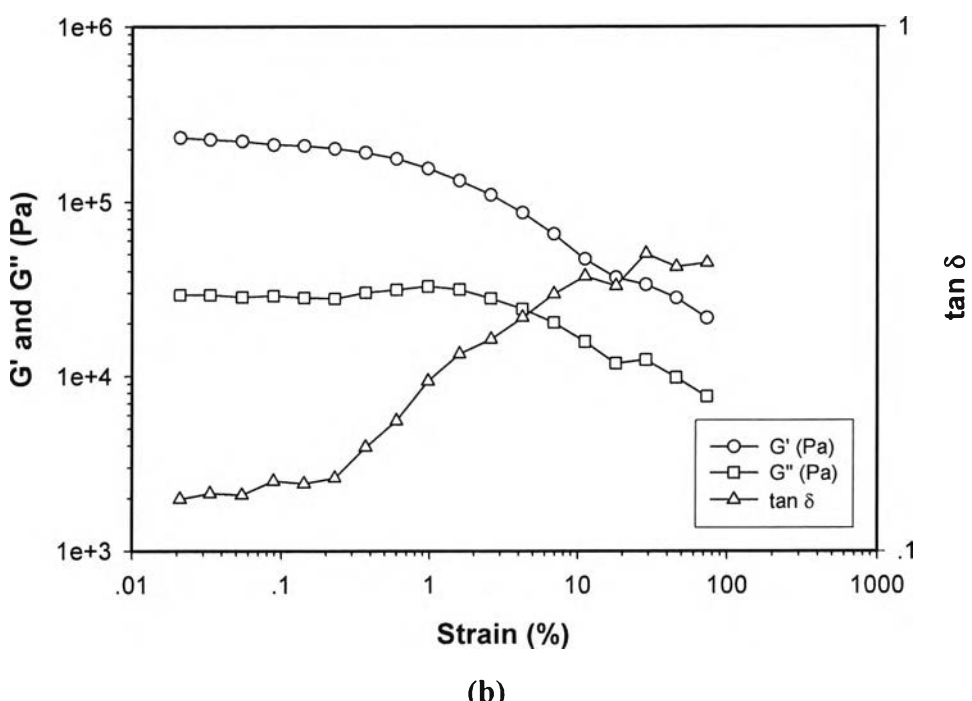


(b)

**Figure L6** Responses of the storage and the loss moduli ( $\Delta G'(\omega)$  and  $\Delta G''(\omega)$ ) of polymer blend between PP and AR71 at 20% v/v of PPP (AR 20%PPP) vs. electric field strength, frequency 1.0 rad/s, strain 0.1%, gap 0.690 mm at  $27^{\circ}\text{C}$ : (a)  $\Delta G'(\omega)$ , (b)  $\Delta G''(\omega)$  when  $G'_0 = 39,859$  Pa and  $G''_0 = 5,496$  Pa.



(a)



(b)

**Figure L7** Strain sweep test of polymer blend between PP and AR71 at 30% v/v of PPP (AR 30%PPP), frequency 1.0 rad/s,  $27^{\circ}$  C, gap 0.590 mm at a)  $E = 0$  V/mm, b)  $E = 2000$  V/mm.

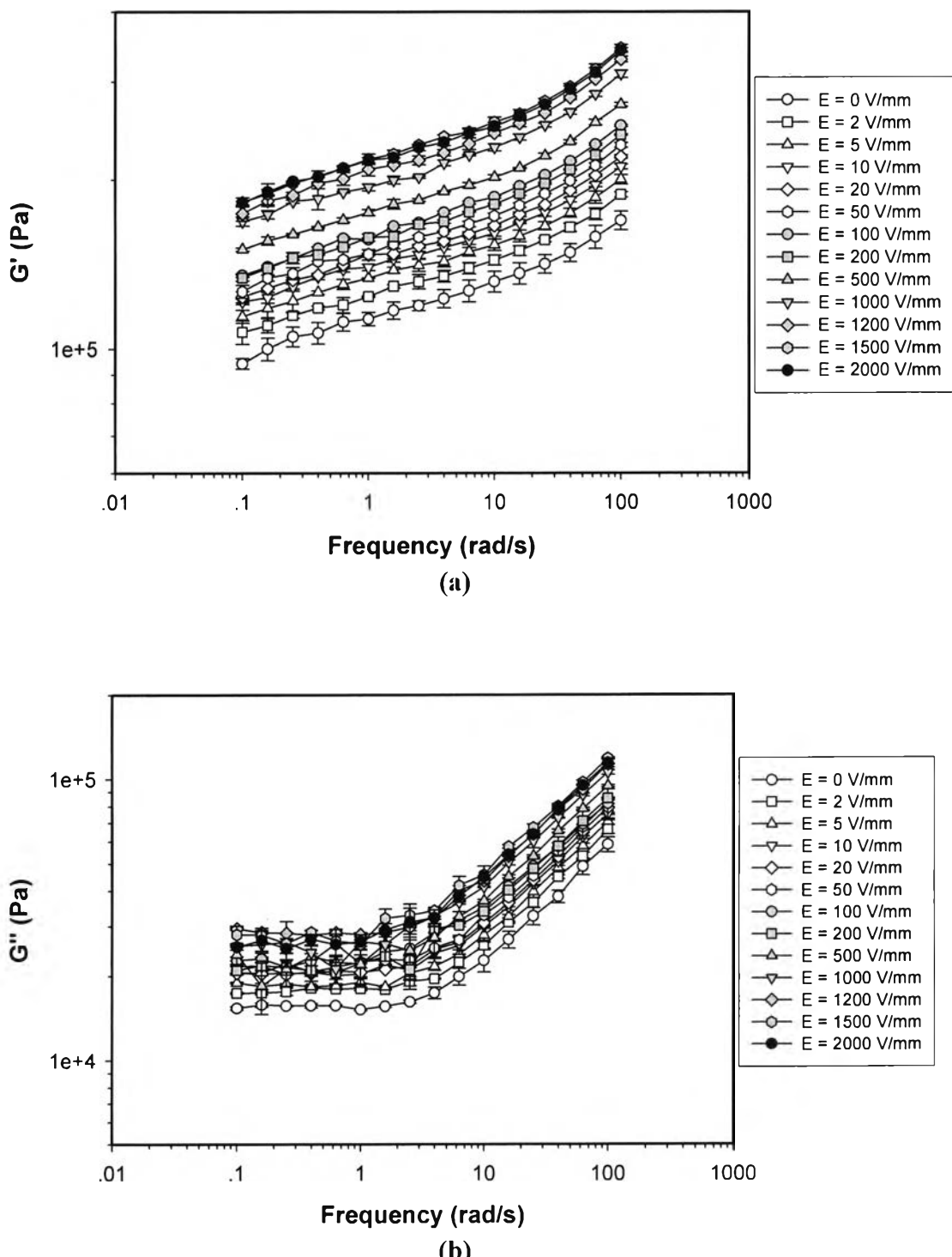


**Figure L8** Frequency sweep test of polymer blend between PP and AR71 at 30% v/v of PPP (AR 30%PPP), strain 0.1%, 27° C, gap 0.590 mm at various electric field strengths: a) G'(Pa), b) G'' (Pa).

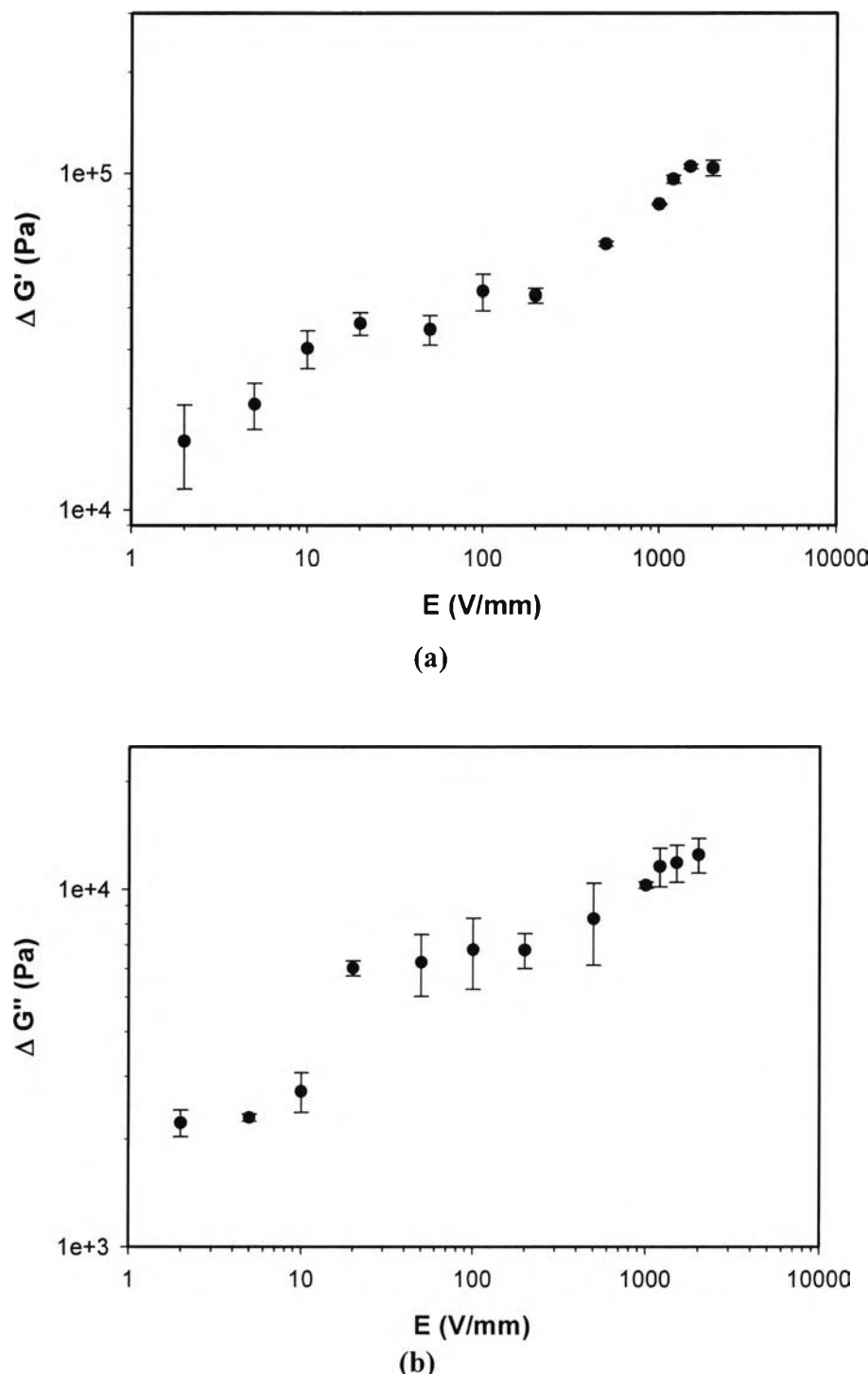
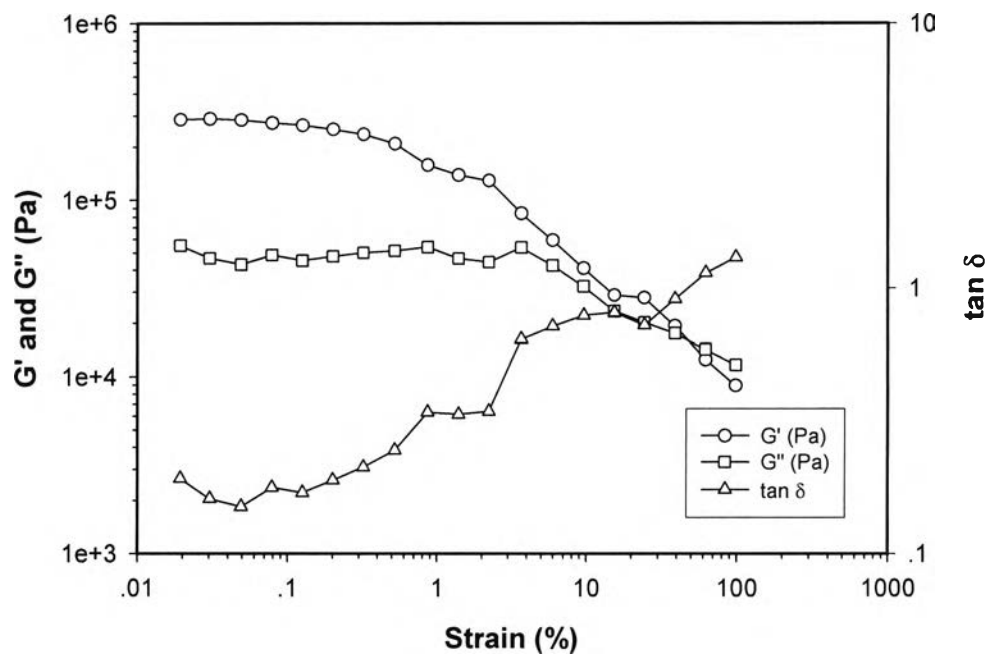
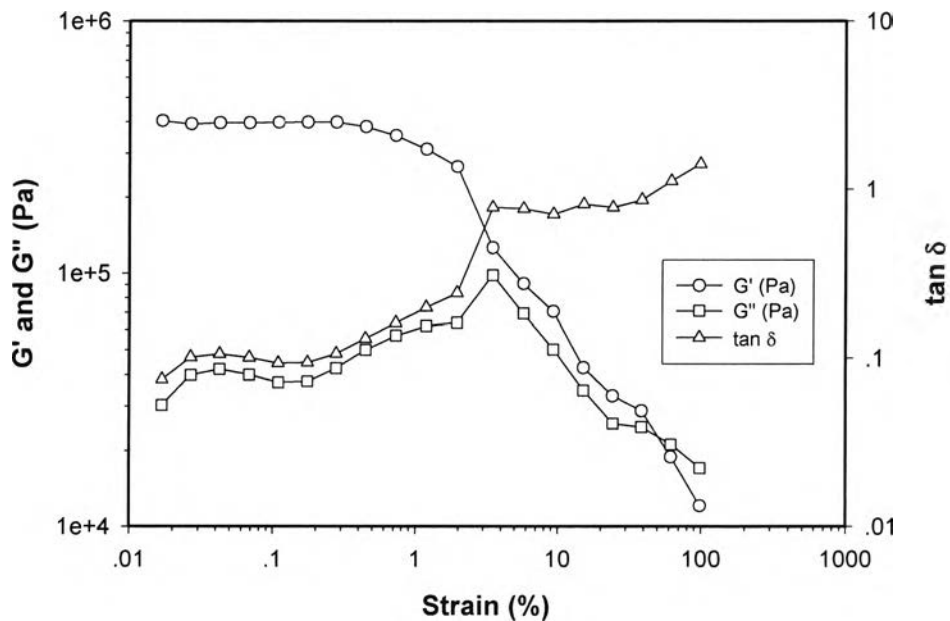


**Figure L9** Responses of the storage and the loss moduli ( $\Delta G'(\omega)$  and  $\Delta G''(\omega)$ ) of polymer blend between PP and AR71 at 30% v/v of PPP (AR 30%PPP) vs. electric field strength, frequency 1.0 rad/s, strain 0.1%, gap 0.590 mm at 27°C: (a)  $\Delta G'(\omega)$ , (b)  $\Delta G''(\omega)$  when  $G'_0 = 115,420$  Pa and  $G''_0 = 15,284$  Pa.



(a)



(b)

**Figure L10** Strain sweep test of polymer blend between PP and AR71 at 40% v/v of PPP (AR 40%PPP), frequency 1.0 rad/s, 27° C, gap 0.710 mm at a)  $E = 0$  V/mm, b)  $E = 2000$  V/mm.

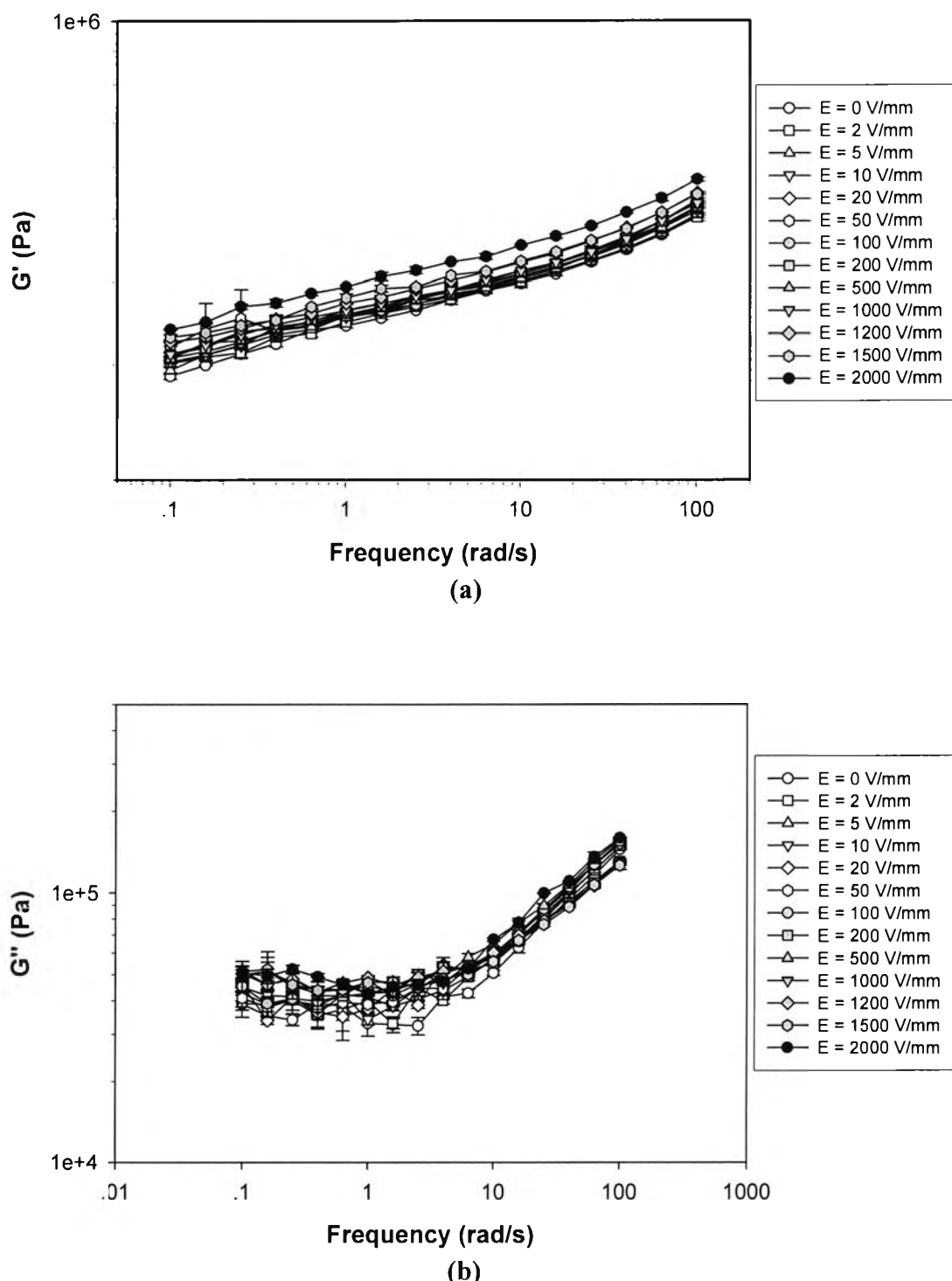


**Figure L11** Frequency sweep test of polymer blend between PP and AR71 at 40% v/v of PPP (AR 40%PPP), strain 0.1%,  $27^{\circ}$  C, gap 0.710 mm at various electric field strengths: a)  $G'$  (Pa), b)  $G''$  (Pa).

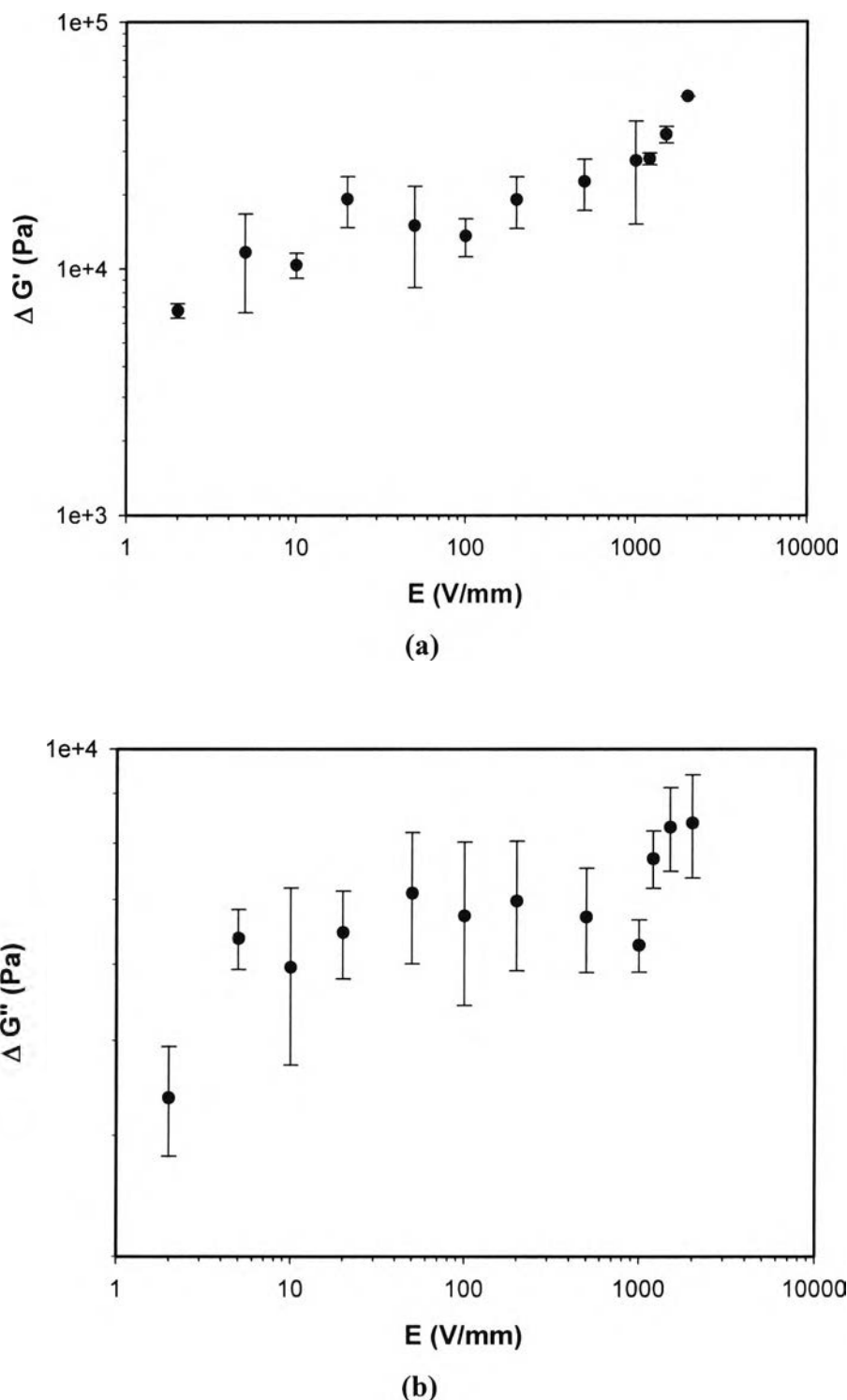


**Figure L12** Responses of the storage and the loss moduli ( $\Delta G'(\omega)$  and  $\Delta G''(\omega)$ ) of polymer blend between PP and AR71 at 40% v/v of PPP (AR 40%PPP) vs. electric field strength, frequency 1.0 rad/s, strain 0.1%, gap 0.710 mm at 27°C: (a)  $\Delta G'(\omega)$ , (b)  $\Delta G''(\omega)$  when  $G'_0 = 343,330$  Pa and  $G''_0 = 35,323$  Pa.

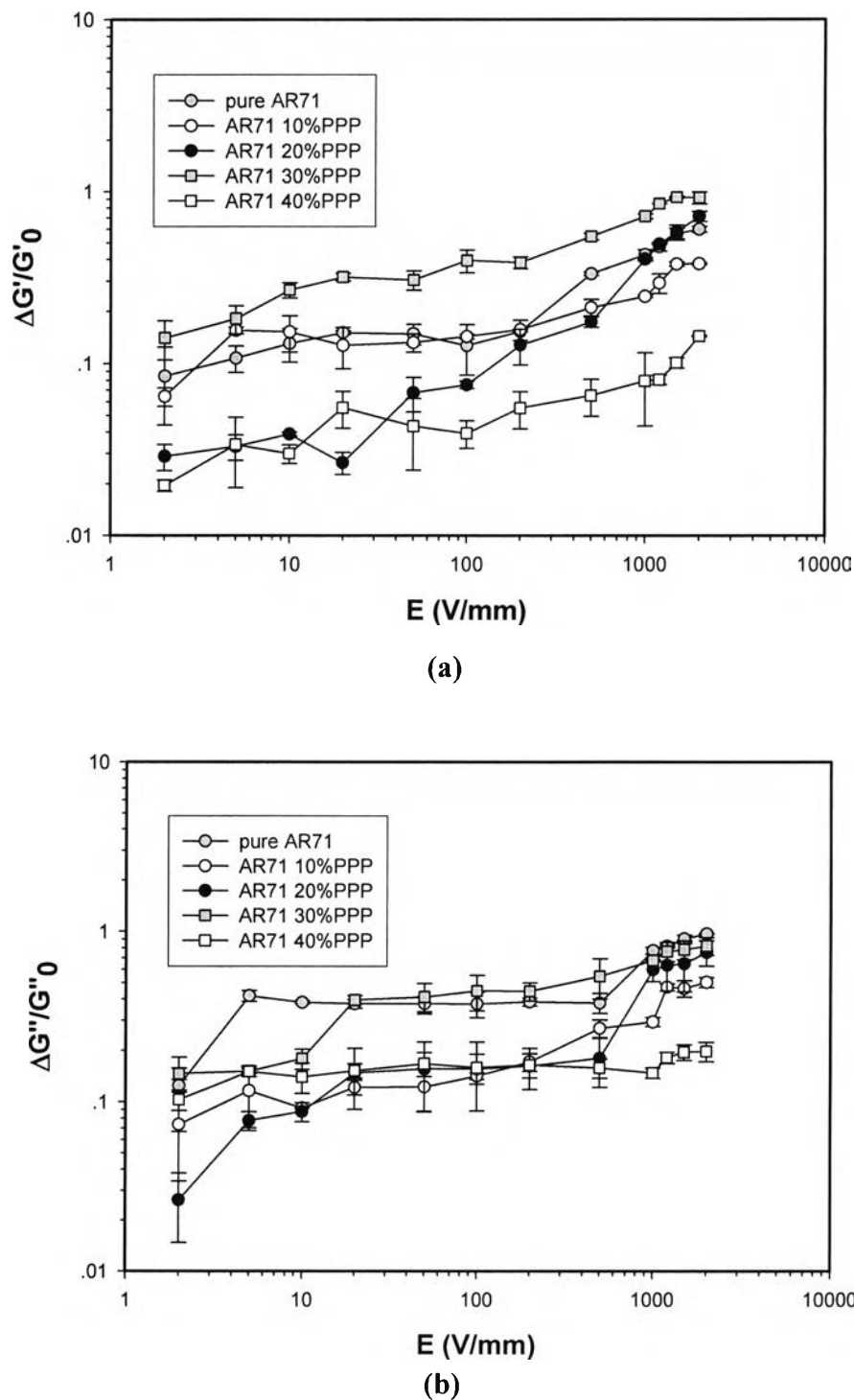


**Figure L13** Sensitivity of the polymer blends between AR71 and PPP at various PPP ratios, 27°C, various electric field strength, frequency 1 rad/s: (a)  $\Delta G'/G'_0$ ; (b)  $\Delta G''/G''_0$ .

## Appendix M Dielectric Constant Measurements

The dielectric constant values of all elastomers and blends were measured by an LCR meter (HP, model 4284A) connected to the rheometer (Rheometric Scientific, ARES) with a 25 mm parallel plate fixture. The thickness of the specimens is typically 1 mm and the diameter is about 25 mm. The top and bottom sides of the specimens were coated with silver adhesive to improve the electrical contact between the specimens and the electrodes. The measurements were carried at temperatures between 300 and 370 K. AC voltage applied was varied between 1 and 10 V, depending on materials. The dielectric constant at a frequency of 20 Hz will be referred to as the dielectric constant of the materials.

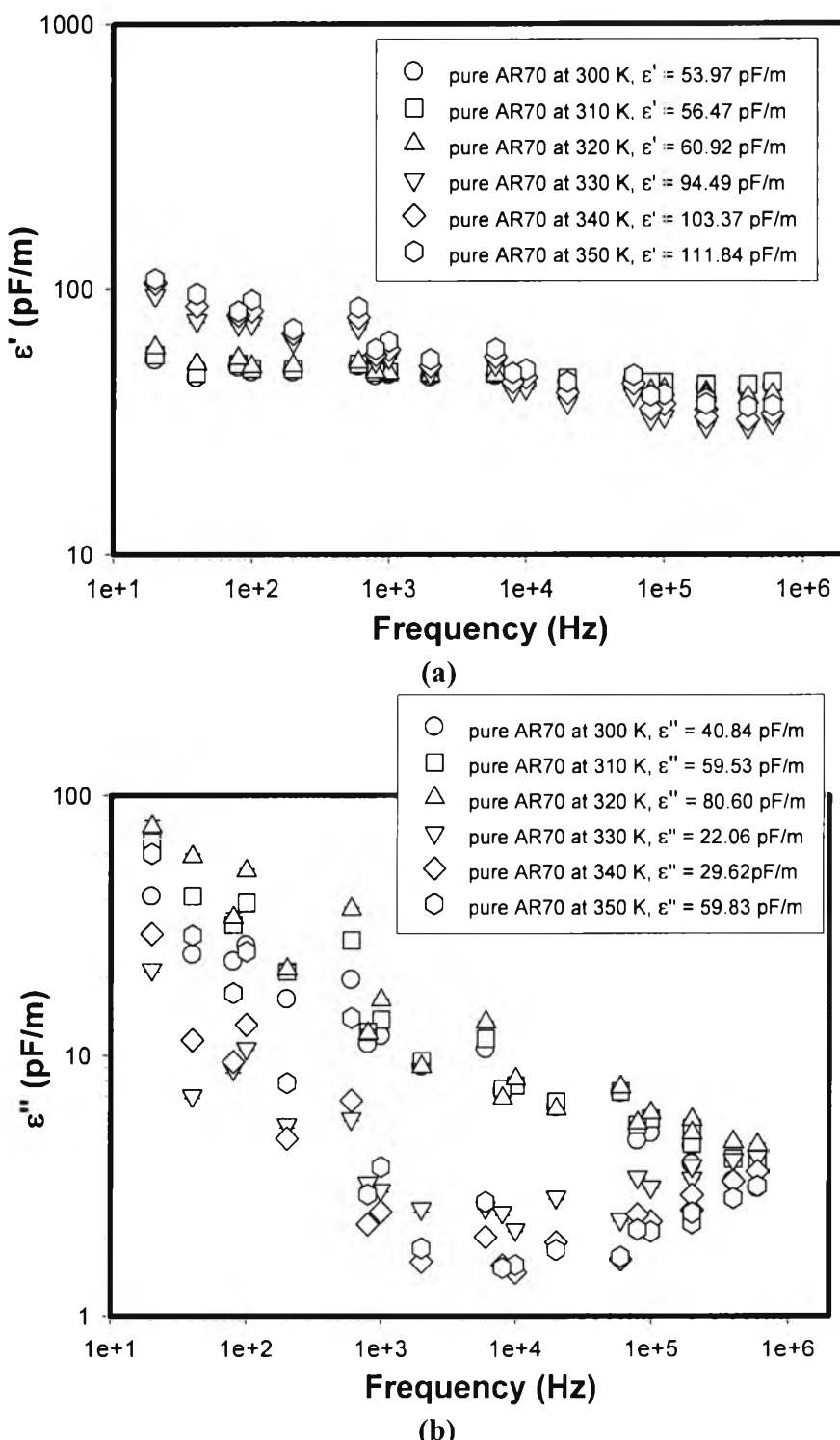


**Figure M1** Dielectric analysis of pure AR70 matrices at various temperatures, gap = 1.130 mm, E = 1 V, with silver coating: (a) dielectric constant vs. frequency; (b) dielectric loss factor vs. frequency.

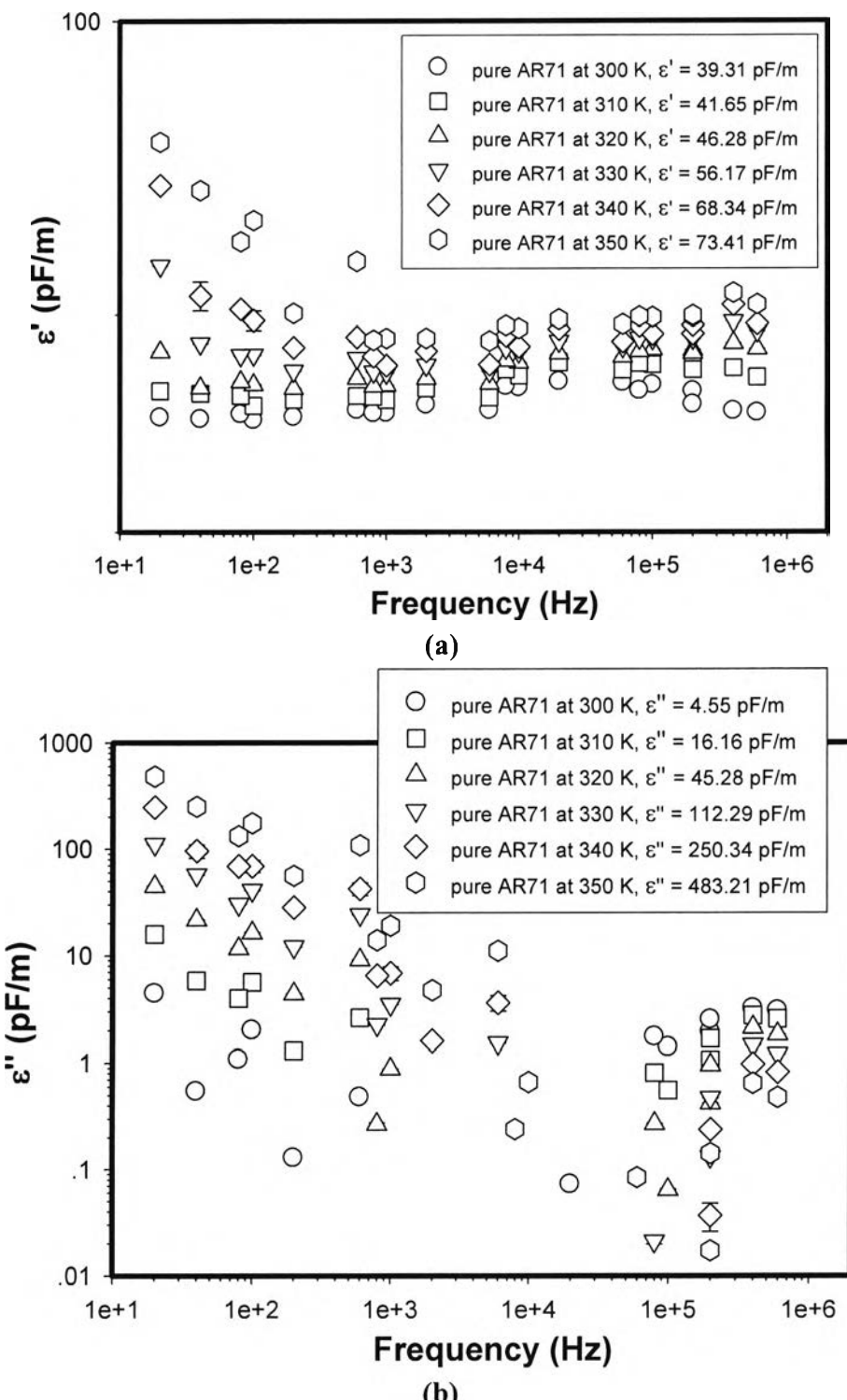


**Figure M2** Dielectric analysis of pure AR71 matrices at various temperatures, gap = 0.850 mm, E = 5 V, without silver coating: (a) dielectric constant vs. frequency; (b) dielectric loss factor vs. frequency.

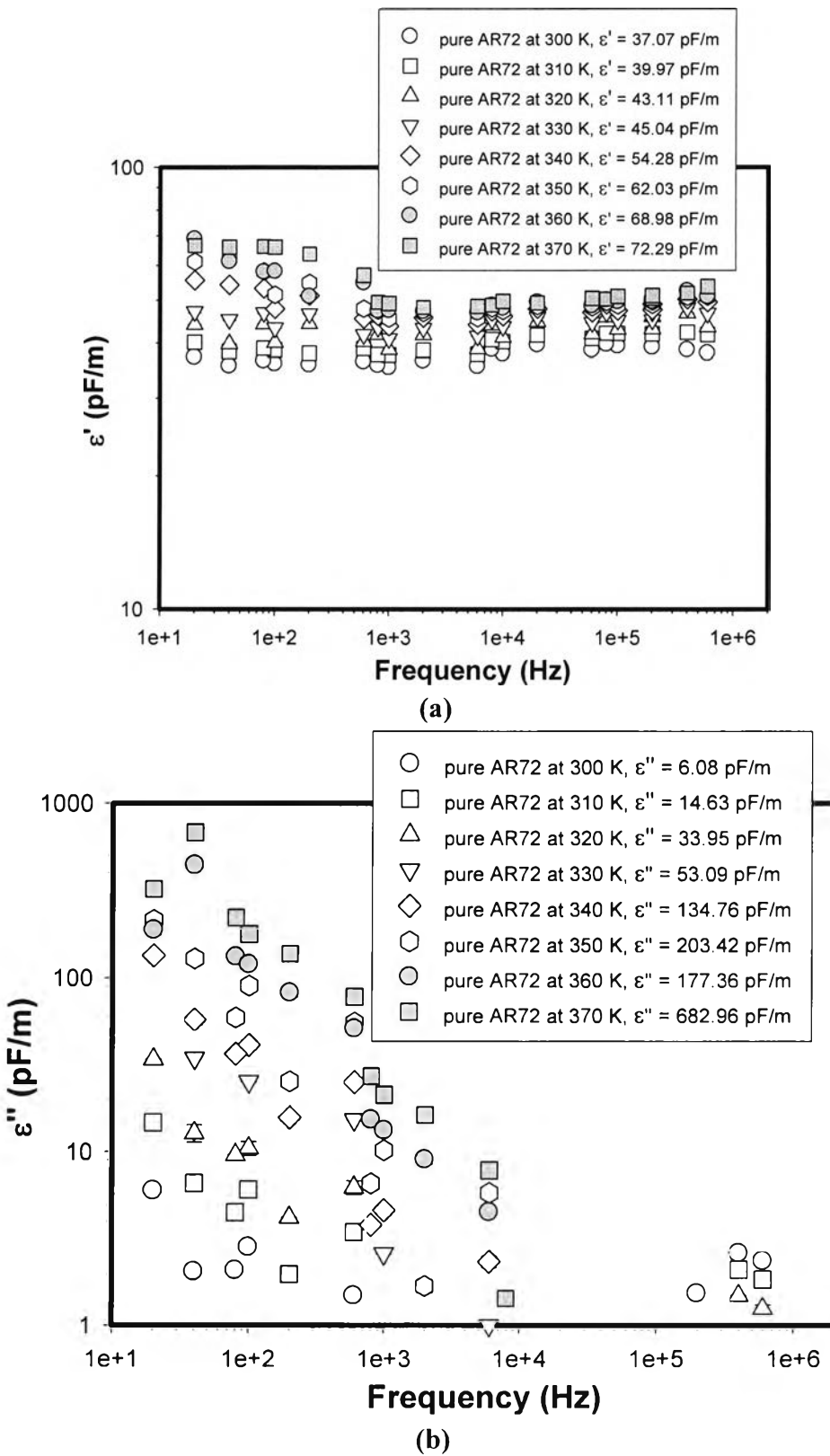


**Figure M3** Dielectric analysis of pure AR72 matrices at various temperatures, gap = 0.715 mm, E = 10 V, without silver coating: (a) dielectric constant vs. frequency; (b) dielectric loss factor vs. frequency.

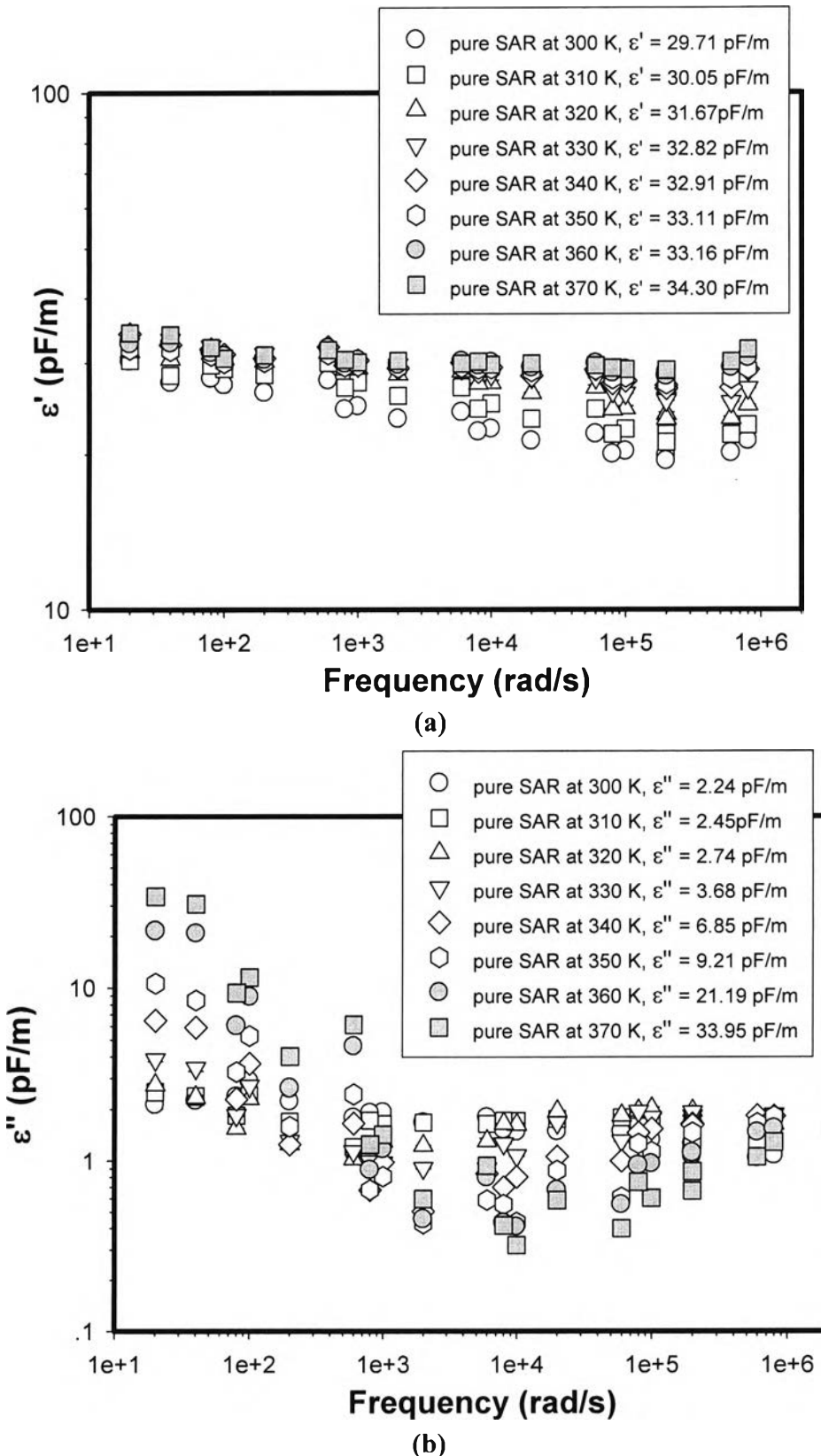


**Figure M4** Dielectric analysis of pure SAR matrices at various temperatures, gap = 0.380 mm, V = 5 V: (a) dielectric constant vs. frequency; (b) dielectric loss factor vs. frequency.

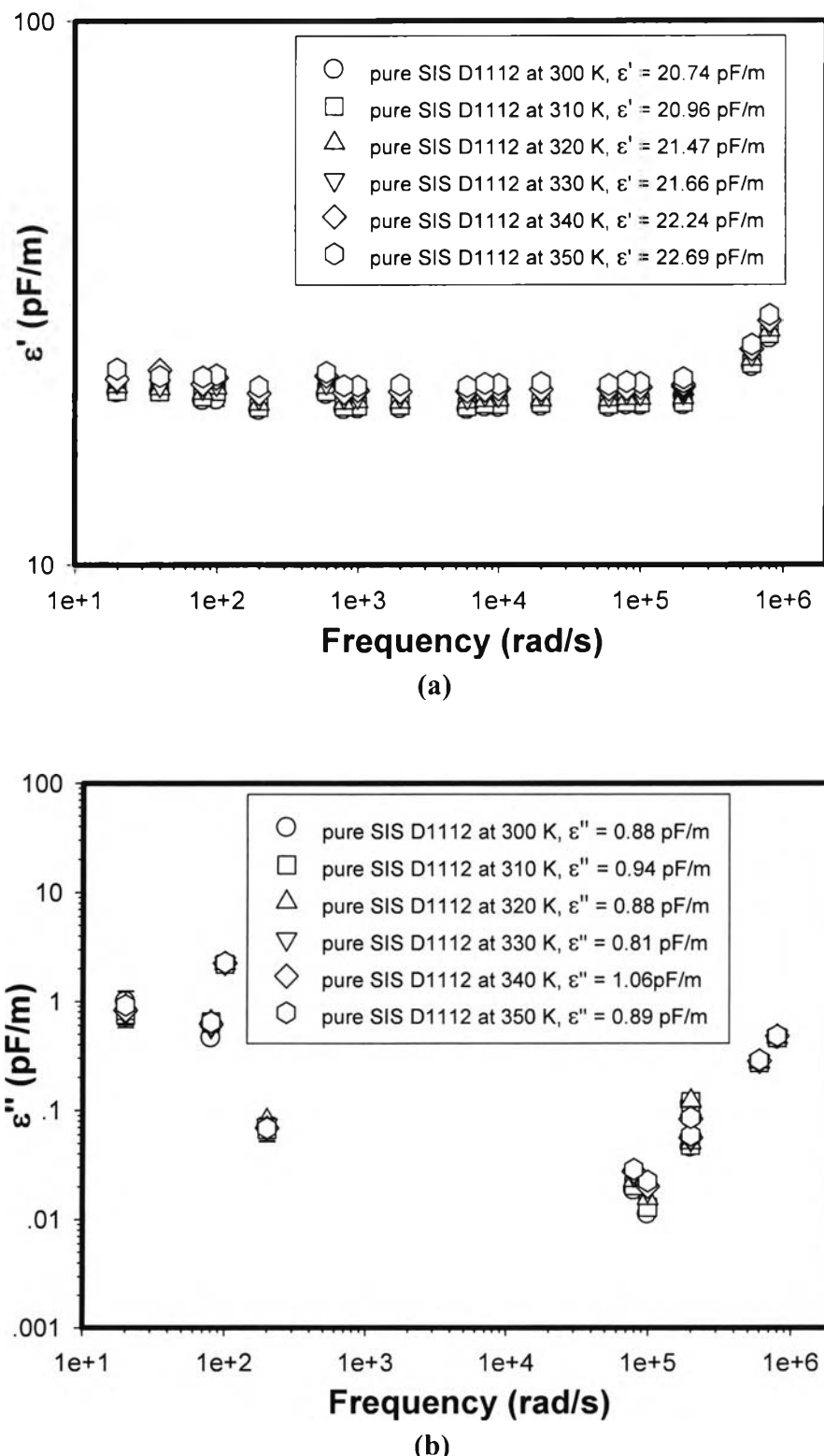
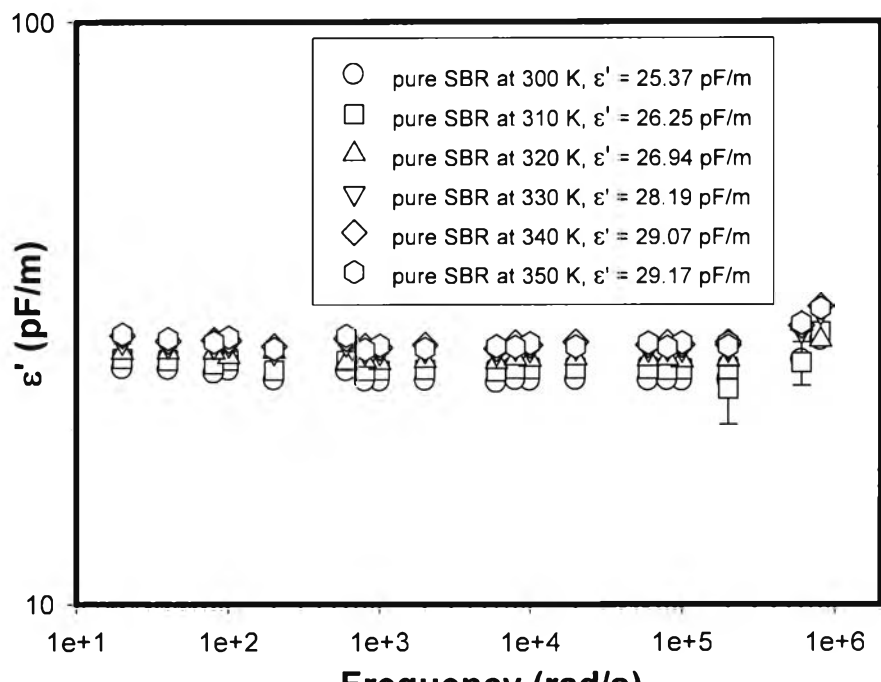
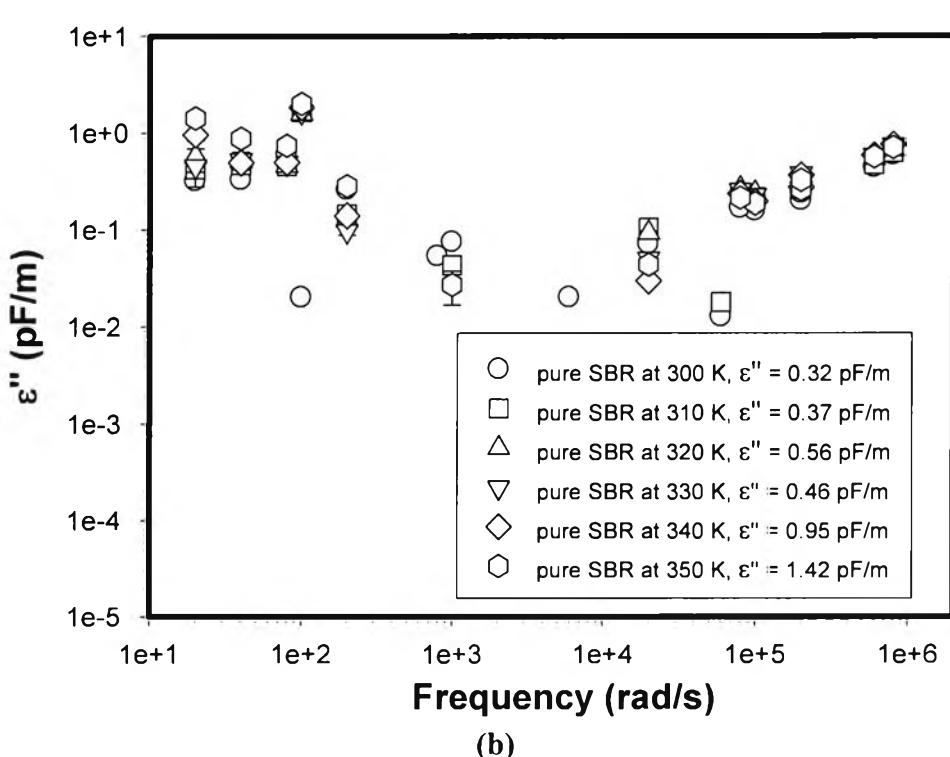


**Figure M5** Dielectric analysis of pure SIS matrices at various temperatures, gap = 0.710 mm, V = 1 V: (a) dielectric constant vs. frequency; (b) dielectric loss factor vs. frequency.



(a)



(b)

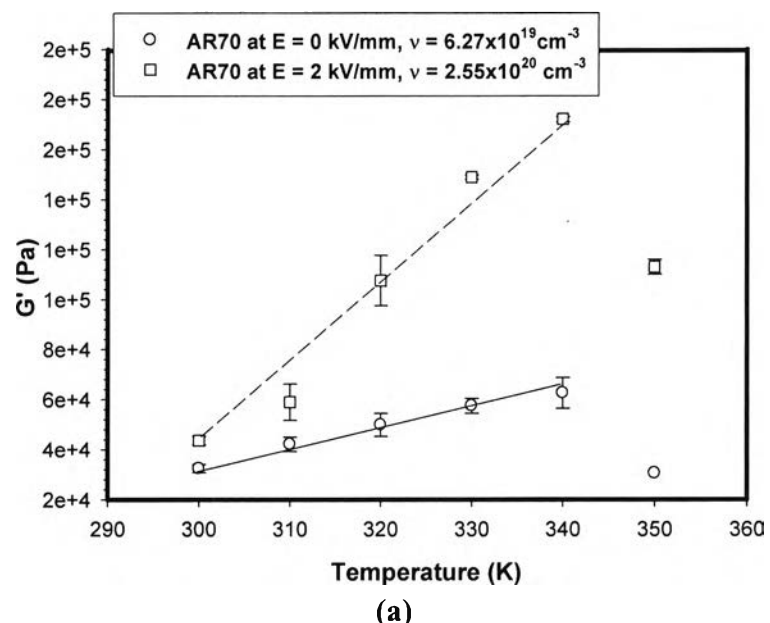
**Figure M6** Dielectric analysis of pure SBR matrices at various temperatures, gap = 0.440 mm, V = 1 V: (a) dielectric constant vs. frequency; (b) dielectric loss factor vs. frequency.

**Appendix N Electrical Conductivity of the Elastomers at Various Temperatures**

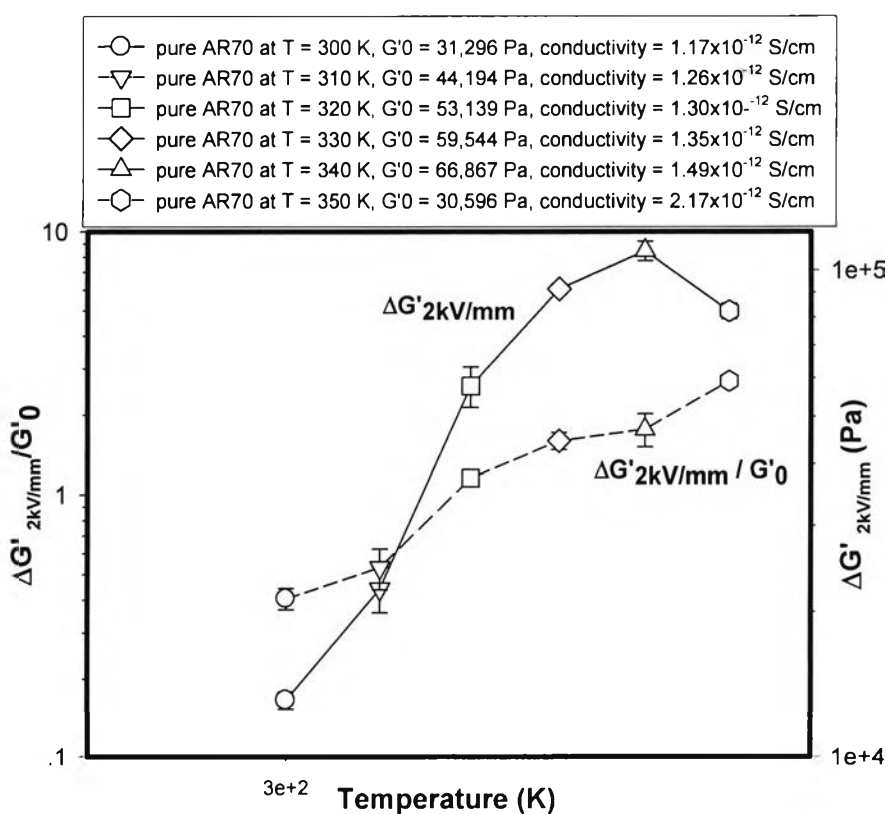
**Table N1** The conductivity value of the elastomers at various temperatures

<b>Temperature (K)</b>	<b>Conductivity of various types of elastomer (S/cm)</b>					
	<b>AR70</b>	<b>AR71</b>	<b>AR72</b>	<b>SAR</b>	<b>SIS D1112</b>	<b>SBR</b>
<b>300</b>	1.17E-12	4.39E-12	2.87E-12	1.27E-10	2.05E-18	1.47E-15
<b>310</b>	1.26E-12	4.58E-12	2.96E-12	1.45E-10	2.27E-18	1.93E-15
<b>320</b>	1.30E-12	5.44E-12	3.02E-12	1.63E-10	2.66E-18	1.98E-15
<b>330</b>	1.35E-12	7.19E-12	3.04E-12	2.18E-10	2.51E-18	1.99E-15
<b>340</b>	1.49E-12	7.21E-12	3.03E-12	3.85E-10	2.42E-18	2.01E-15
<b>350</b>	2.17E-12	1.01E-11	3.04E-12	7.24E-10	2.30E-18	2.03E-15
<b>360</b>	-	-	2.91E-12	-	2.34E-18	2.03E-15
<b>370</b>	-	-	2.85E-12	-	-	1.91E-15

**Appendix O Electrorheological Properties of the Elastomers at Various Temperatures**



(a)



(b)

**Figure O1** Effect of temperature of the AR70: (a) the storage modulus ( $G'$ ) at  $E = 0$  and  $2$  kV/mm at various temperatures using one sample for all temperatures tested; (b) the sensitivity of storage modulus ( $\Delta G'/G'_0$ ) vs. temperature and the storage modulus response  $\Delta G'$  at  $E = 2$  kV/mm ( $\Delta G'$  at  $2$  kV/mm) vs. temperature.

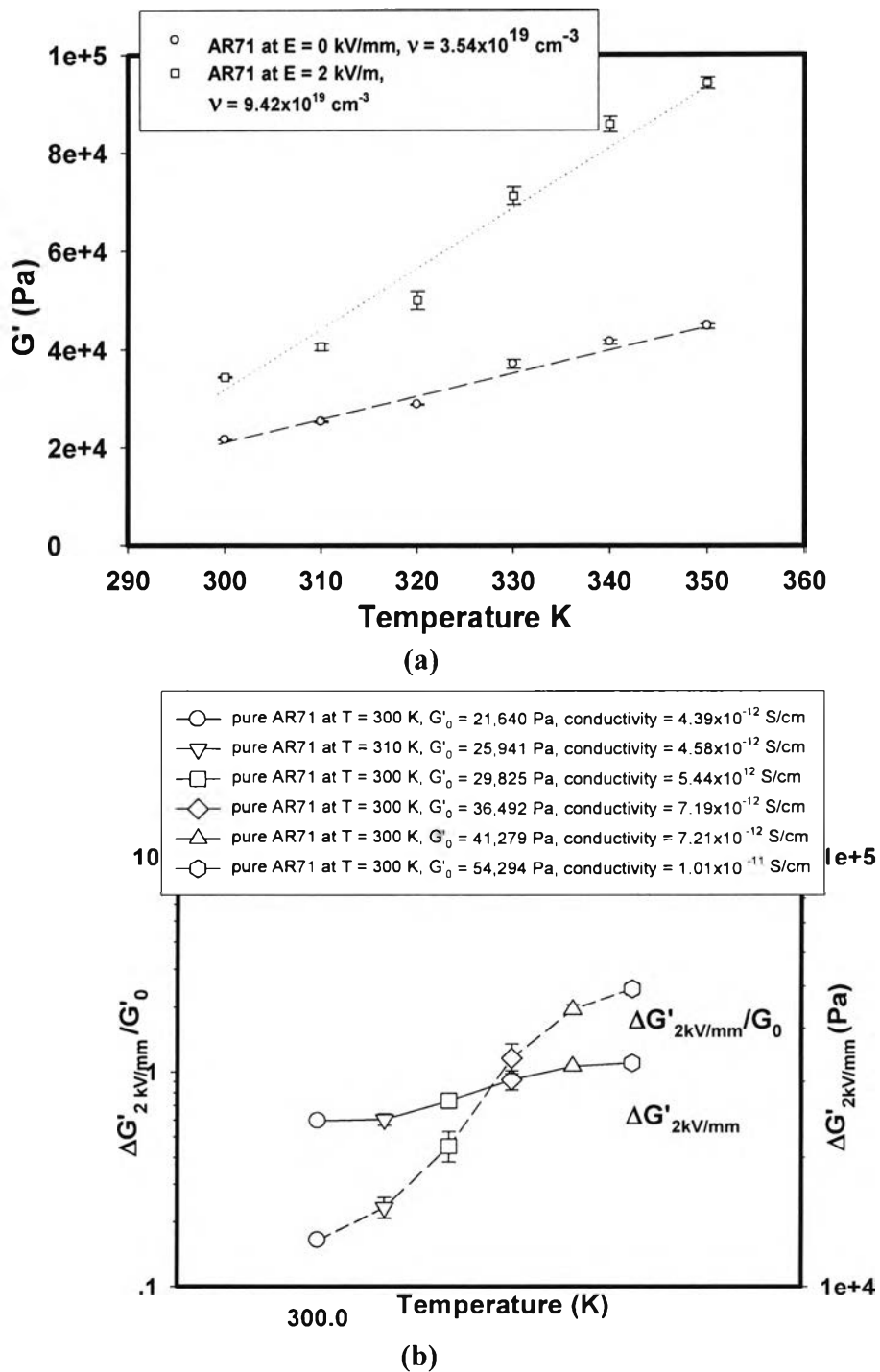


**Figure O2** Effect of temperature for the AR71 on: (a) the storage modulus ( $G'$ ) at  $E = 0$  and 2 kV/mm at various temperatures for one sample at all temperatures tested; (b) the sensitivity of storage modulus ( $\Delta G'/G'_0$ ) vs. temperature and the storage modulus response  $\Delta G$  at  $E = 2$  kV/mm ( $\Delta G'_{2\text{kV/mm}}$ ) vs. temperature.

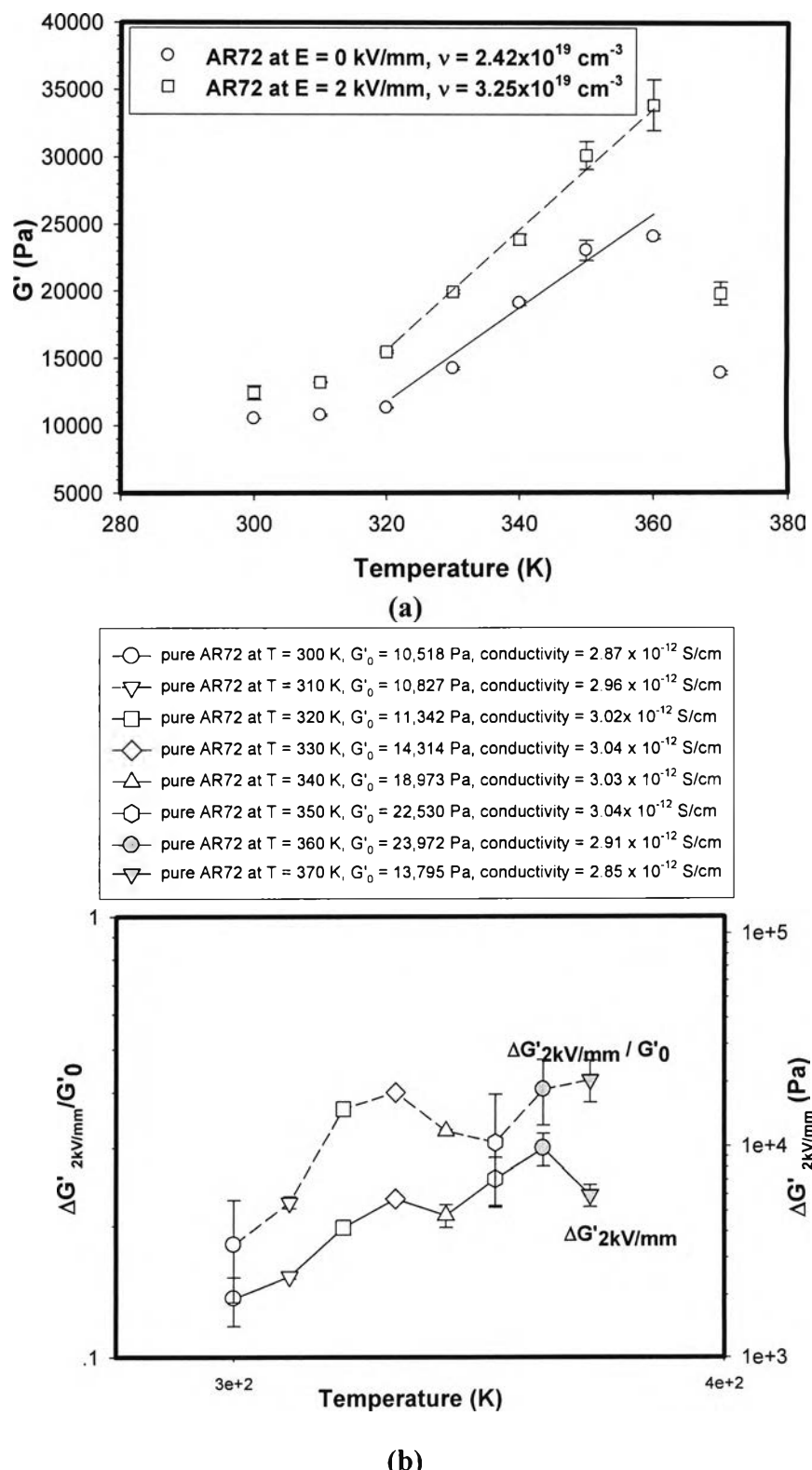


**Figure O3** Effect of temperature of the AR72: (a) the storage modulus ( $G'$ ) at  $E = 0$  and 2 kV/mm at various temperatures using one sample for all temperatures tested;

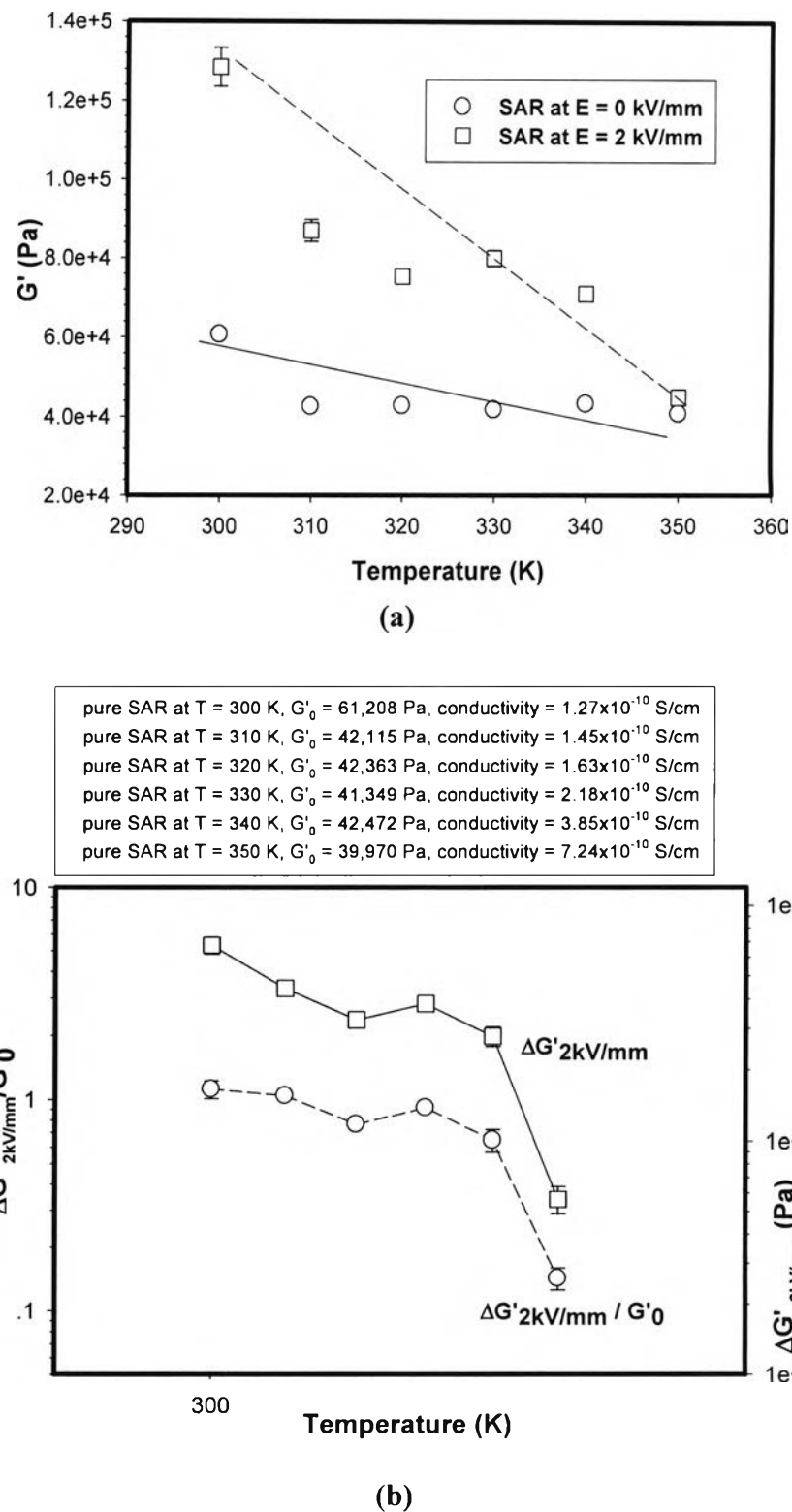


**Figure O4** Effect of temperature of the SAR: (a) the storage modulus ( $G'$ ) at  $E = 0$  and  $2 \text{ kV/mm}$  at various temperatures using one sample for all temperatures tested; (b) the sensitivity of storage modulus ( $\Delta G'/G'_0$ ) vs. temperature and the storage modulus response  $\Delta G'$  at  $E = 2 \text{ kV/mm}$  ( $\Delta G'_{2\text{kV/mm}}$ ) vs. temperature.

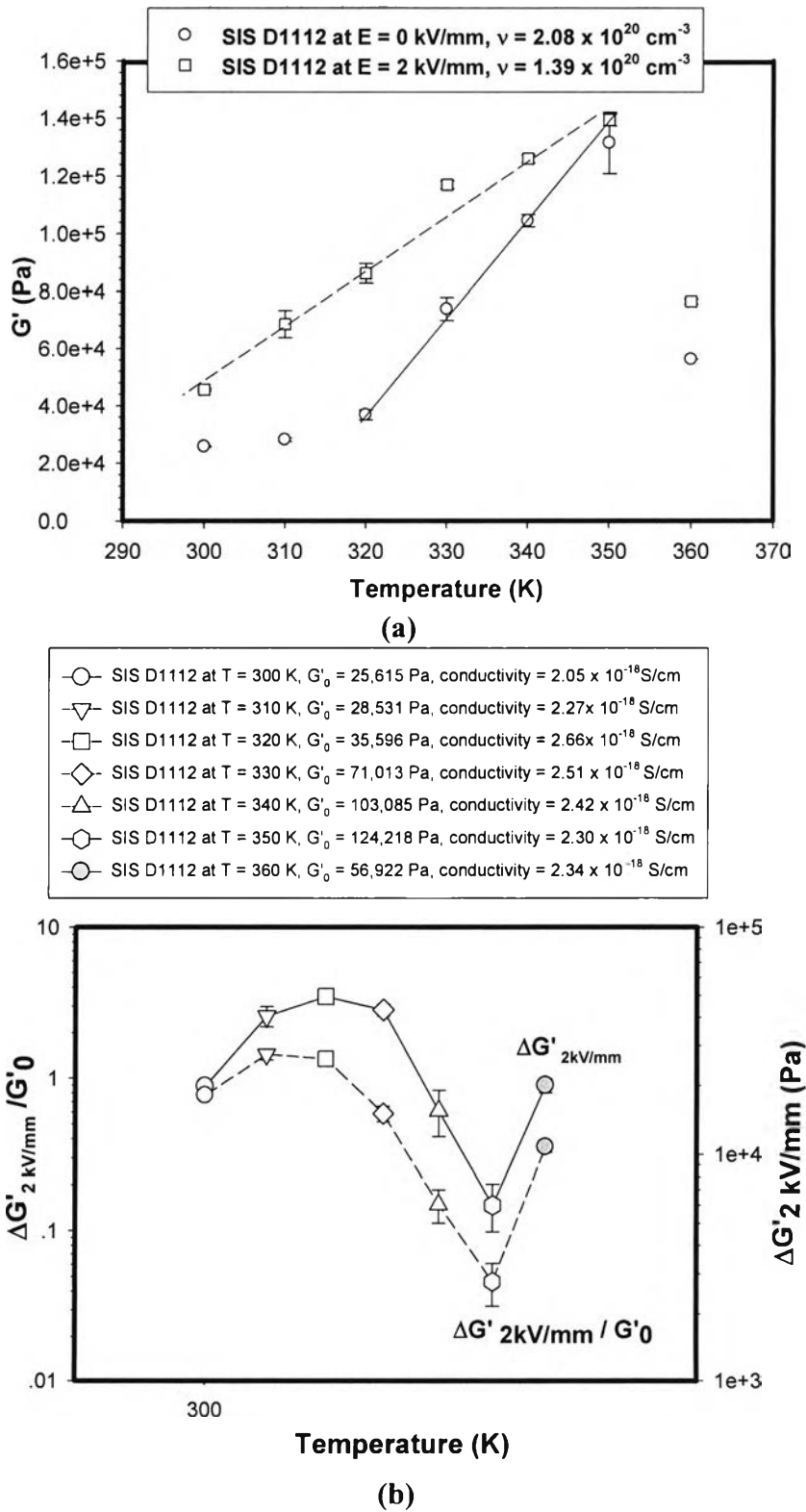


**Figure 05** Effect of temperature of the SIS D1112: (a) the storage modulus ( $G'$ ) at  $E = 0$  and 2 kV/mm at various temperatures using one sample for all temperatures tested; (b) the sensitivity of storage modulus ( $\Delta G'/G'_0$ ) vs. temperature and the storage modulus response  $\Delta G'$  at  $E = 2$  kV/mm ( $\Delta G'_{2\text{kV/mm}}$ ) vs. temperature.

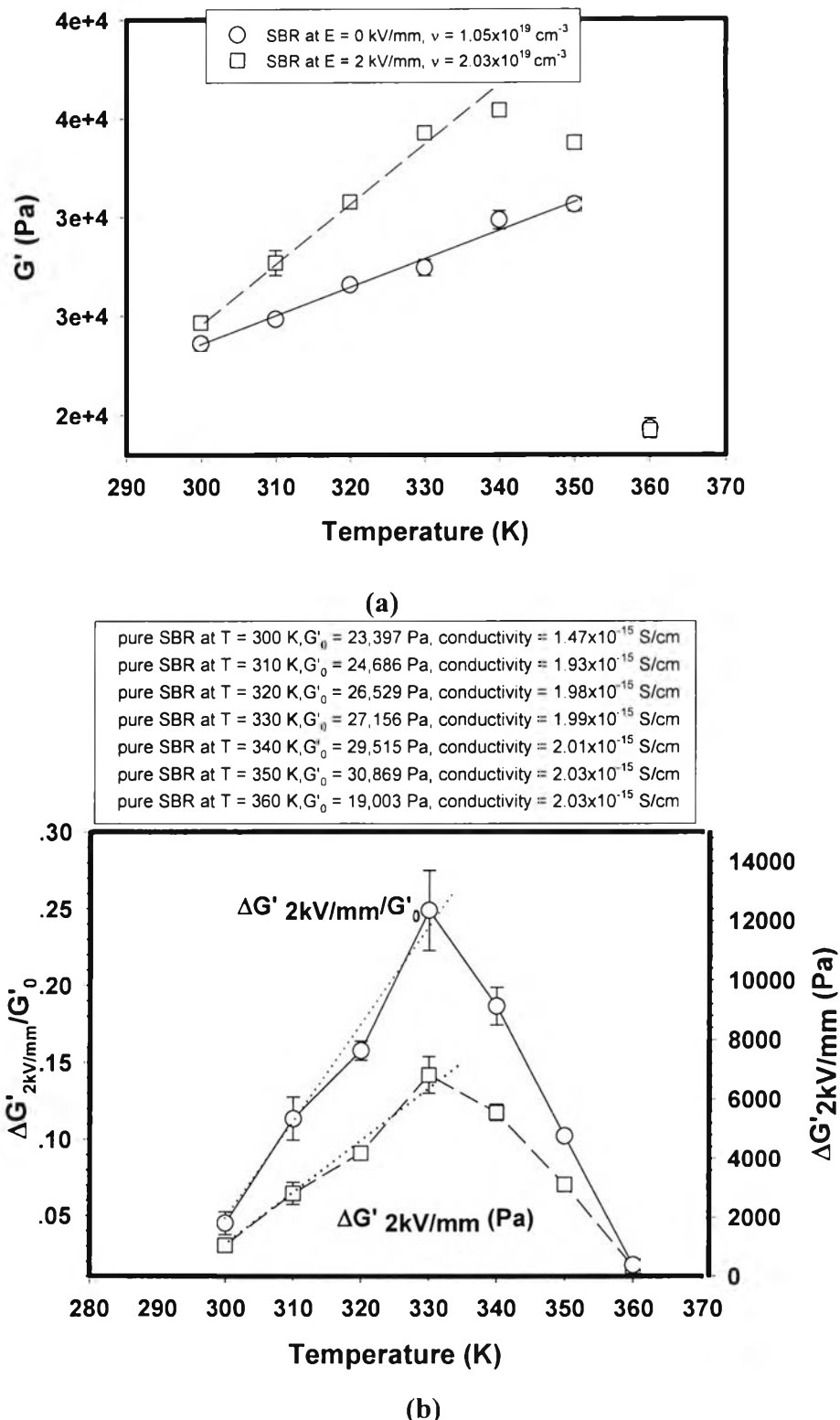


**Figure O6** Effect of temperature of the SBR: (a) the storage modulus ( $G'$ ) at  $E = 0$  and 2 kV/mm at various temperatures using one sample for all temperatures tested; (b) the sensitivity of storage modulus ( $\Delta G'/G'_0$ ) vs. temperature and the storage modulus response  $\Delta G'$  at  $E = 2$  kV/mm ( $\Delta G'_{2\text{kV/mm}}$ ) vs. temperature.

## Appendix P %Element of the Elastomers

The percentages of elements (Cu, Zn, Fe, Cl, Na, C, and O) in the elastomers were characterized and determined by an EDX (Energy Dispersive X-Ray Fluorescence Spectrometer, OXFORD Pentafet, model 6111); it was also connected to a scanning electron microscope (JEOL, model JSM-5200).

**Table P1** Elemental analysis of SAR/01 by EDX technique

<b>Element</b>	%Atomic				
	<b>1</b>	<b>2</b>	<b>3</b>	<b>average</b>	<b>SD</b>
C	78.31	78.14	78.22	78.22	0.09
O	20.70	20.89	20.45	20.68	0.22
Na	0.46	0.16	0.54	0.39	0.20
Cl	0.04	0.08	0.07	0.06	0.02
Fe	0.13	0.22	0.18	0.18	0.05
Cu	0.05	0.21	0.25	0.17	0.11
Zn	0.31	0.30	0.29	0.30	0.01

**Table P2** Elemental analysis of SAR/02 by EDX technique

<b>Element</b>	%Atomic				
	<b>1</b>	<b>2</b>	<b>3</b>	<b>average</b>	<b>SD</b>
C	78.64	77.99	76.97	77.87	0.84
O	20.64	21.17	22.52	21.44	0.97
Na	0.10	0.14	0.09	0.11	0.03
Cl	0.07	0.09	0.08	0.08	0.01
Fe	0.23	0.15	0.10	0.16	0.07
Cu	0.04	0.17	0.11	0.11	0.07
Zn	0.37	0.29	0.27	0.31	0.05

**Table P3** Elemental analysis of AR70/01 by EDX technique

Element	%Atomic				
	1	2	3	average	SD
C	65.67	67.28	65.95	66.30	0.81
O	33.87	32.22	33.49	33.19	0.86
Na	0.26	0.34	0.4	0.33	0.07
Cl	0.17	0.11	0.14	0.14	0.03
Fe	0.01	0.02	0.01	0.01	0.01
Cu	0.02	0.02	0.01	0.02	0.01
Zn	0.00	0.01	0.00	0.00	0.01

**Table P4** Elemental analysis of SIS/01 by EDX technique

Element	%Atomic				
	1	2	3	average	SD
C	99.85	99.88	99.77	99.83	0.06
O	0.09	0.05	0.09	0.08	0.02
Na	0.03	0.01	0.05	0.03	0.02
Cl	0.02	0.00	0.00	0.01	0.01
Fe	0.00	0.00	0.01	0.00	0.01
Cu	0.00	0.02	0.03	0.02	0.02
Zn	0.01	0.04	0.05	0.03	0.02

\*\*note

Scanning electron micrographs (JEOL, model JSM-5200)

Magnification = X2,000

Accelerating voltage = 20.00 kV

Element	%Atomic		
	SAR	AR70	SIS
C	78.22±0.09	66.30±0.81	99.83±0.06
O	20.68±0.22	33.19±0.86	0.08±0.02
Na	0.39±0.05	0.33±0.07	0.03±0.02
Cl	0.06±0.02	0.14±0.03	0.01±0
Fe	0.18±0.55	0.01±0	0.00±0
Cu	0.17±0.11	0.02±0	0.02±0
Zn	0.30±0.01	0.00±0	0.03±0

## Appendix Q Identification of Characteristic Peaks in FT-IR Spectrum of the Elastomers

The six elastomers were characterized by an FT-IR spectrometer in order to identify their functional groups. The FT-IR spectrometer (Thermo Nicolet, Nexus 670) was operated in absorption mode with 32 scans at resolution of  $\pm 4 \text{ cm}^{-1}$ , covering a wavenumber range between 400 and  $4,000 \text{ cm}^{-1}$ , using a deuterated triglycine sulfate detector. The specimens were prepared as thin films (thickness  $\approx 0.5 \text{ mm}$ ).

**Table Q1** FT-IR spectrum of acrylic elastomers (AR70)

Wavenumber ( $\text{cm}^{-1}$ )	Functional group	Wavenumber from references	Reference
2960	C-H stretching	3000	Gunzler <i>et al.</i>
1728	C=O stretching on ester group	1715	Lu <i>et al.</i>
1410	CO-CH <sub>2</sub>	1405	Lu <i>et al.</i>
1390	CH <sub>3</sub>	1380	Gunzler <i>et al.</i>
1260	(CH <sub>3</sub> ) <sub>3</sub> C	1255-1240	Amornsin <i>et al.</i>
1150	C-O on ester group	1200-1100	Gunzler <i>et al.</i>

**Table Q2** FT-IR spectrum of acrylic elastomers (AR71)

Wavenumber ( $\text{cm}^{-1}$ )	Functional group	Wavenumber from references	References
2990	C-H stretching	3000	Gunzler <i>et al.</i>
1728	C=O stretching on ester group	1715	Lu <i>et al.</i>
1410	CO-CH <sub>2</sub>	1405	Lu <i>et al.</i>
1380	CH <sub>3</sub>	1380	Gunzler <i>et al.</i>
1260	(CH <sub>3</sub> ) <sub>3</sub> C	1255-1240	Amornsin <i>et al.</i>
1155	C-O on ester group	1200-1100	Gunzler <i>et al.</i>
1040	O-CH <sub>2</sub> -C	1050	Gunzler <i>et al.</i>

**Table Q3** FT-IR spectrum of acrylic elastomers (AR72)

<b>Wavenumber (cm<sup>-1</sup>)</b>	<b>Functional group</b>	<b>Wavenumber from references</b>	<b>References</b>
2960	C-H stretching	3000	Gunzler <i>et al.</i>
1730	C=O stretching on ester group	1715	Lu <i>et al.</i>
1415	CO-CH <sub>2</sub>	1405	Lu <i>et al.</i>
1260	(CH <sub>3</sub> ) <sub>3</sub> C	1255-1240	Amornsin <i>et al.</i>
1160	C-O on ester group	1200-1100	Gunzler <i>et al.</i>
1050	O-CH <sub>2</sub> -C	1050	Gunzler <i>et al.</i>

**Table Q4** FT-IR spectrum of styrene-acrylic copolymer (SAR)

<b>Wavenumber (cm<sup>-1</sup>)</b>	<b>Functional group</b>	<b>Wavenumber from references</b>	<b>References</b>
2980	C-H stretching	3000	Gunzler <i>et al.</i>
1728	C=O stretching on ester group	1715	Lu <i>et al.</i>
1470	C=C vibration on benzene ring	1500-1430	Gunzler <i>et al.</i>
1160	C-O on ester group	1200-1100	Gunzler <i>et al.</i>
764	C-H stretching on mono-substituted benzene ring	751 <sub>±</sub> 15	Gunzler <i>et al.</i>
702	C-H stretching on mono-substituted benzene ring	697 <sub>±</sub> 11	Gunzler <i>et al.</i>

**Table Q5** FT-IR spectrum of styrene-isoprene-styrene triblock copolymer (SIS)

<b>Wavenumber (cm<sup>-1</sup>)</b>	<b>Functional group</b>	<b>Wavenumber from references</b>	<b>References</b>
2960, 2930, 2860	C-H stretching on -CH <sub>2</sub> -	3000-2900	Gunzler <i>et al.</i>
1450	C=C vibration on benzene ring	1500-1430	Gunzler <i>et al.</i>
1380	CH <sub>3</sub>	1380	Gunzler <i>et al.</i>
1100-1020	C-O on ester group	1200-1100	Gunzler <i>et al.</i>
889	di- substituted of isoprene	895-885	Gunzler <i>et al.</i>
760	C-H stretching on mono-substituted benzene ring	751 <sub>±</sub> 15	Gunzler <i>et al.</i>
698	C-H stretching on mono-substituted benzene ring	697 <sub>±</sub> 11	Gunzler <i>et al.</i>

**Table Q6** FT-IR spectrum of styrene-butadiene rubber (SBR)

<b>Wavenumber (cm<sup>-1</sup>)</b>	<b>Functional group</b>	<b>Wavenumber from references</b>	<b>References</b>
3003	Mono-substituted of butadiene		Gunzler <i>et al.</i>
2980-2900	C-H stretching on -CH <sub>2</sub> -	3000-2900	Gunzler <i>et al.</i>
1620-1600	C-C stretching on mono-substituted of benzene ring	1600-1585	Gunzler <i>et al.</i>
1450	C=C vibration on benzene ring	1500-1430	Gunzler <i>et al.</i>
1020	=CH-R on butadiene	1010	Gunzler <i>et al.</i>
966	1,2 tran- C-H wagging of butadiene	970	Gunzler <i>et al.</i>
760	C-H stretching on mono-substituted benzene ring	751 <sub>±</sub> 15	Gunzler <i>et al.</i>
698	C-H stretching on mono-substituted benzene ring	697 <sub>±</sub> 11	Gunzler <i>et al.</i>

**\*\*\*note**

- X. Lu, C. Tan, J. Xu, and C. He, Synthetic Metals, 138, p.429-440, 2003
- H. Gunzler, H-U Gremlich, IR Spectroscopy, Wiley-VCH.
- M. Amornsin, A. Petchsom, Principles and Techniques of Instrumental Analysis, Chulalongkorn University.

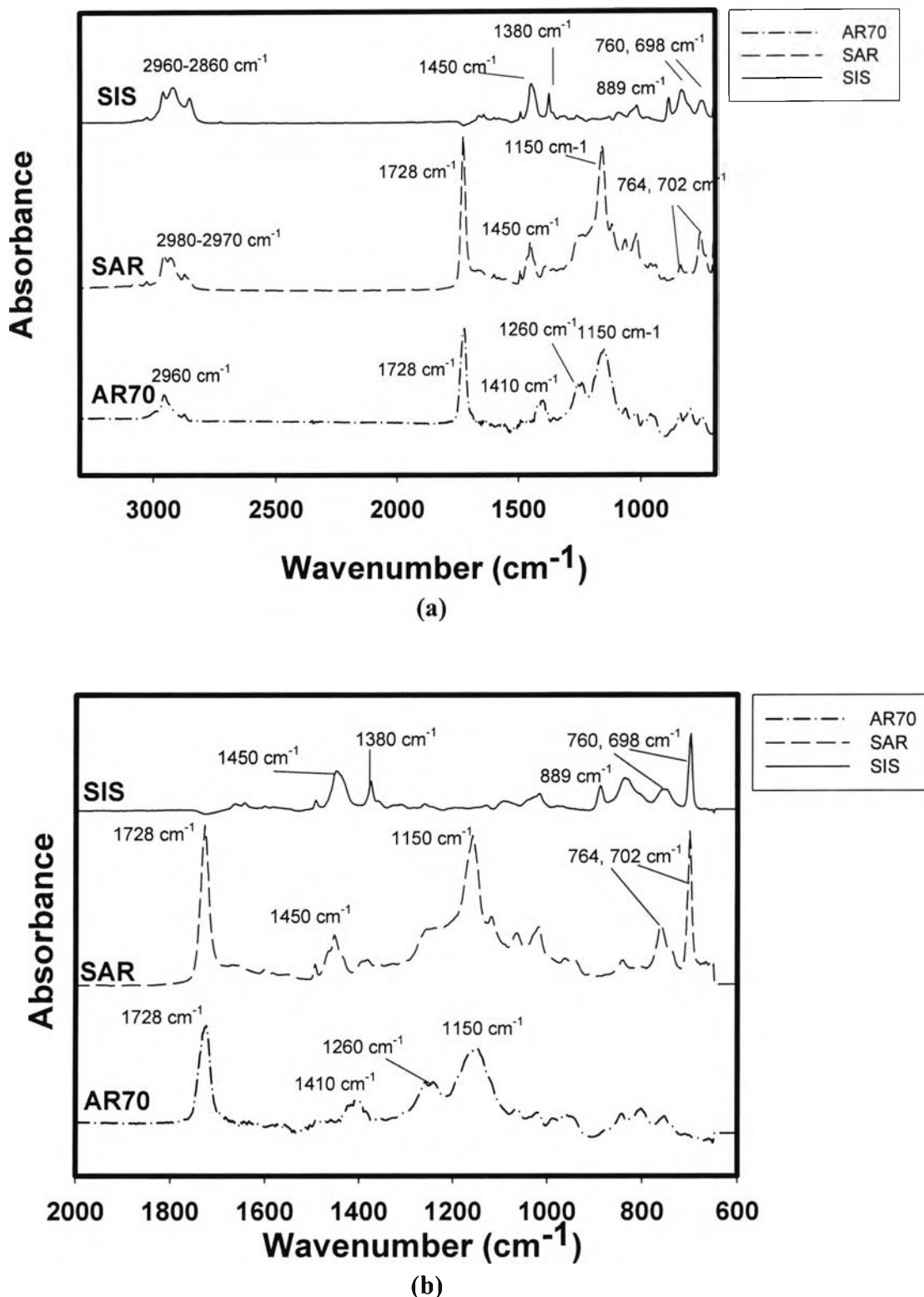
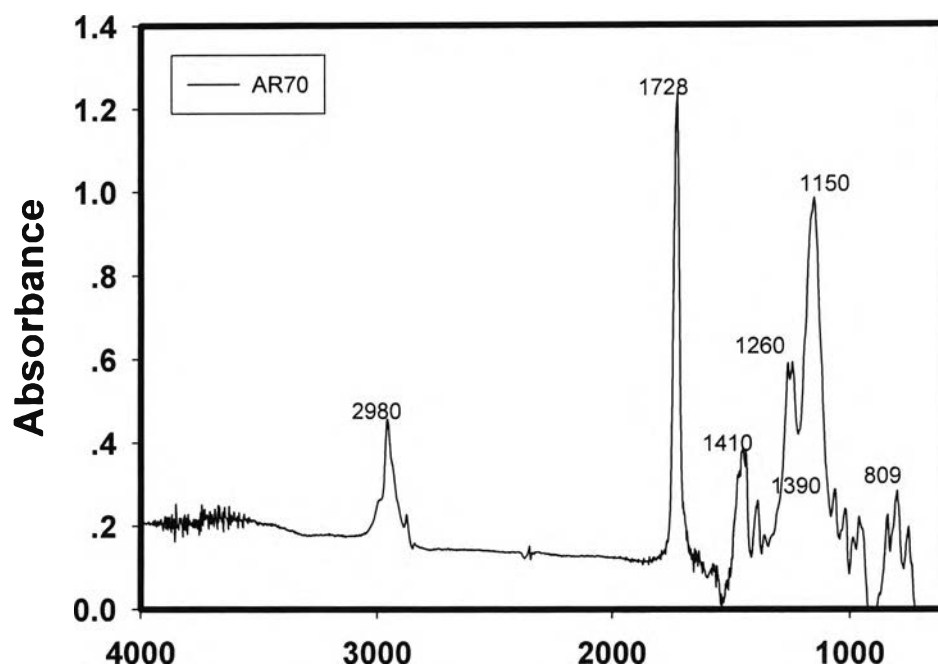
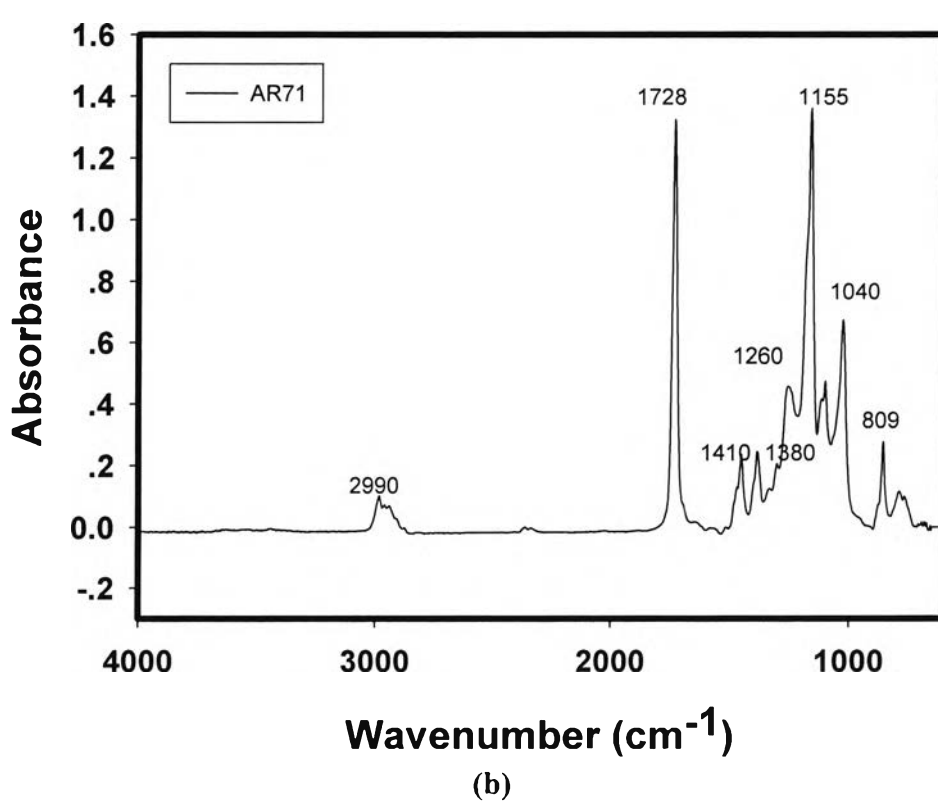


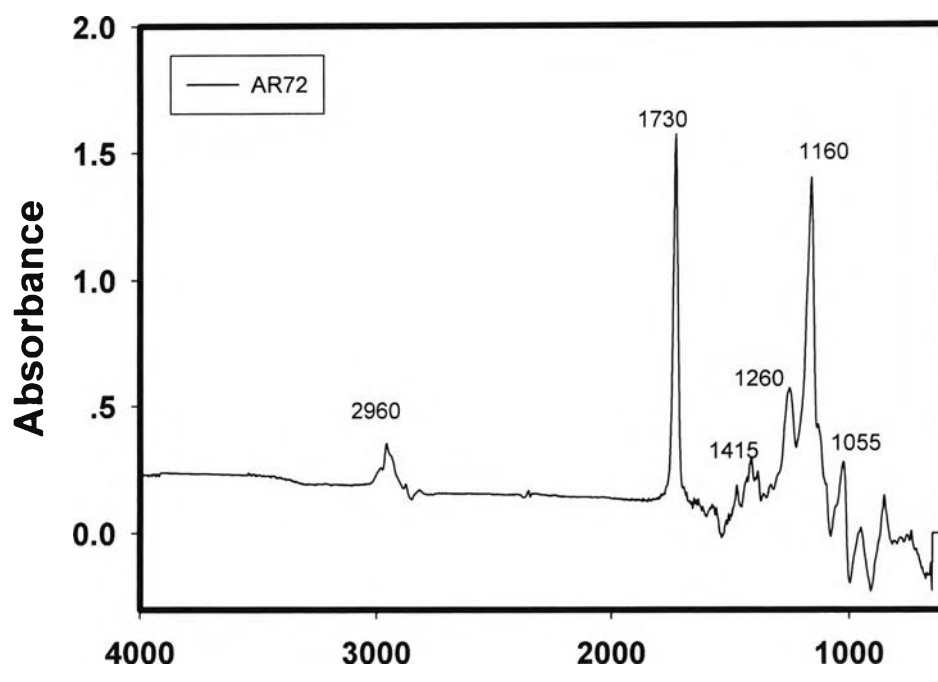
**Figure Q1** FT-IR spectra of acrylic elastomers (AR70), styrene-acrylic copolymer (SAR) and styrene-isoprene-styrene triblock copolymer: (a) wavenumber between 600-3500  $\text{cm}^{-1}$ ; (b) wavenumber between 600-2000  $\text{cm}^{-1}$ .



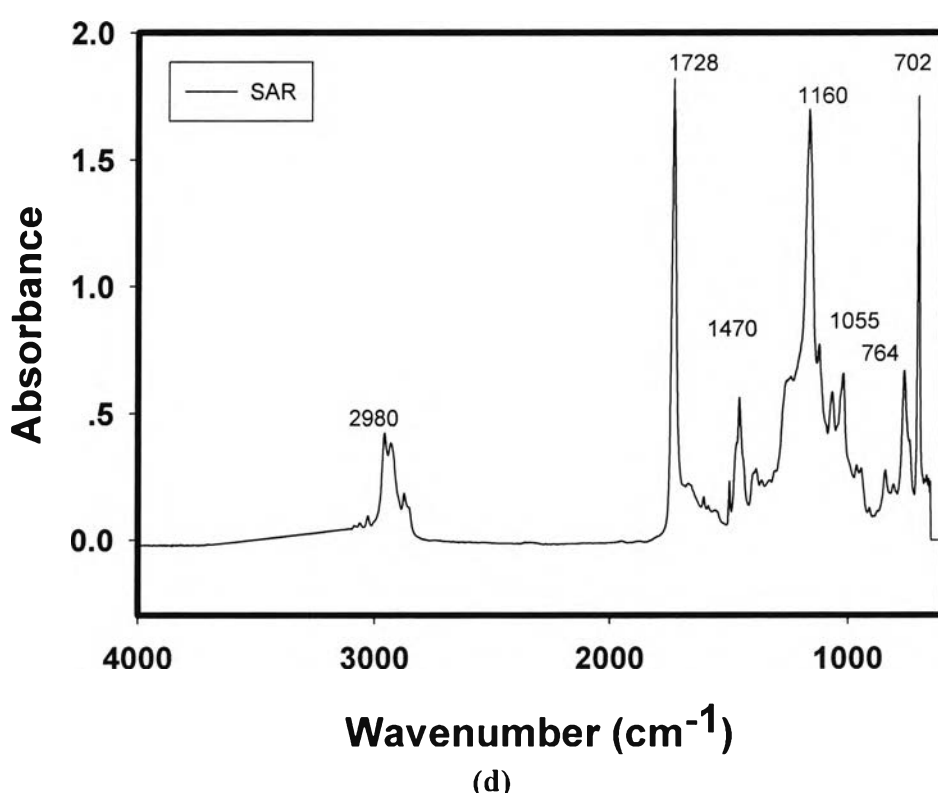
(a)



(b)



(c)



(d)

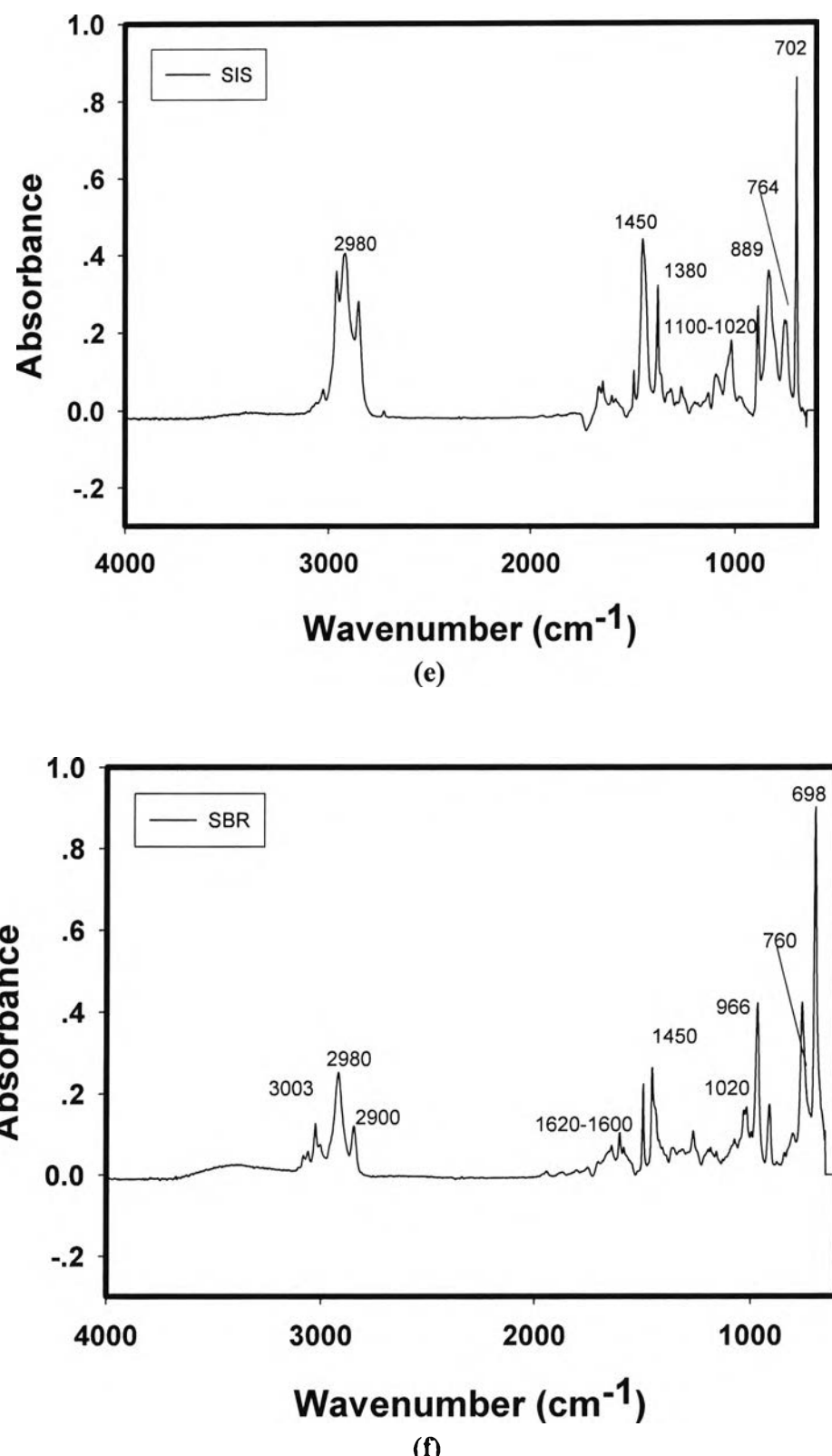


**Figure Q2** FT-IR spectra of the elastomers: (a) AR70; (b) AR71; (c) AR72; (d) SAR; (e) SIS and; (f) SBR.

## Appendix R Deflection Distance, Angle and Dielectrophoresis Force of the Six Elastomers under DC Electric Field

The dielectrophoresis forces were determined by measuring the deflection distances of the elastomers in the vertical cantilever fixture under electric field. The specimens were vertically immersed in the silicone oil (viscosity = 100 cSt) between parallel copper electrode plates (40 mm long, 30 mm width, and 1 mm thick). The gap between the pair of electrodes was 30 mm. A DC voltage was applied with a DC power supply (Goldsun, GPS 3003B) connected to a high voltage power supply (Gamma High Voltage, model UC5-30P and UC5-30N) which can deliver an electric field up to 25 kV. The output voltage from the high voltage power supply was calibrated using a Fluke 40 kV High Voltage Probe. We used a CCD video camera to record the movement during the experiment. Still pictures were captured from the video and the deflection distances in x (d) and y axes (l) at the ends of the specimen were determined by using Scion Image software (version 4.0.3). The electric field strength was varied between 0–600 V/mm at room temperature,  $300 \pm 1$  K. Both the voltage and the current were monitored. We calculated the resisting elastic force of the specimens under electric field using the non-linear deflection theory of a cantilever (Timoshenko et al.) and (Kim et al., 2007), which can be calculated from

the standard curve between  $\frac{F_e l_0^2}{EI}$  and  $\frac{d}{l_0}$  ( $l_0$  = initial length of specimens)

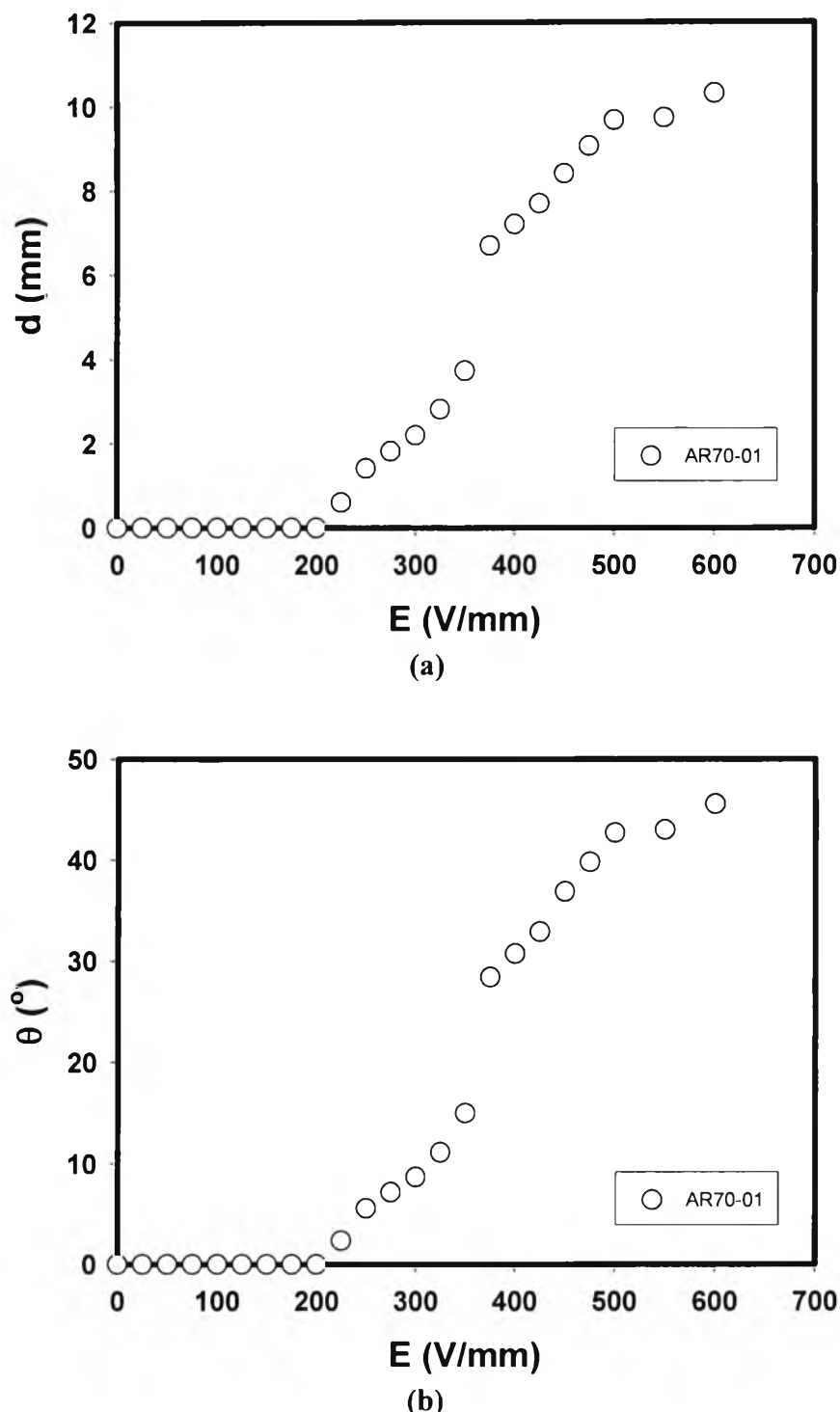
(Timoshenko et al.).

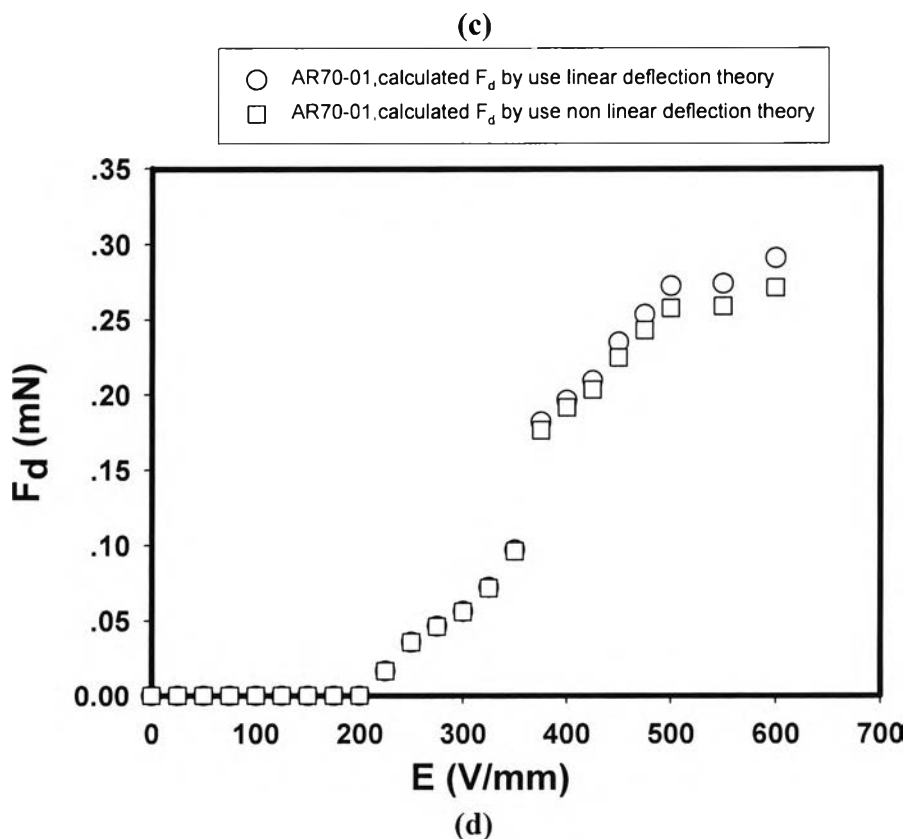
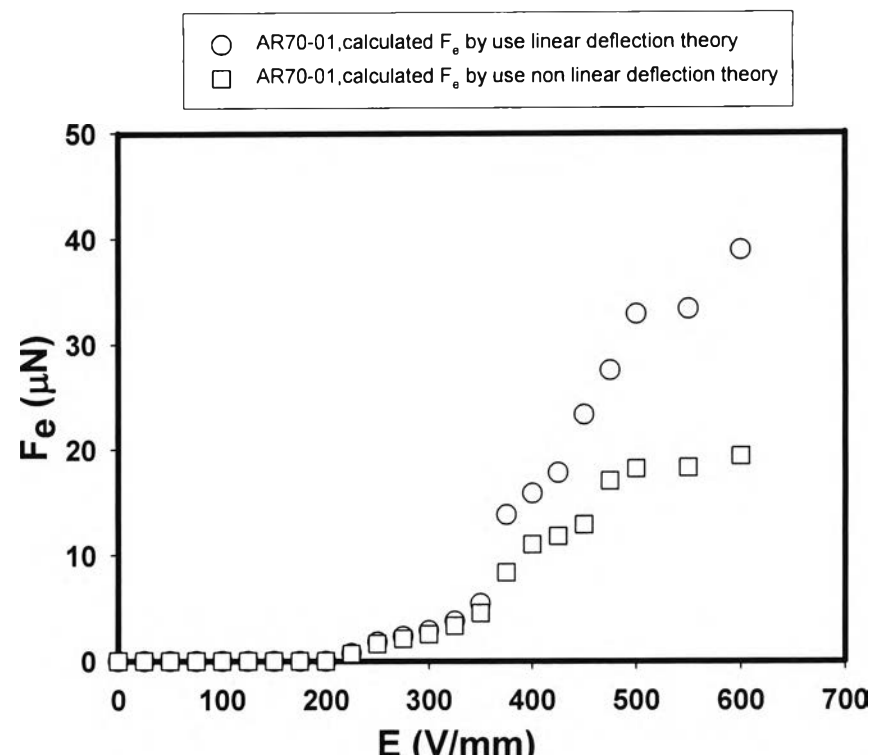
where  $F_e$  is the elastic force,  $d$  is the deflection distance in the horizontal axis,  $l$  is the deflection distance in the vertical axis,  $E$  is the Young's modulus —which is equal to  $2G(1+v)$ , where  $G$  is the shear storage modulus taken to be  $G'(\omega = 1 \text{ rad/s})$  at various electric field strengths and,  $v$  is the Poisson's ratio (0.5 for an incompressible sample)— and  $I$  is the moment of inertia  $\frac{1}{12}t^3w$ , where  $t$  is the thickness of the film

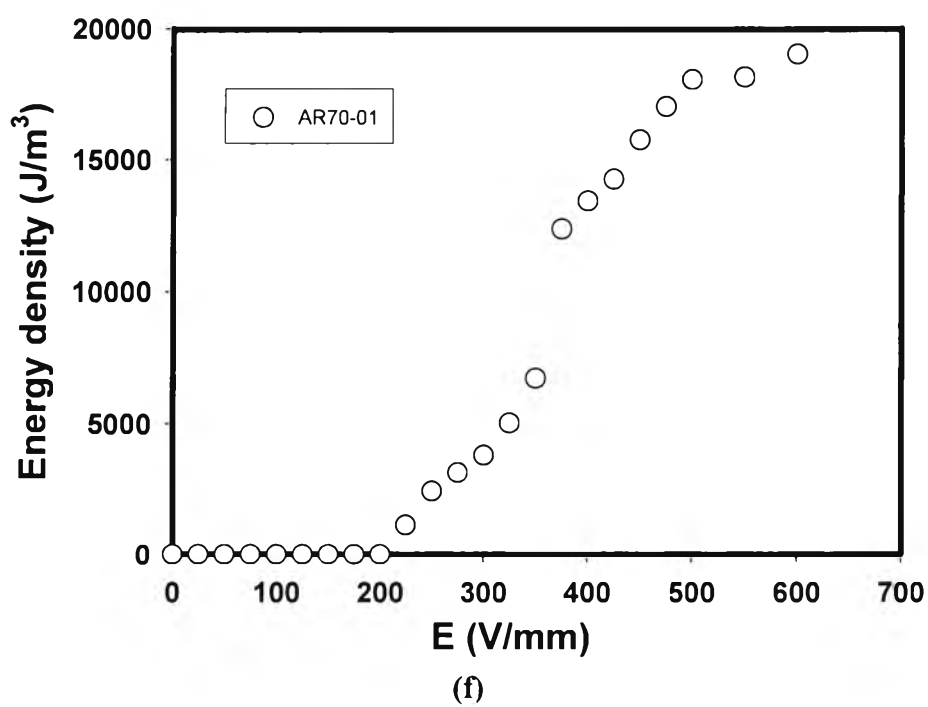
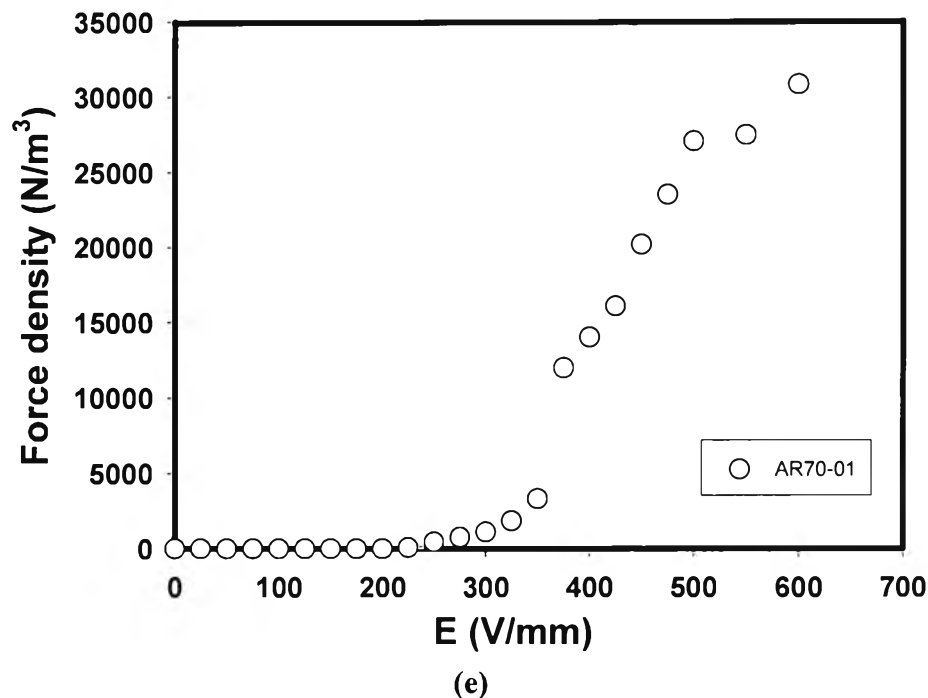
and  $w$  is the width of the film. The dielectrophoresis force can be calculated from the static horizontal force balance consisting of the elastic force and the corrective gravity force term ( $mgsin\theta$ ):

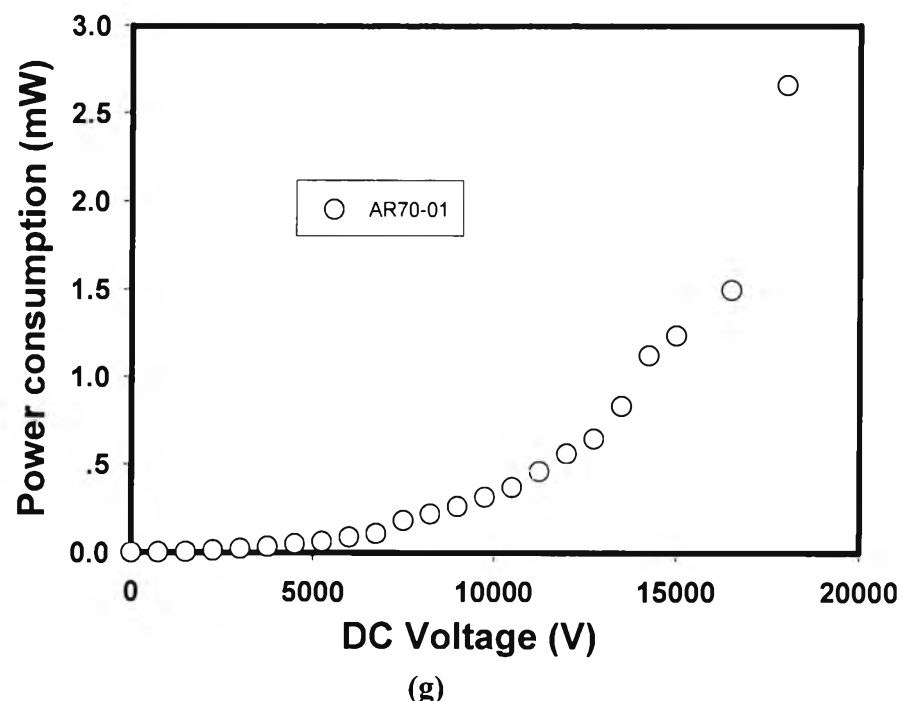
$$F_d = F_e + mg \sin \theta , \quad (\text{R1})$$

where  $g = 9.8 \text{ m.s}^{-2}$ ,  $m$  = mass of the specimen, and  $\theta$  is the deflection angle.

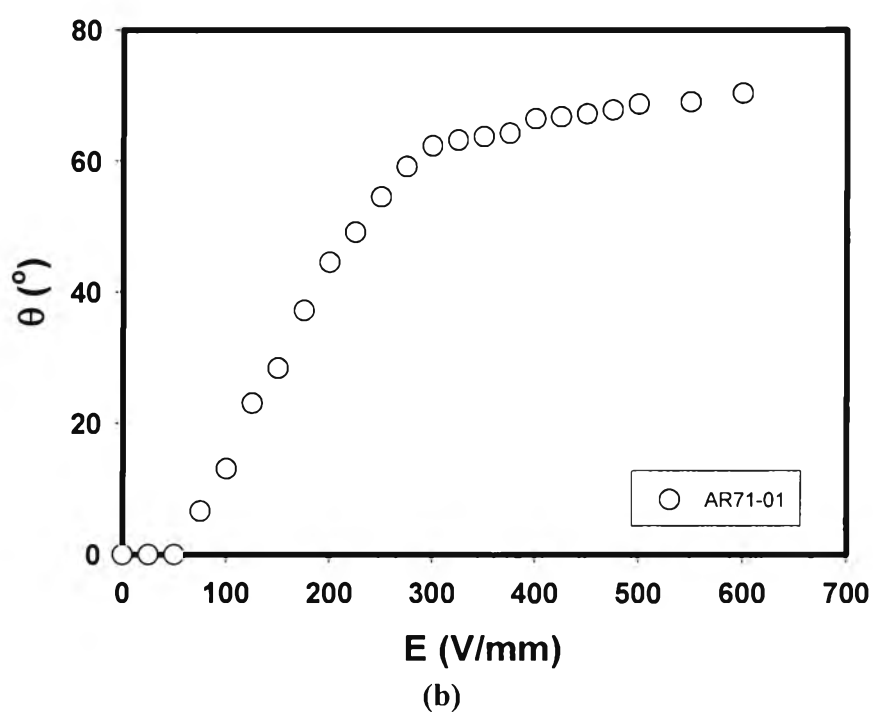
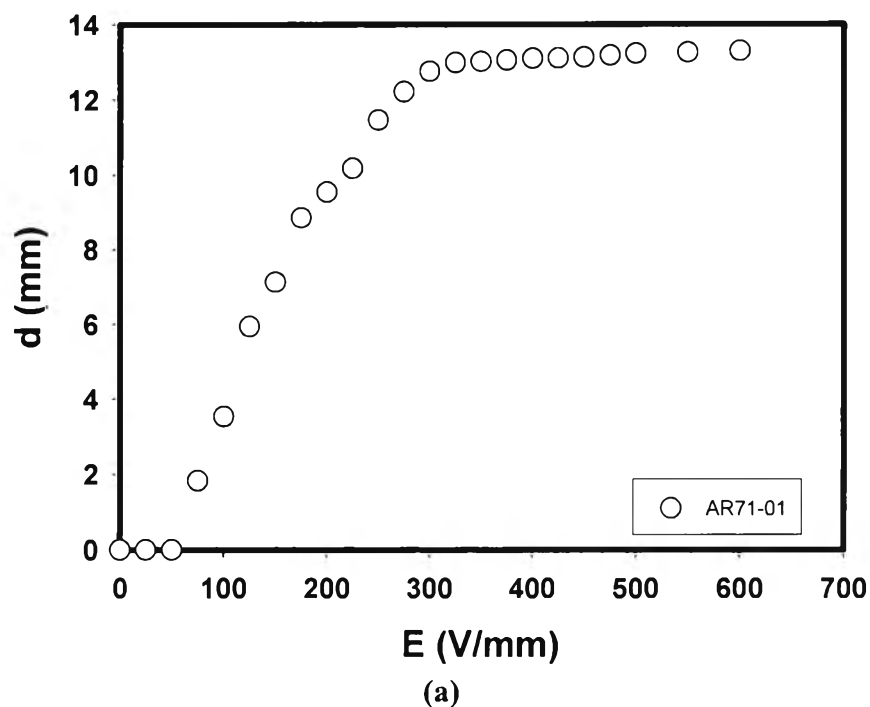


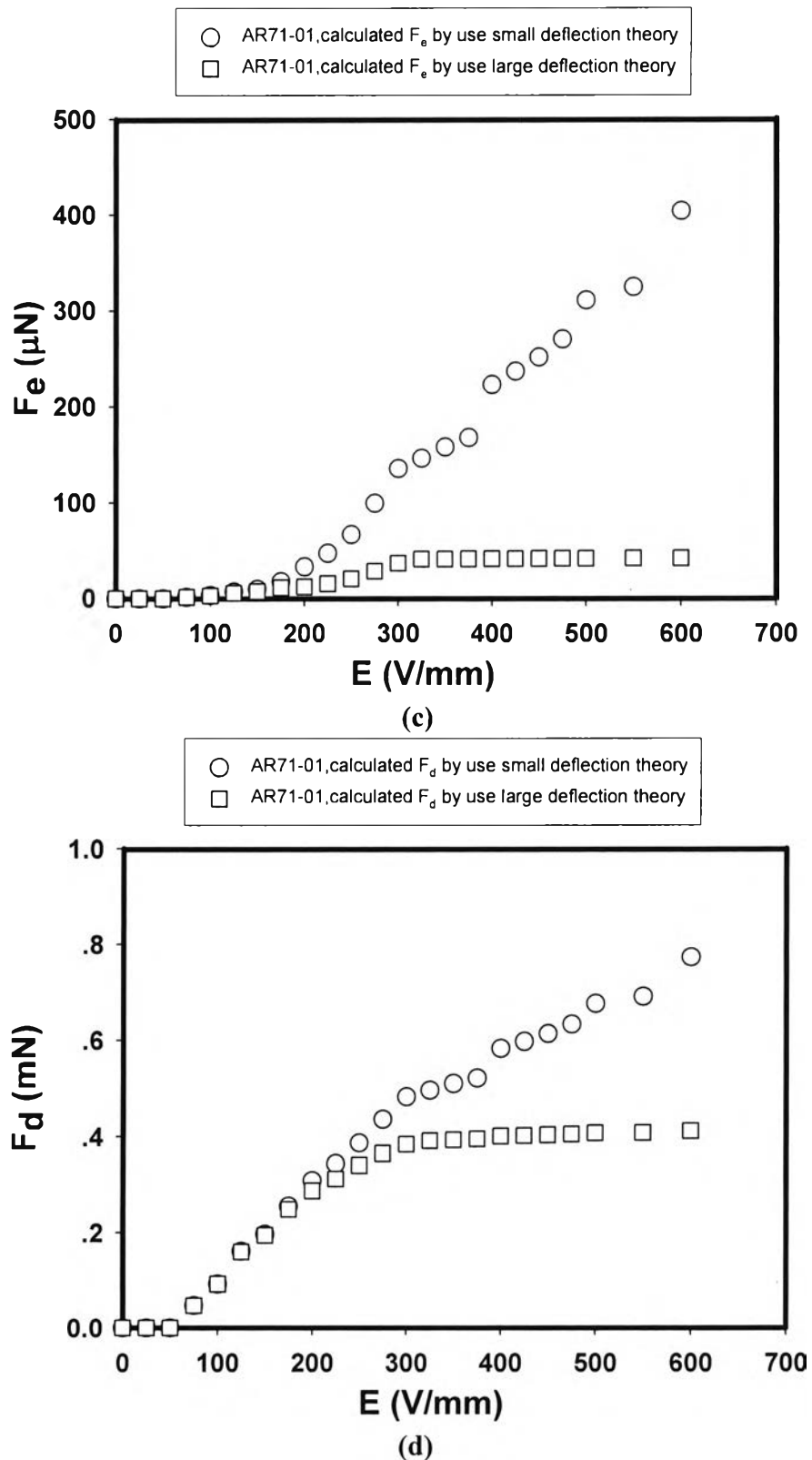


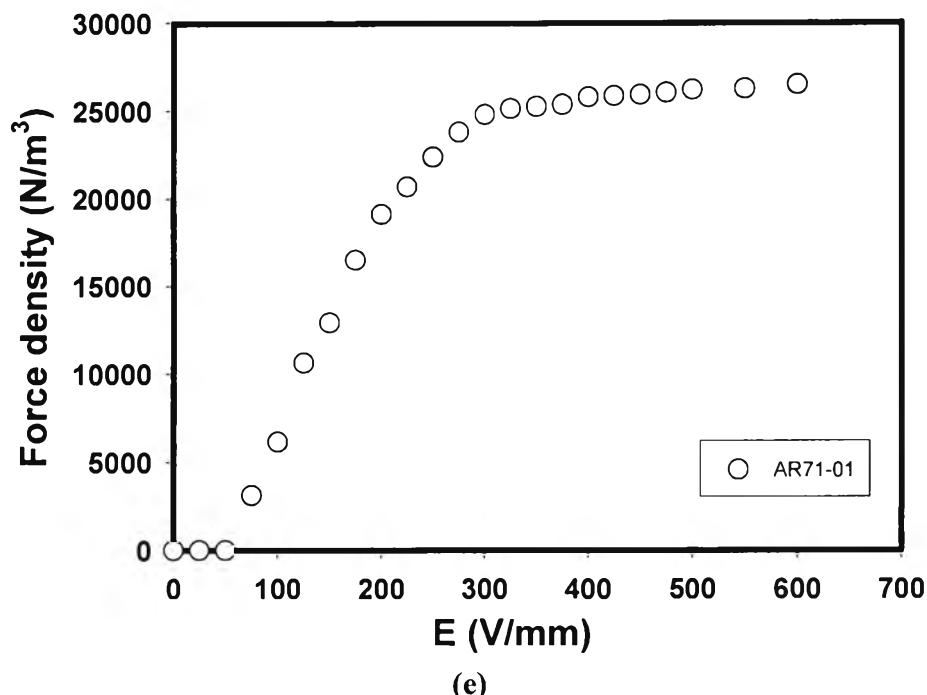




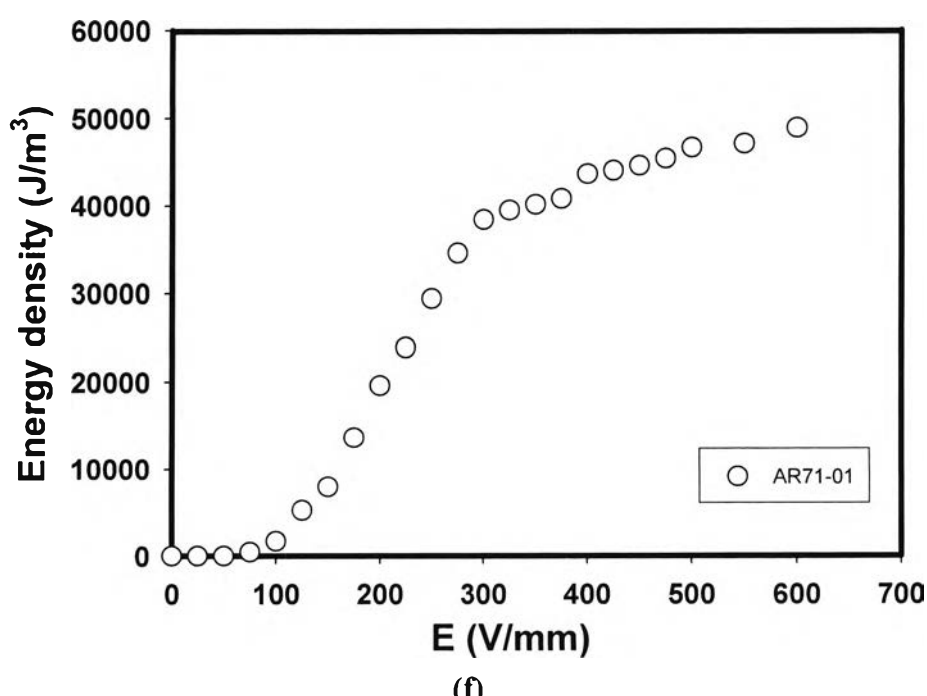
**Figure R1** Electromechanical responses of AR70-01 at various electric field strengths: (a) deflection lengths; (b) deflection angles; (c) elastic force ( $F_e$ ); (d) dielectrophoretic forces ( $F_d$ ); (e) force density; (f) energy density; (g) power consumption.



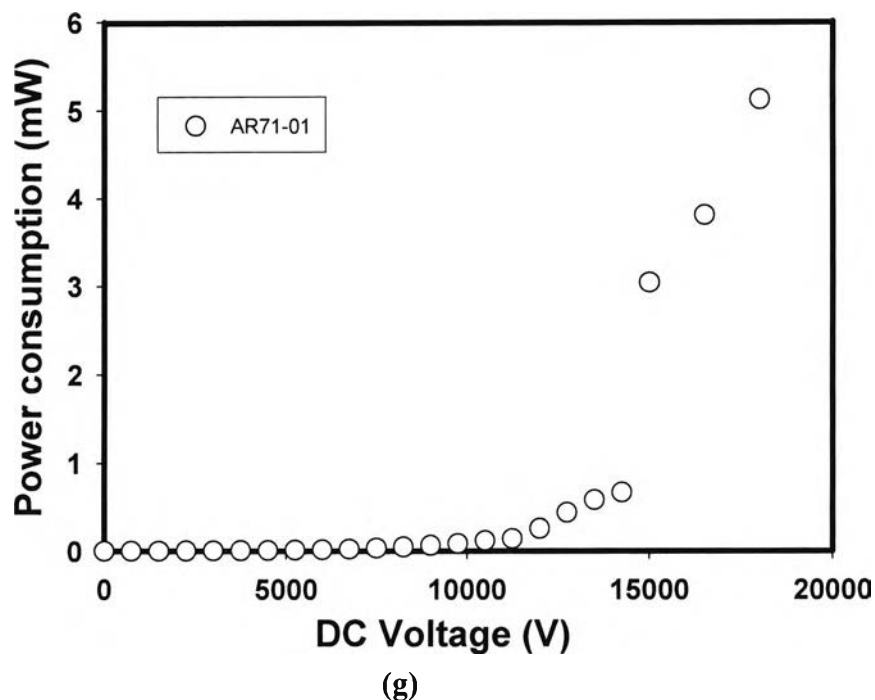




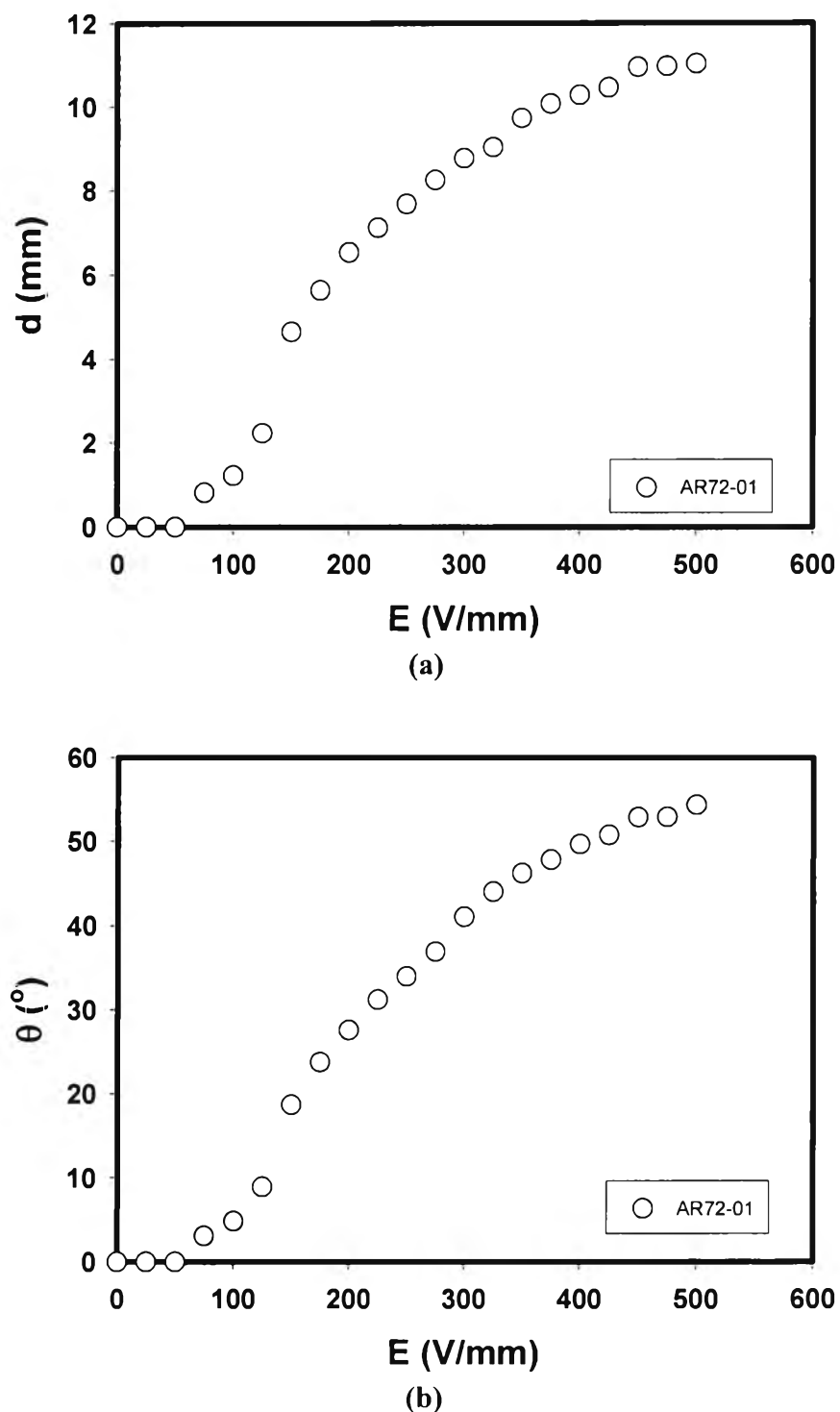
(e)

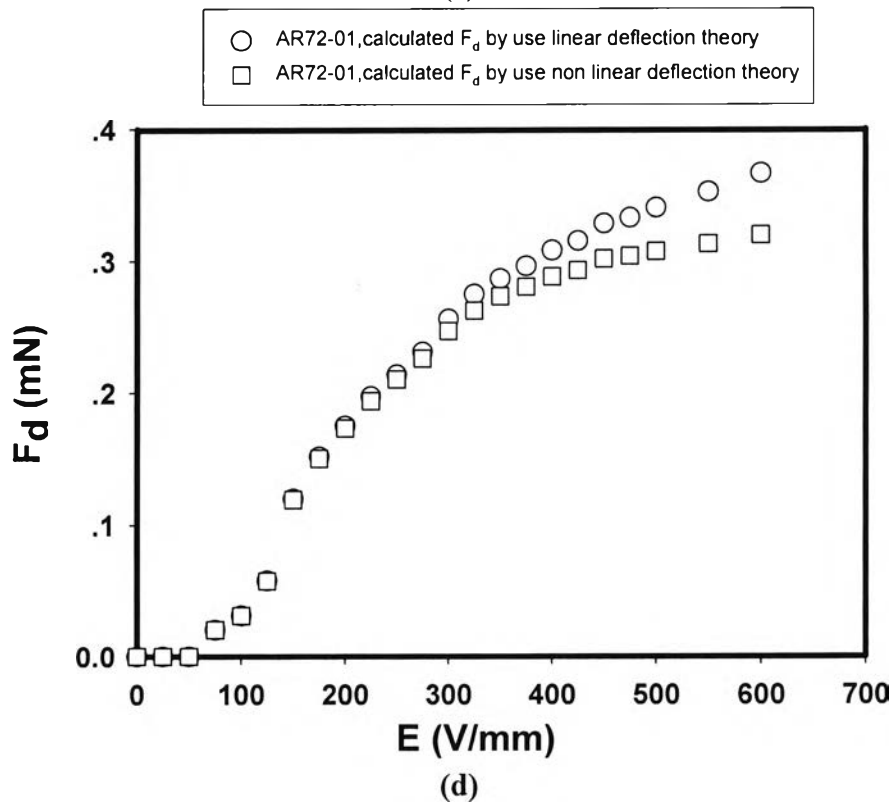
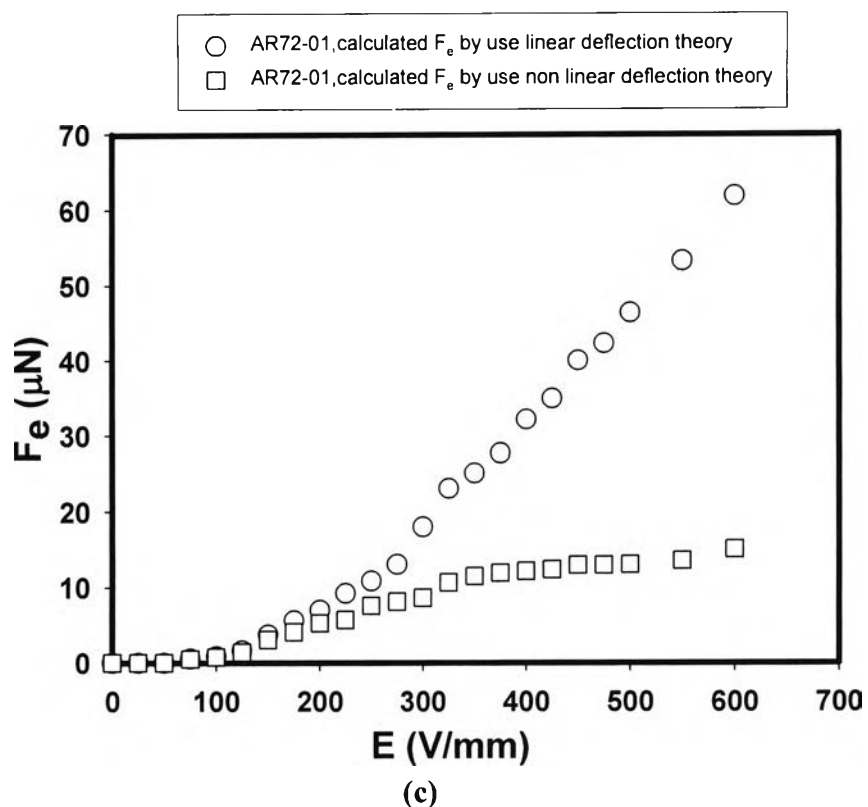


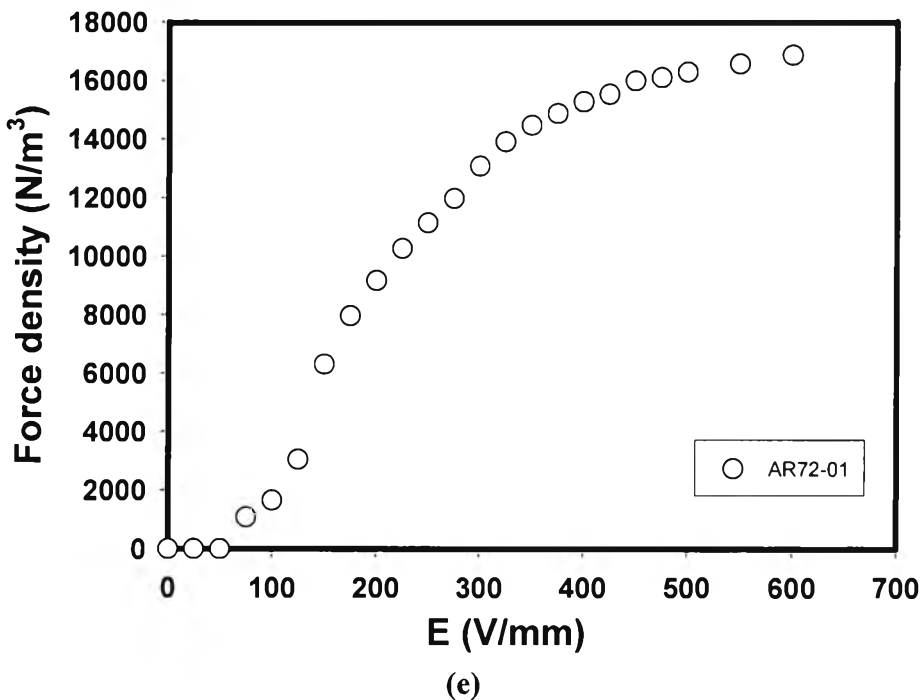
(f)



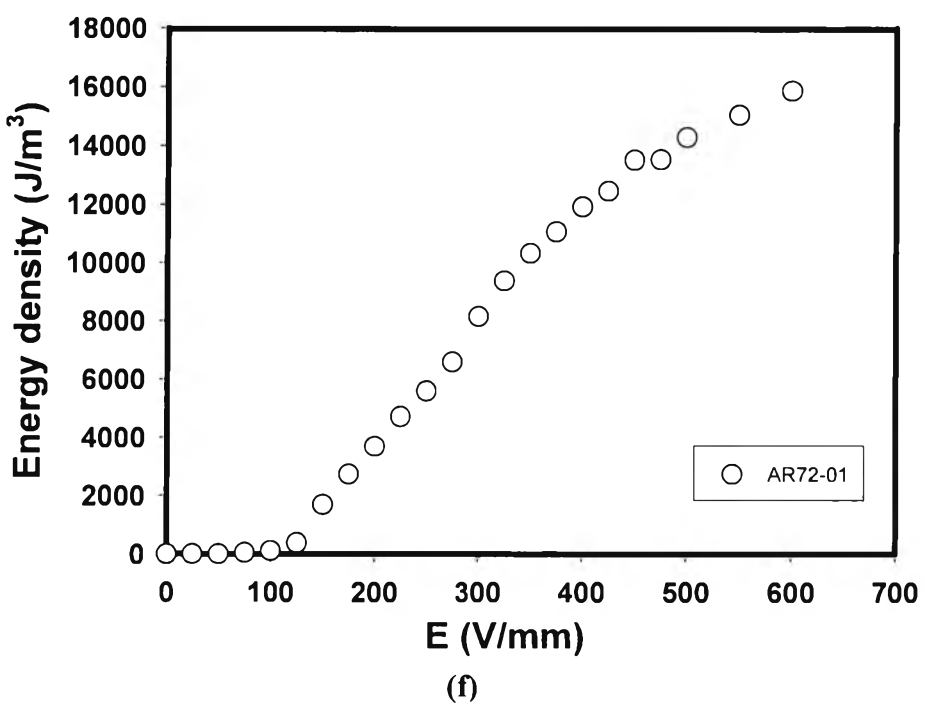
**Figure R2** Electromechanical responses of AR71-01 at various electric field strengths: (a) deflection lengths; (b) deflection angles; (c) elastic force ( $F_e$ ); (d) dielectrophoretic forces ( $F_d$ ); (e) force density; (f) energy density; (g) power consumption.







(e)



(f)

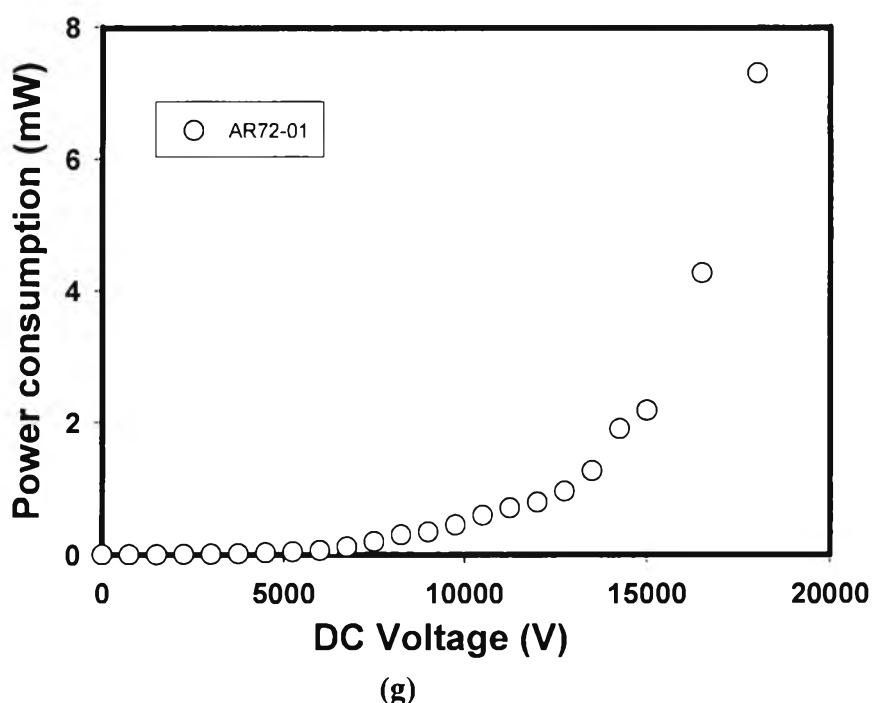
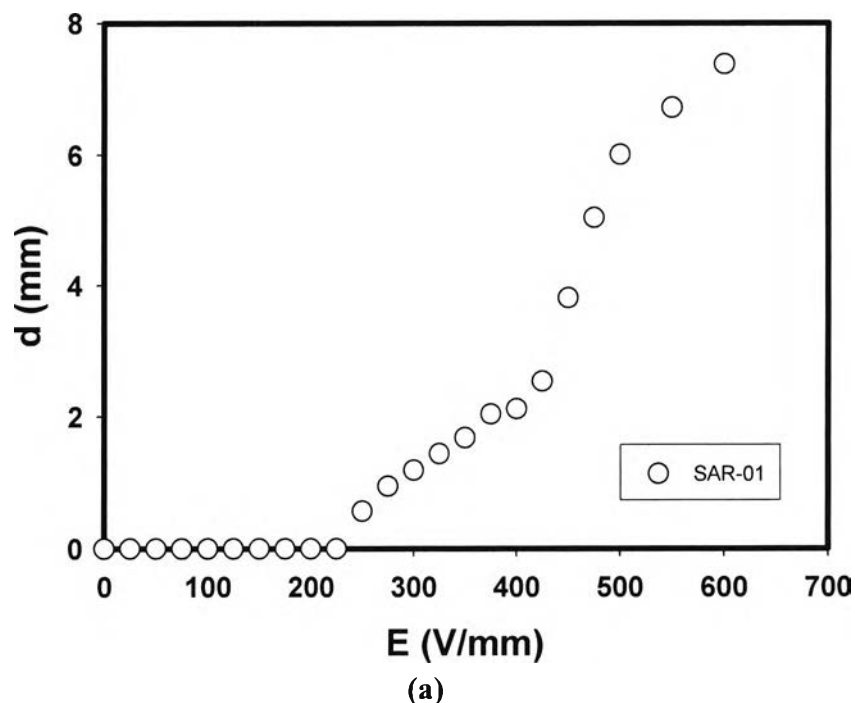
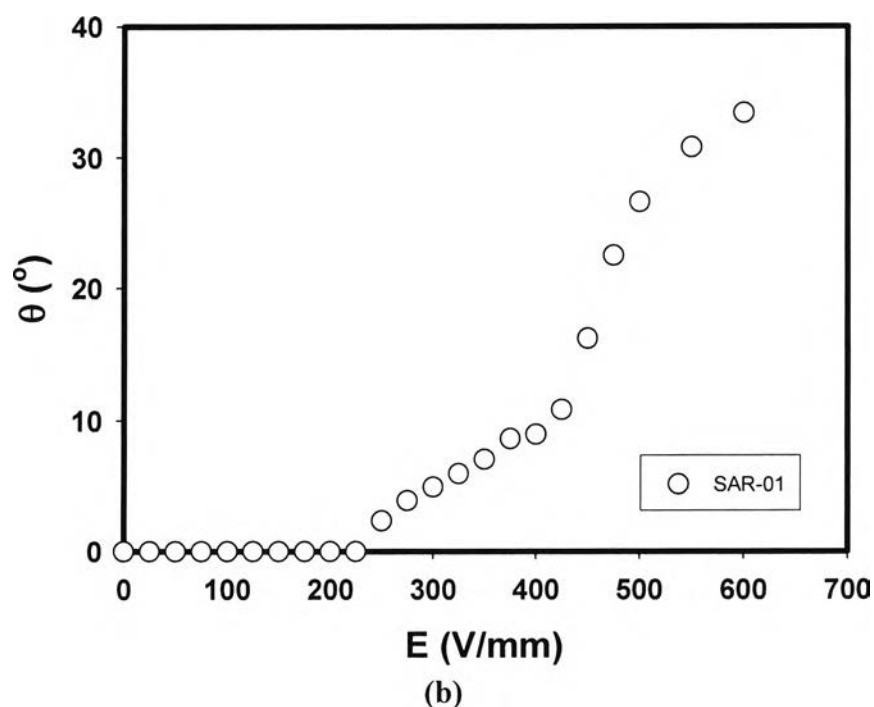


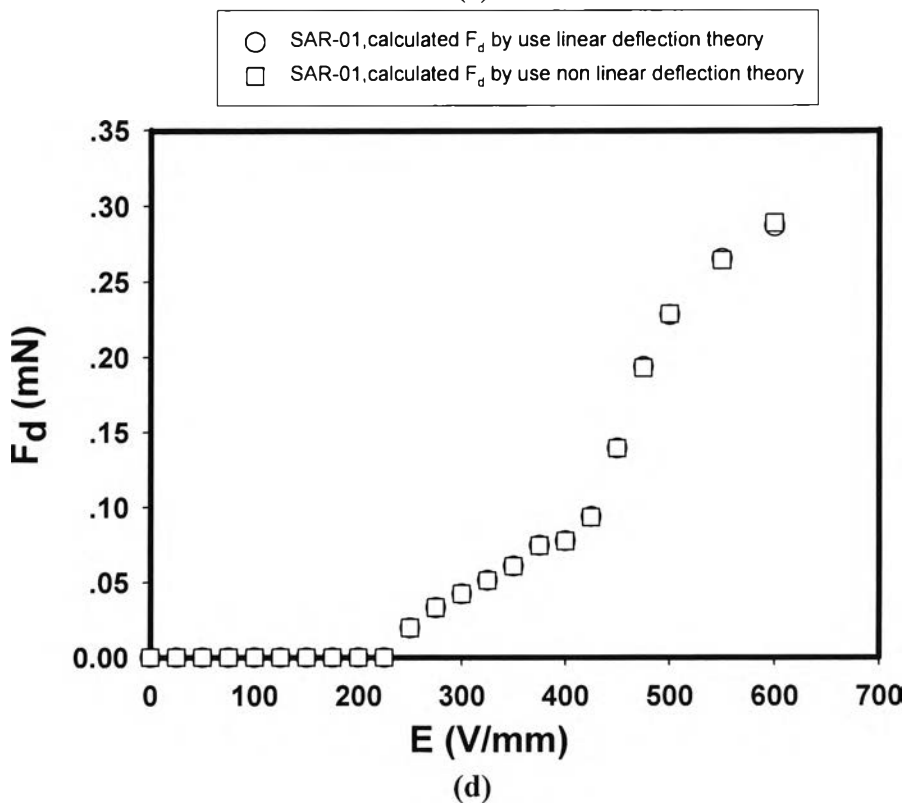
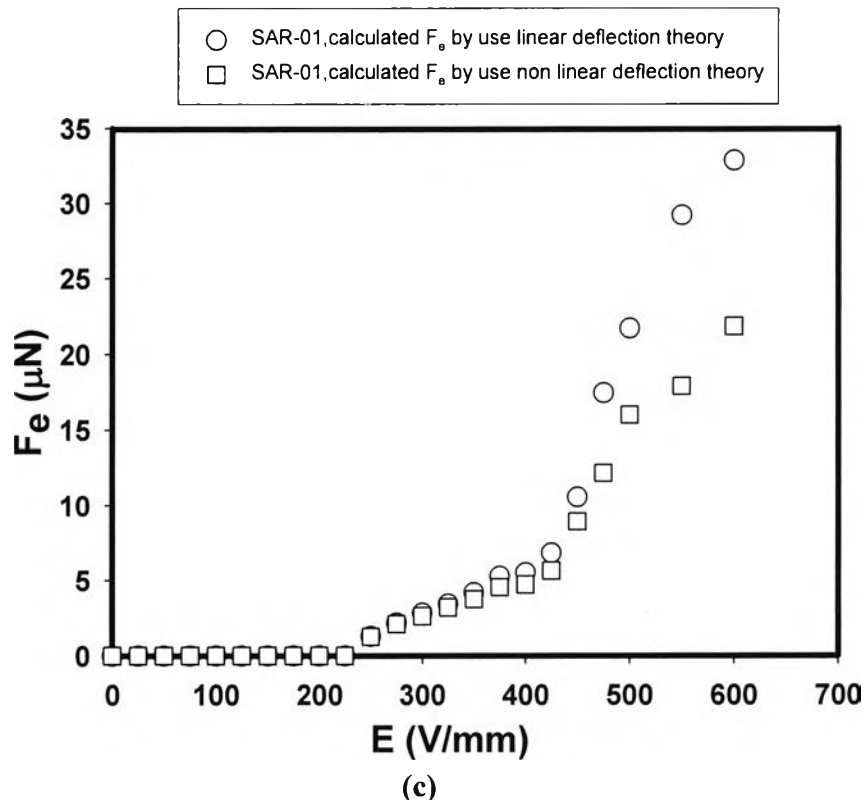
**Figure R3** Electromechanical responses of AR72-01 at various electric field strengths: (a) deflection lengths; (b) deflection angles; (c) elastic force ( $F_e$ ); (d) dielectrophoretic forces ( $F_d$ ); (e) force density; (f) energy density; (g) power consumption

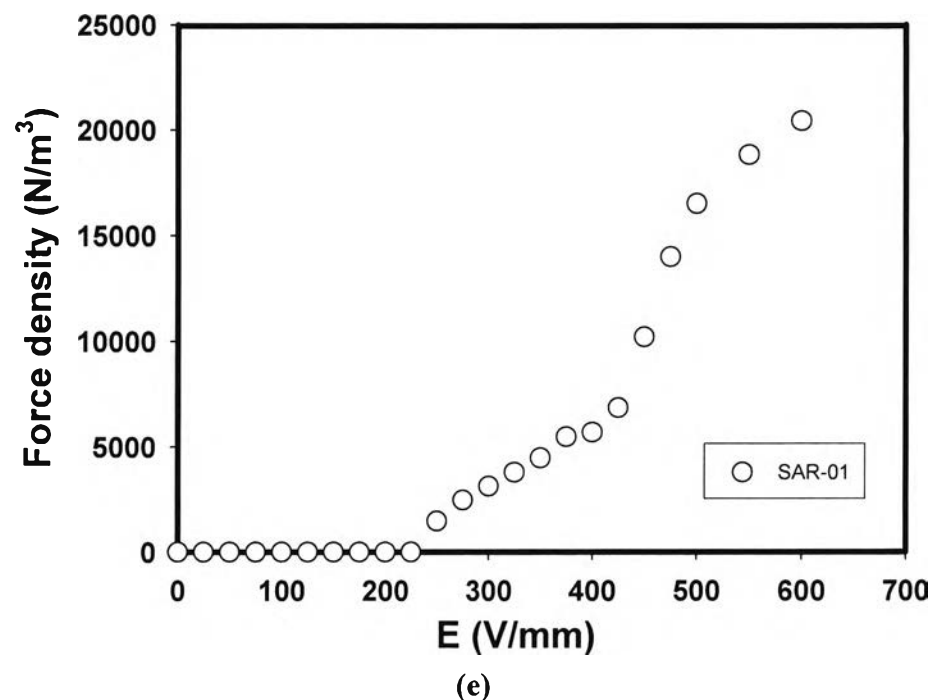


(a)

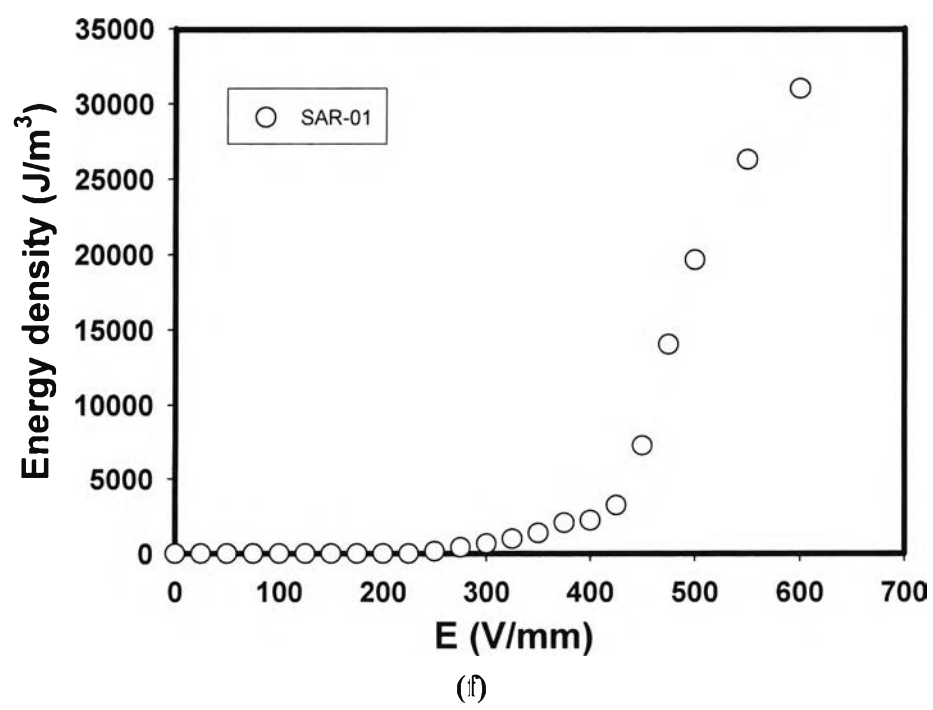


(b)

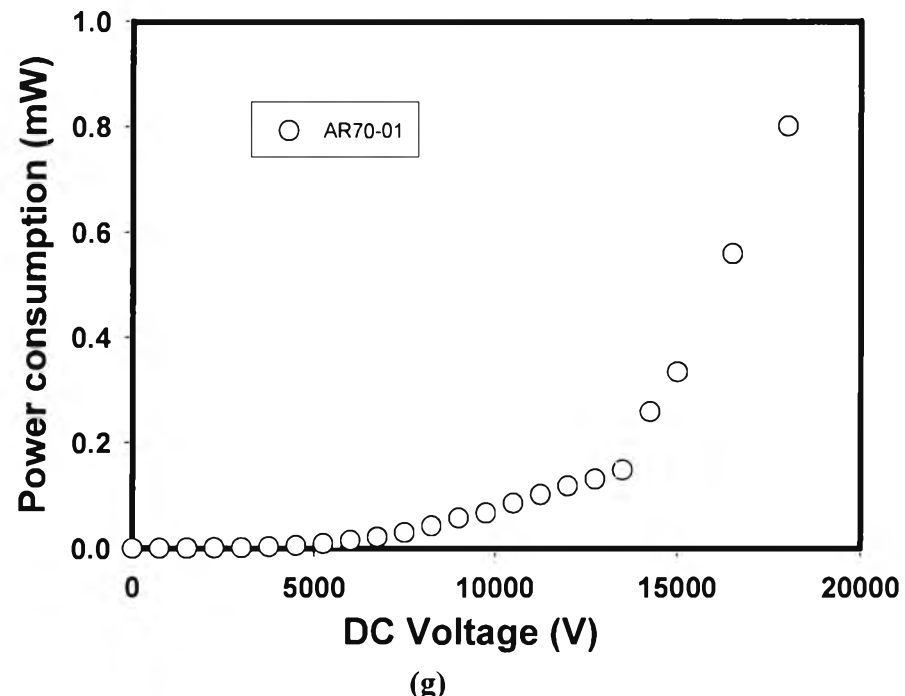




(e)

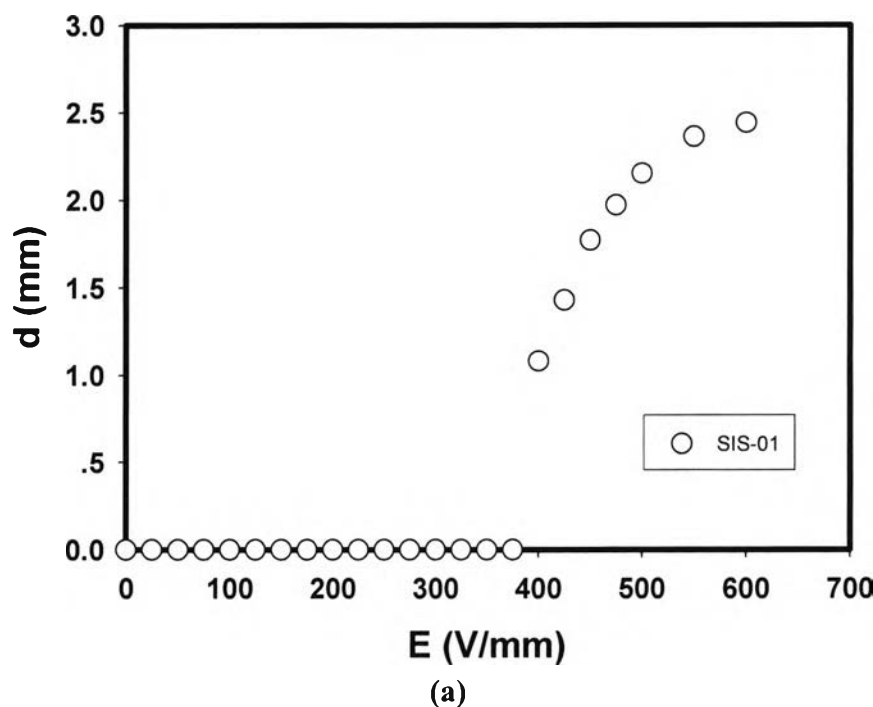


(f)

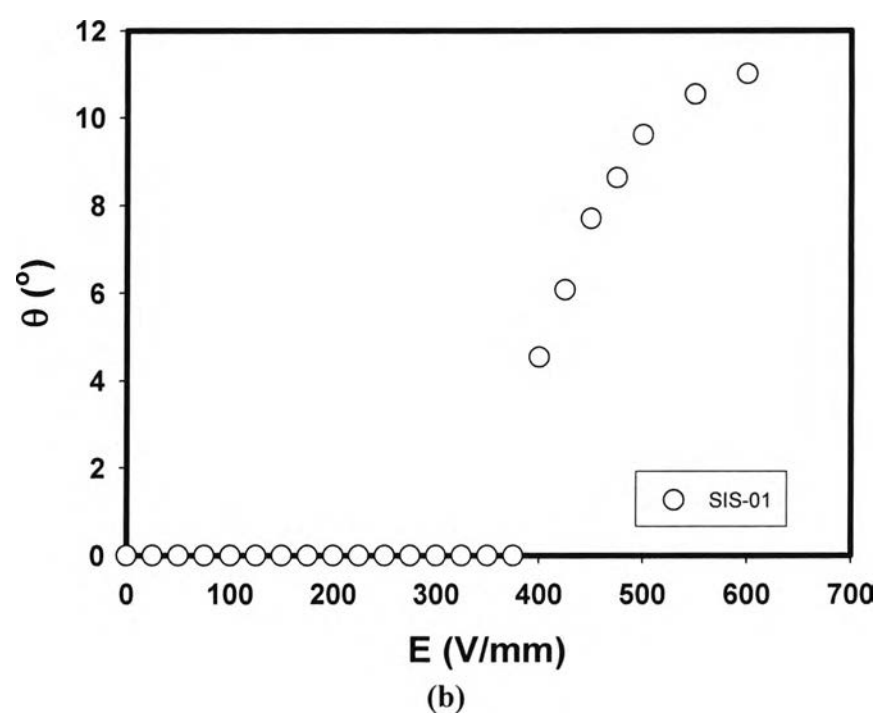


(g)

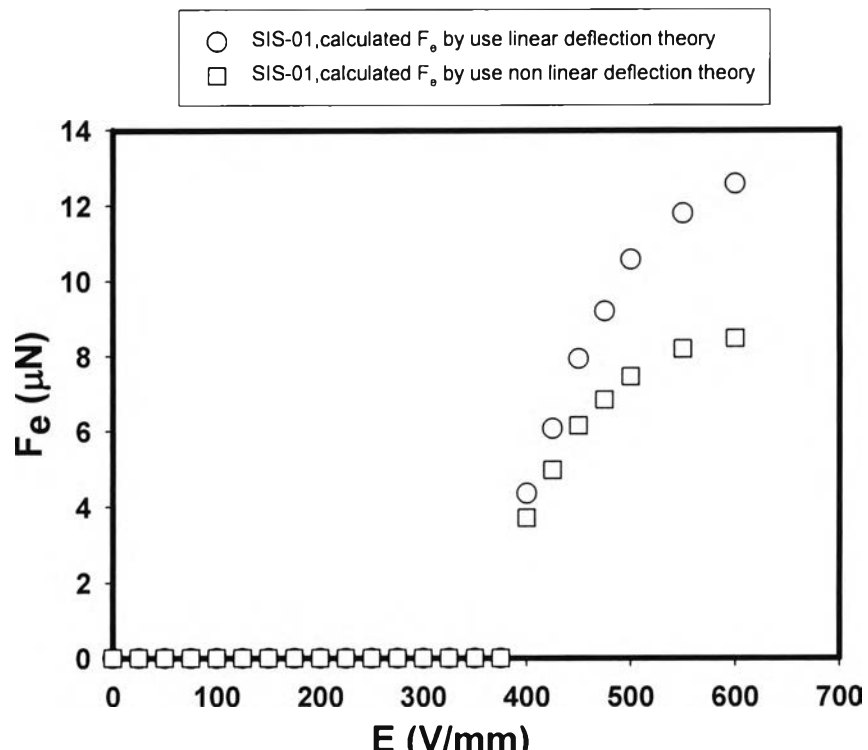
**Figure R4** Electromechanical responses of SAR-01 at various electric field strengths: (a) deflection lengths; (b) deflection angles; (c) elastic force ( $F_e$ ); (d) dielectrophoretic forces ( $F_d$ ); (e) force density; (f) energy density; (g) power consumption.



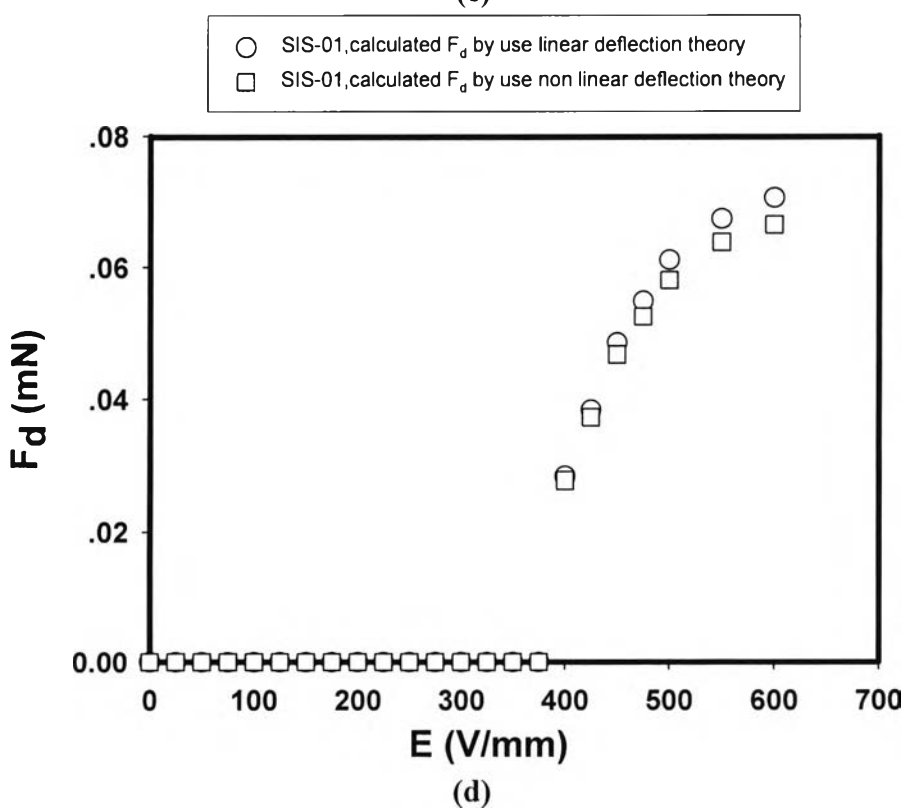
(a)



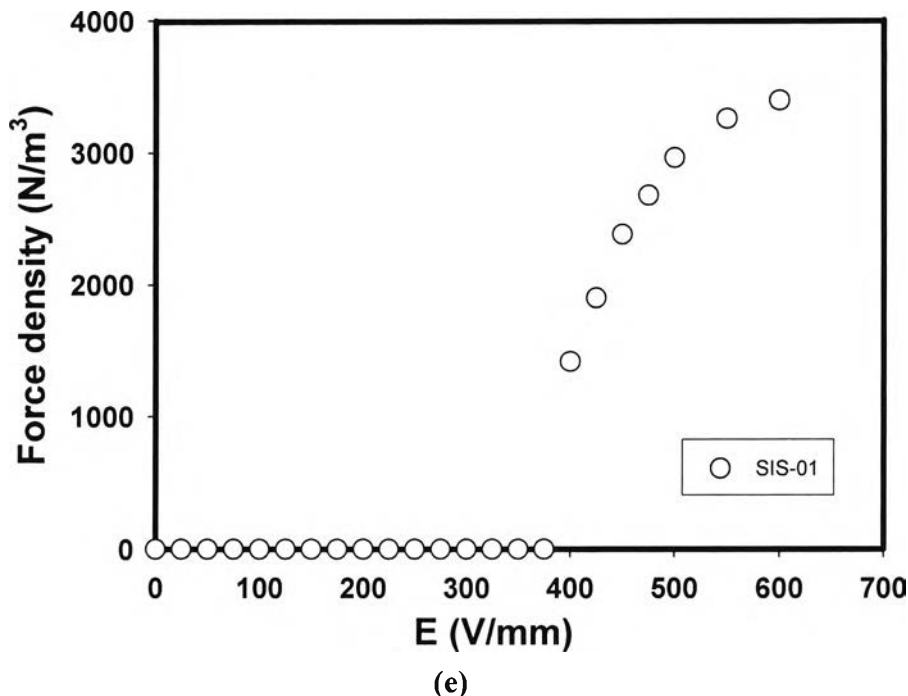
(b)



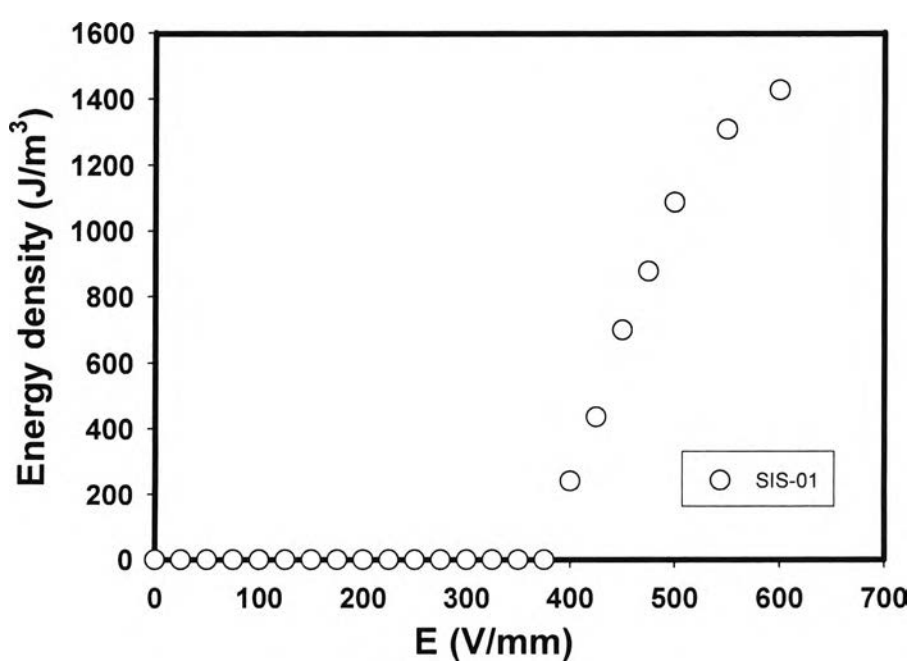
(c)



(d)



(e)



(f)

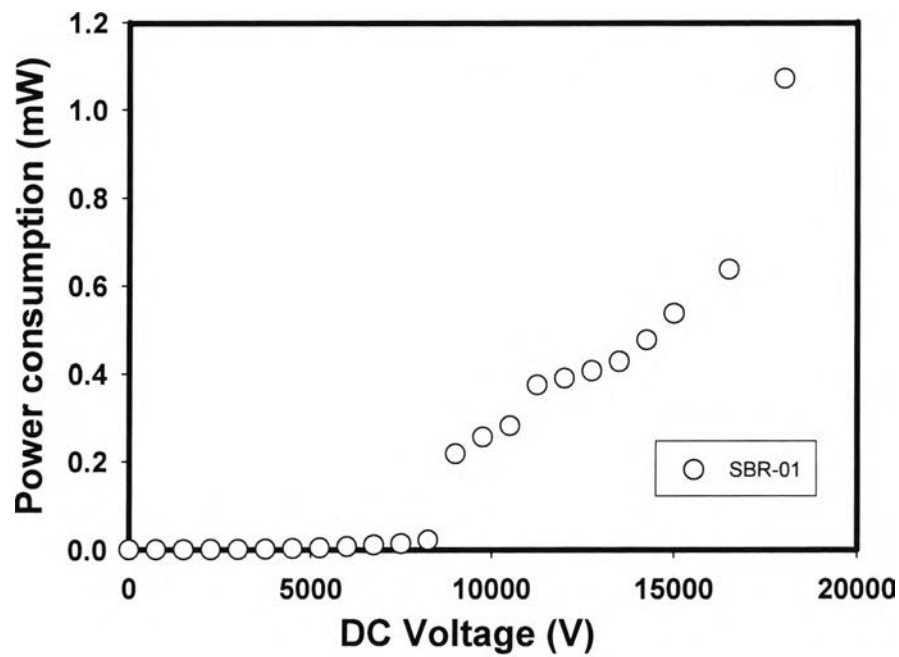
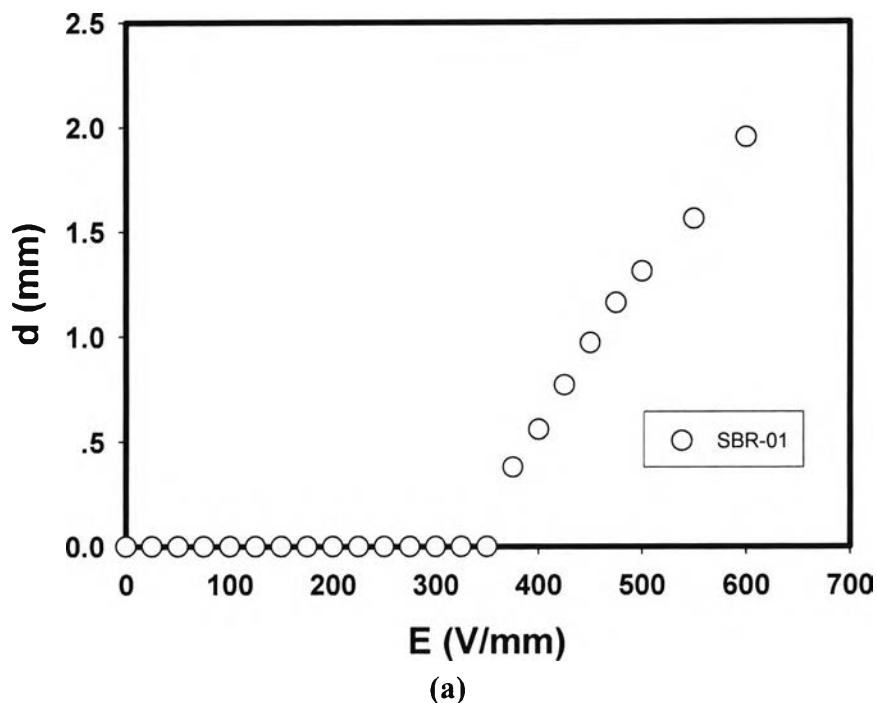
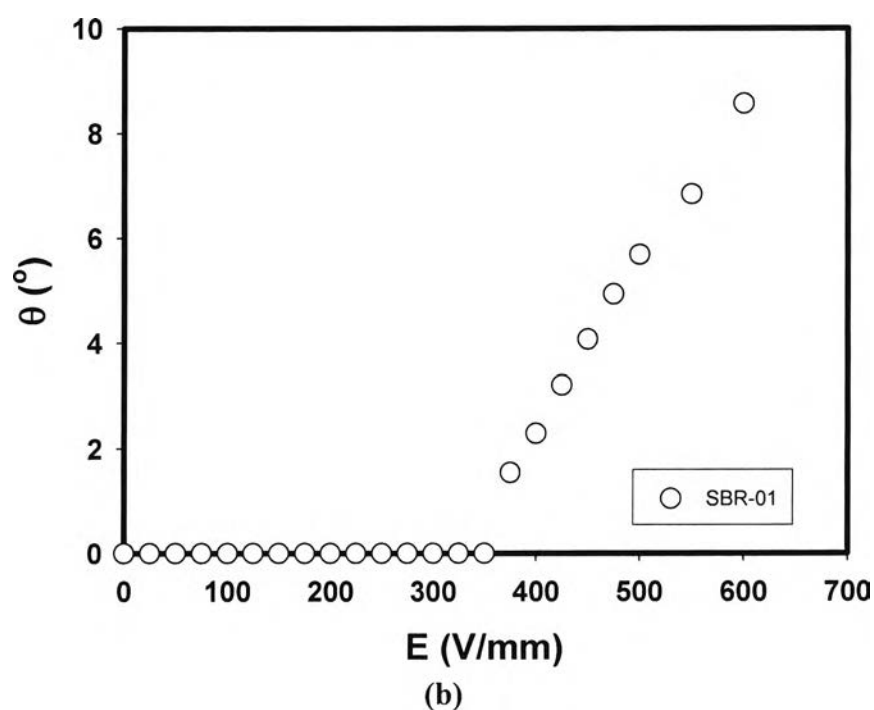


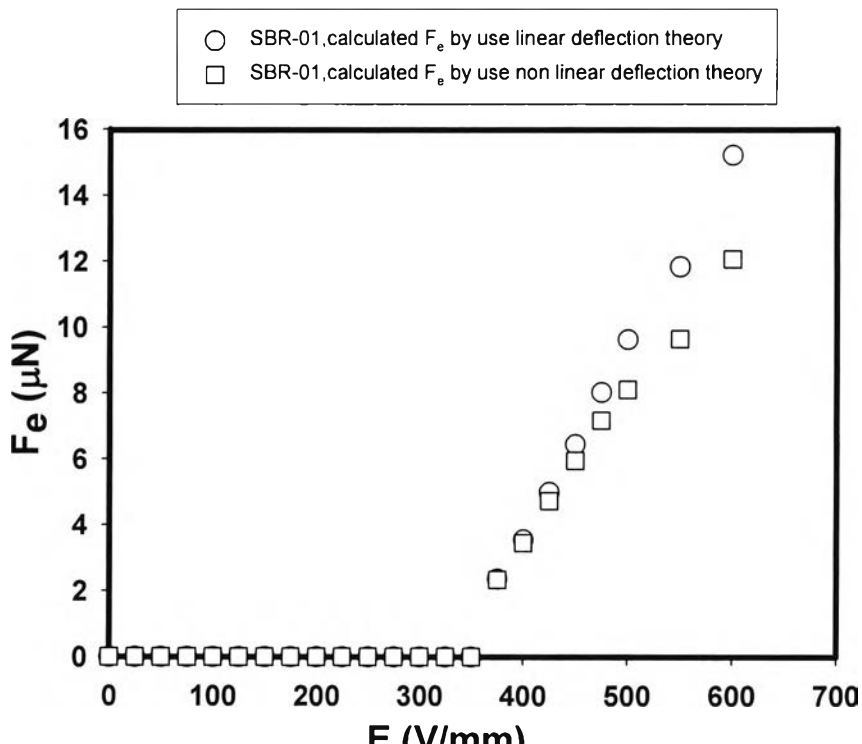
**Figure R5** Electromechanical responses of SIS-01 at various electric field strengths: (a) deflection lengths; (b) deflection angles; (c) elastic force ( $F_e$ ); (d) dielectrophoretic forces ( $F_d$ ); (e) force density; (f) energy density; (g) power consumption.



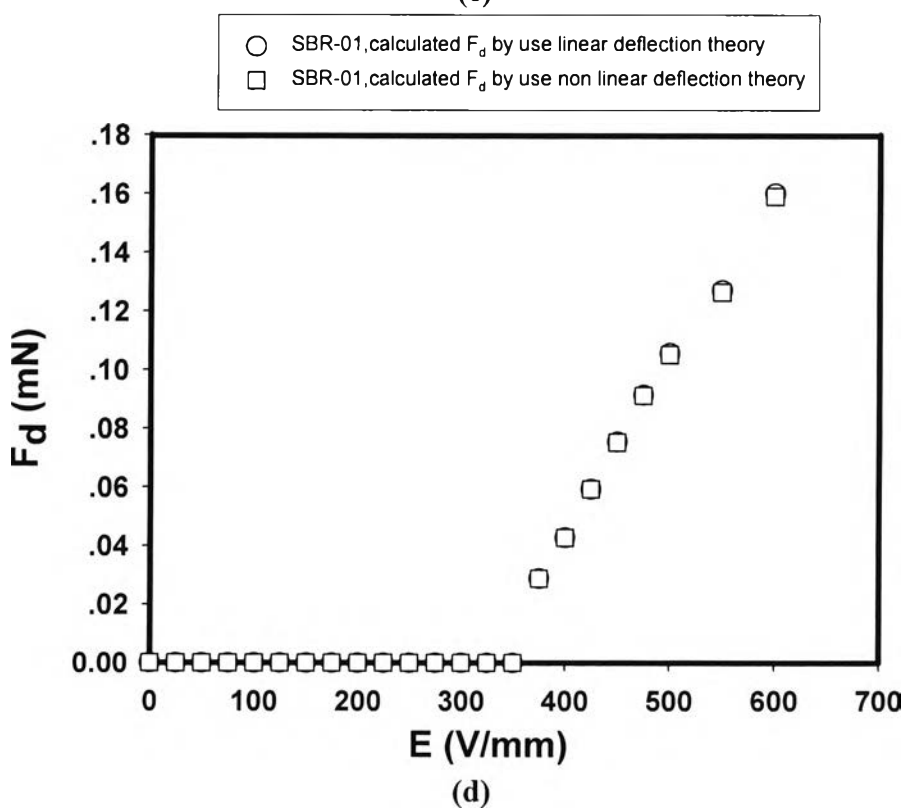
(a)



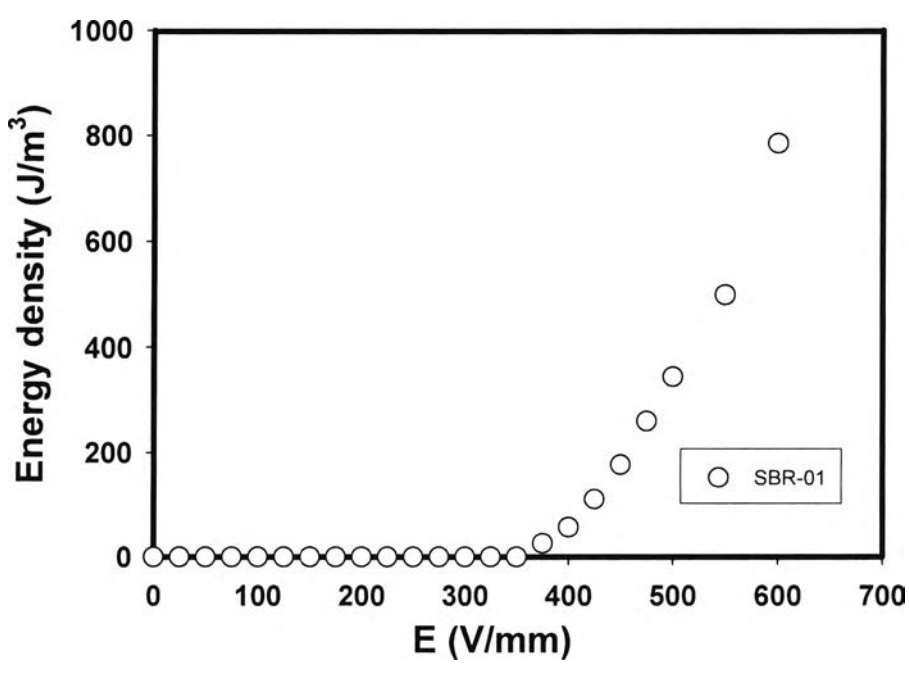
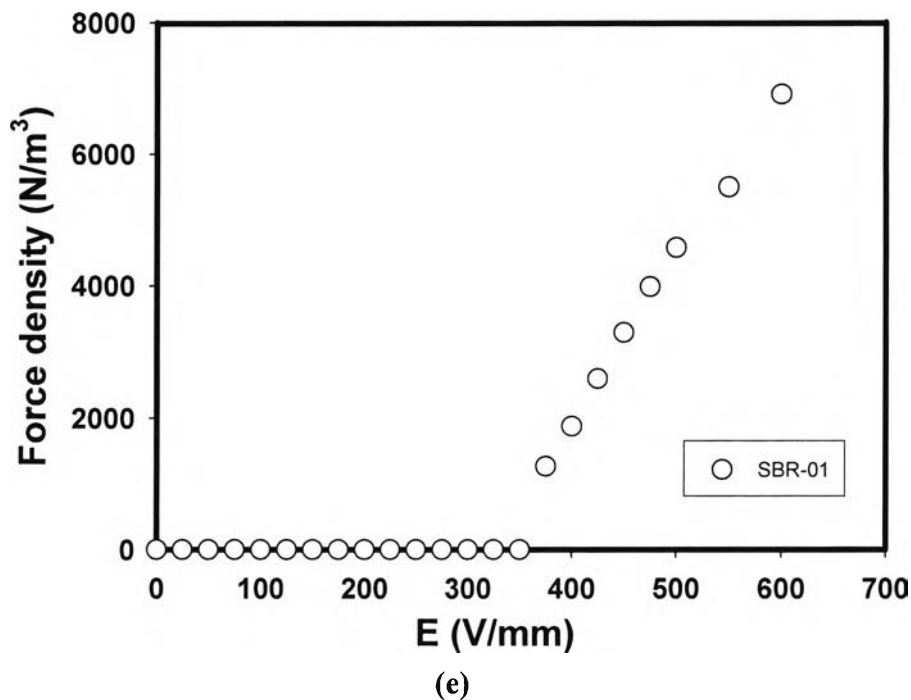
(b)



(c)



(d)



(f)

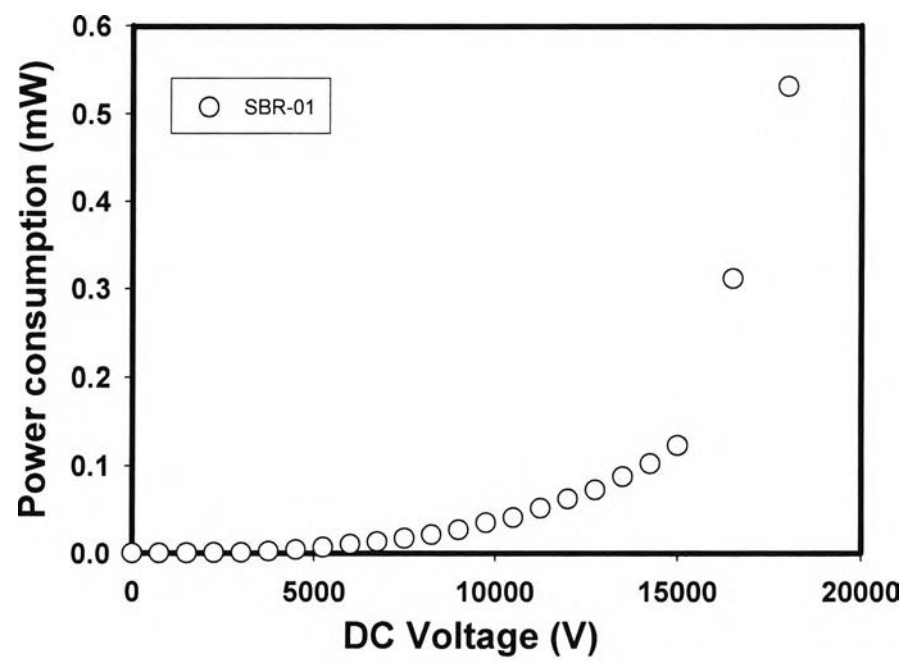


**Figure R6** Electromechanical responses of SBR-01 at various electric field strengths: (a) deflection lengths; (b) deflection angles; (c) elastic force ( $F_e$ ); (d) dielectrophoretic forces ( $F_d$ ); (e) force density; (f) energy density; (g) power consumption.

## **Appendix S Deflection Distance, Angle and Dielectrophoresis Force of the Acrylic Elastomers (AR71) and Styrene Copolymers (SAR and SBR) under AC Electric Field**

The dielectrophoresis forces were determined by measuring the deflection distances of the elastomers in the vertical cantilever fixture under electric field. The specimens were vertically immersed in the silicone oil (viscosity = 100 cSt) between parallel copper electrode plates (40 mm long, 30 mm width, and 1 mm thick). The gap between the pair of electrodes was 10 mm. An AC field was applied with a function generator (Tektonix, model CFG 253) connected to a high voltage power supply (Trek, model 609E-6) which can deliver an electric field up to 4 kV. The output voltage and frequency from the high voltage power supply was detected using an oscilloscope (BK Precision, model 2120B). We used a CCD video camera to record the movement during the experiment. Still pictures were captured from the video and the deflection distances in x ( $d$ ) and y axes ( $l$ ) at the ends of the specimen were determined by using Scion Image software (version 4.0.3). The electric field strength was varied between 0–800 V/mm at room temperature,  $300 \pm 1$  K. Both the voltage and the current were monitored. We calculated the resisting elastic force of the specimens under electric field using the non-linear deflection theory of a cantilever (Timoshenko et al.) and (Kim et al., 2007), which can be calculated from the standard curve between  $\frac{F_e l_0^2}{EI}$  and  $\frac{d}{l_0}$  ( $l_0$  = initial length of specimens)

(Timoshenko et al.).

where  $F_e$  is the elastic force,  $d$  is the deflection distance in the horizontal axis,  $l$  is the deflection distance in the vertical axis,  $E$  is the Young's modulus —which is equal to  $2G(1+v)$ , where  $G$  is the shear storage modulus taken to be  $G'(\omega = 1 \text{ rad/s})$  at various electric field strengths and,  $v$  is the Poisson's ratio (0.5 for an incompressible sample)— and  $I$  is the moment of inertia  $\frac{1}{12}t^3w$ , where  $t$  is the thickness of the film and  $w$  is the width of the film. The dielectrophoresis force can be calculated from the static horizontal force balance consisting of the elastic force and the corrective gravity force term ( $mgsin\theta$ ):

$$F_d = F_e + mg \sin \theta , \quad (\text{S1})$$

where  $g = 9.8 \text{ m.s}^{-2}$ ,  $m$  = mass of the specimen, and  $\theta$  is the deflection angle.

**Table S1** Dimensions of specimens

<b>Samples</b>	<b>Width, w (mm)</b>	<b>Length, l (mm)</b>	<b>Thickness , t (mm)</b>	<b>Weight (g)</b>	<b>Volume (mm<sup>3</sup>)</b>	<b>Maximum F<sub>d</sub> (mN)</b>	<b>Maximum F<sub>d</sub>/volume (N/m<sup>3</sup>)</b>	<b>Maximum F<sub>d</sub>/thickness (N/m)</b>
<b>AR71 at E = 200 V/mm</b>	2.25	10.39	0.65	0.017	15.19	0.011	724	0.02
<b>AR71 at E = 300 V/mm</b>	2.21	10.55	0.76	0.021	17.72	0.021	1,185	0.03
<b>AR71 at E = 500 V/mm</b>	2.34	11.40	0.51	0.015	13.60	0.024	1,764	0.05
<b>AR71 at E = 600 V/mm</b>	2.31	12.58	0.73	0.026	21.20	0.040	1,886	0.06
<b>AR71 at E = 800 V/mm</b>	2.13	12.24	0.79	0.024	20.59	0.185	8,984	0.23
<b>SAR at E = 600 V/mm</b>	2.13	12.30	0.69	0.019	18.08	0.027	1,493	0.04
<b>SAR at E = 800 V/mm</b>	2.44	12.75	0.73	0.025	22.71	0.071	3,126	0.10
<b>SBR at E = 800 V/mm</b>	2.28	11.97	0.66	0.019	17.90	0.008	469	0.01

**Table S2** Dimensions of specimens

<b>Samples</b>	<b>Width, w (mm)</b>	<b>Length, l (mm)</b>	<b>Thickness , t (mm)</b>	<b>Weight (g)</b>	<b>Volume (mm<sup>3</sup>)</b>	<b>Maximum <math>F_d</math> (mN)</b>	<b>Maximum <math>F_d/volume</math> (N/m<sup>3</sup>)</b>	<b>Maximum <math>F_d/thickness</math> (N/m)</b>
<b>AR71 at E = 800 V/mm</b>	2.19	11.39	0.11	0.003	2.74	0.103	37,588	0.94
<b>AR71 at E = 800 V/mm</b>	2.11	11.72	0.25	0.007	6.18	0.207	33,493	0.83
<b>AR71 at E = 800 V/mm</b>	2.36	11.53	0.52	0.016	14.15	0.177	12,511	0.34
<b>AR71 at E = 800 V/mm</b>	2.13	12.24	0.79	0.024	20.59	0.185	8,984	0.23
<b>AR71 at E = 800 V/mm</b>	2.34	11.65	0.93	0.030	25.35	0.068	2,682	0.07

**Table S3** Dimensions of specimens

<b>Samples</b>	<b>Width, w (mm)</b>	<b>Length, l (mm)</b>	<b>Thickness , t (mm)</b>	<b>Weight (mg)</b>	<b>Volume (mm<sup>3</sup>)</b>	<b>Maximum <math>F_d</math> (mN)</b>	<b>Maximum <math>F_d/volume</math> (N/m<sup>3</sup>)</b>	<b>Maximum <math>F_d/thickness</math> (N/m)</b>
<b>Pure AR71 at E = 800 V/mm</b>	2.11	11.72	0.25	6.55	6.18	0.207	33,493	0.83
<b>AR71:undoped PPP 1% at E = 800 V/mm</b>	2.15	11.59	0.29	8.37	7.22	0.011	1,523	0.04
<b>AR71: undoped PPP 10% at E = 800 V/mm</b>	2.29	12.22	0.28	9.55	7.83	0.006	766	0.02
<b>AR71: undoped PPP 20% at E = 800 V/mm</b>	2.28	12.10	0.22	7.70	6.07	0.002	329	0.01
<b>AR71:doped PPP 1% at E = 800 V/mm</b>	2.18	11.40	0.31	9.09	7.70	0.346	44,940	1.12
<b>AR71:doped PPP 10% at E = 800 V/mm</b>	2.34	11.25	0.30	9.62	7.89	0.419	53,100	1.39
<b>AR71:doped PPP 20% at E = 800 V/mm</b>	2.22	11.63	0.27	8.85	6.97	0.229	32,850	0.85

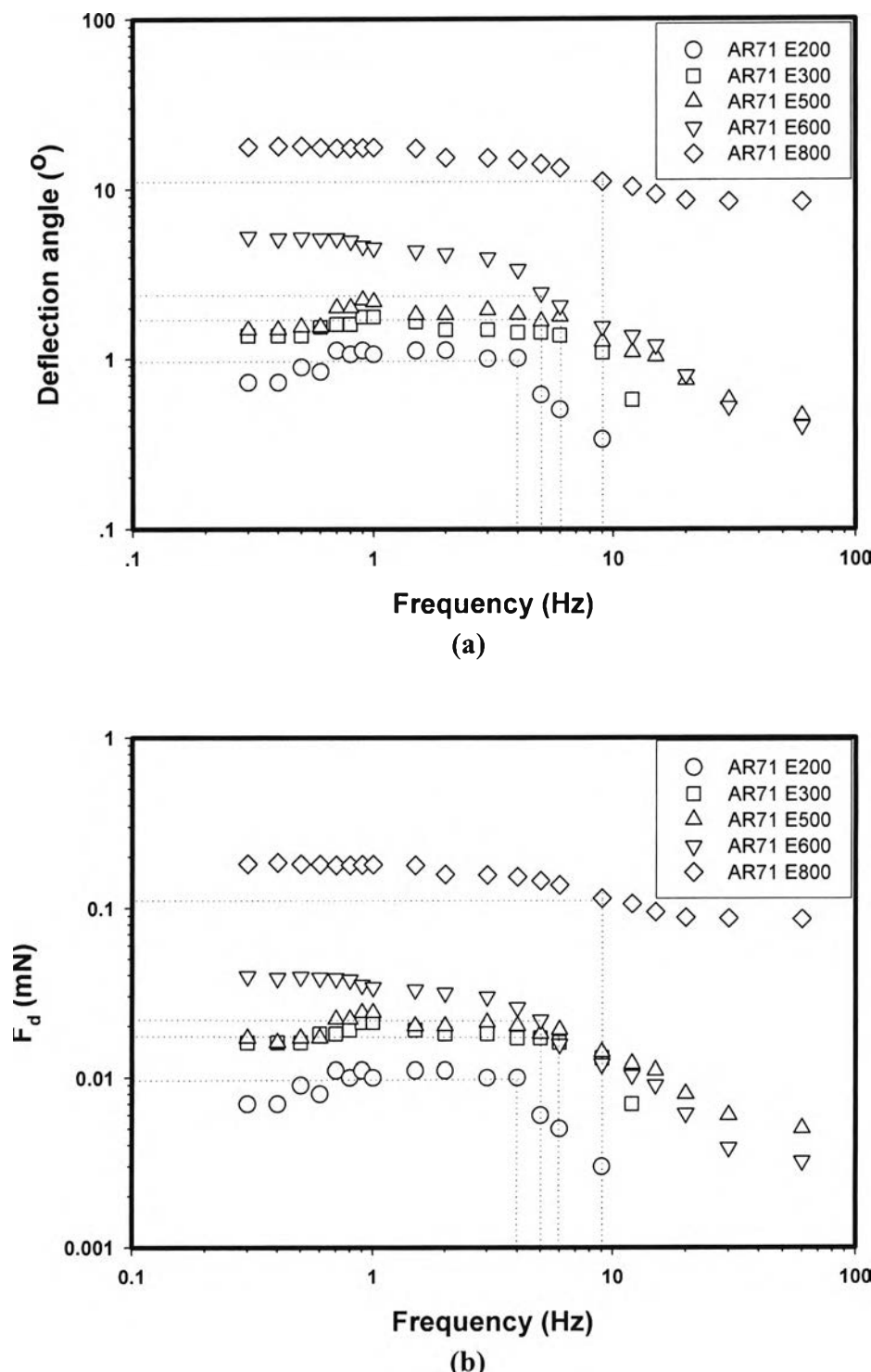


**Figure S1** Electromechanical responses of AR71 at various frequencies and under AC electric field strengths (a) deflection angles; (b) dielectrophoresis forces ( $F_d$ ).

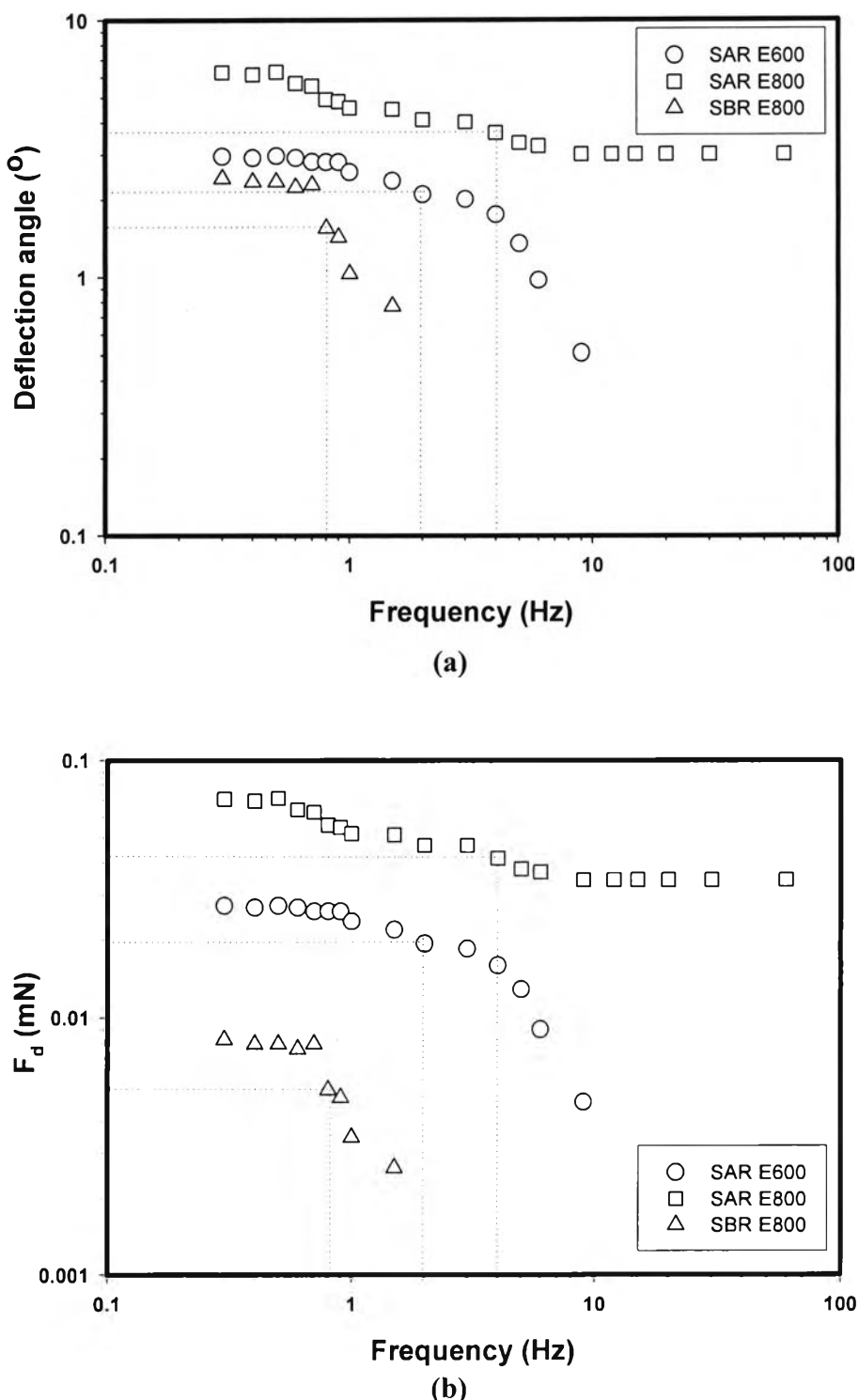


**Figure S2** Electromechanical responses of SAR and SBR at various frequencies and under AC electric field strengths (a) deflection angles; (b) dielectrophoresis forces ( $F_d$ ).

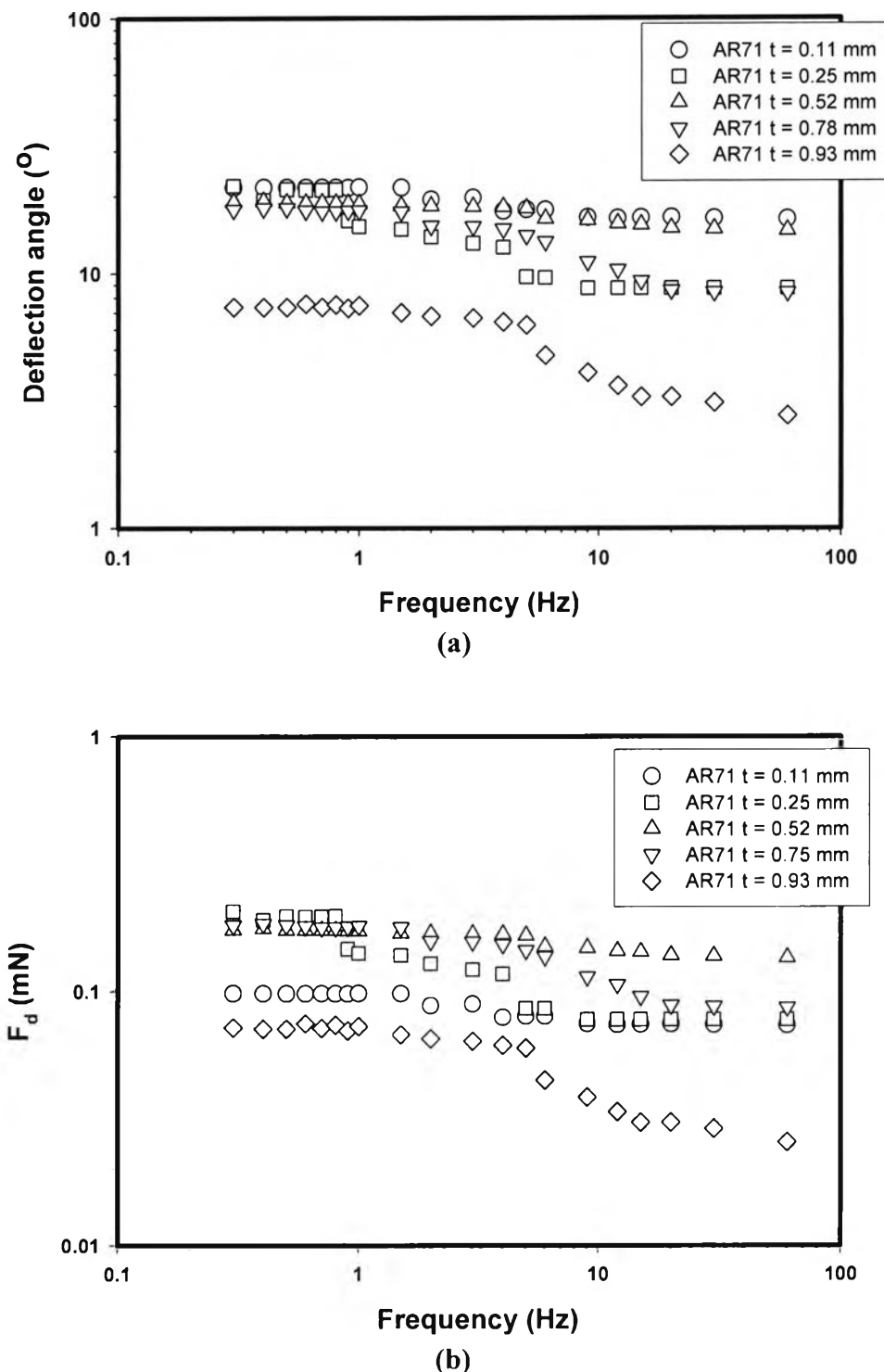


**Figure S3** Electromechanical responses of AR71 at various frequencies and thickness under AC field  $E = 800 \text{ V/mm}$  (a) deflection angles; (b) dielectrophoresis forces ( $F_d$ ).

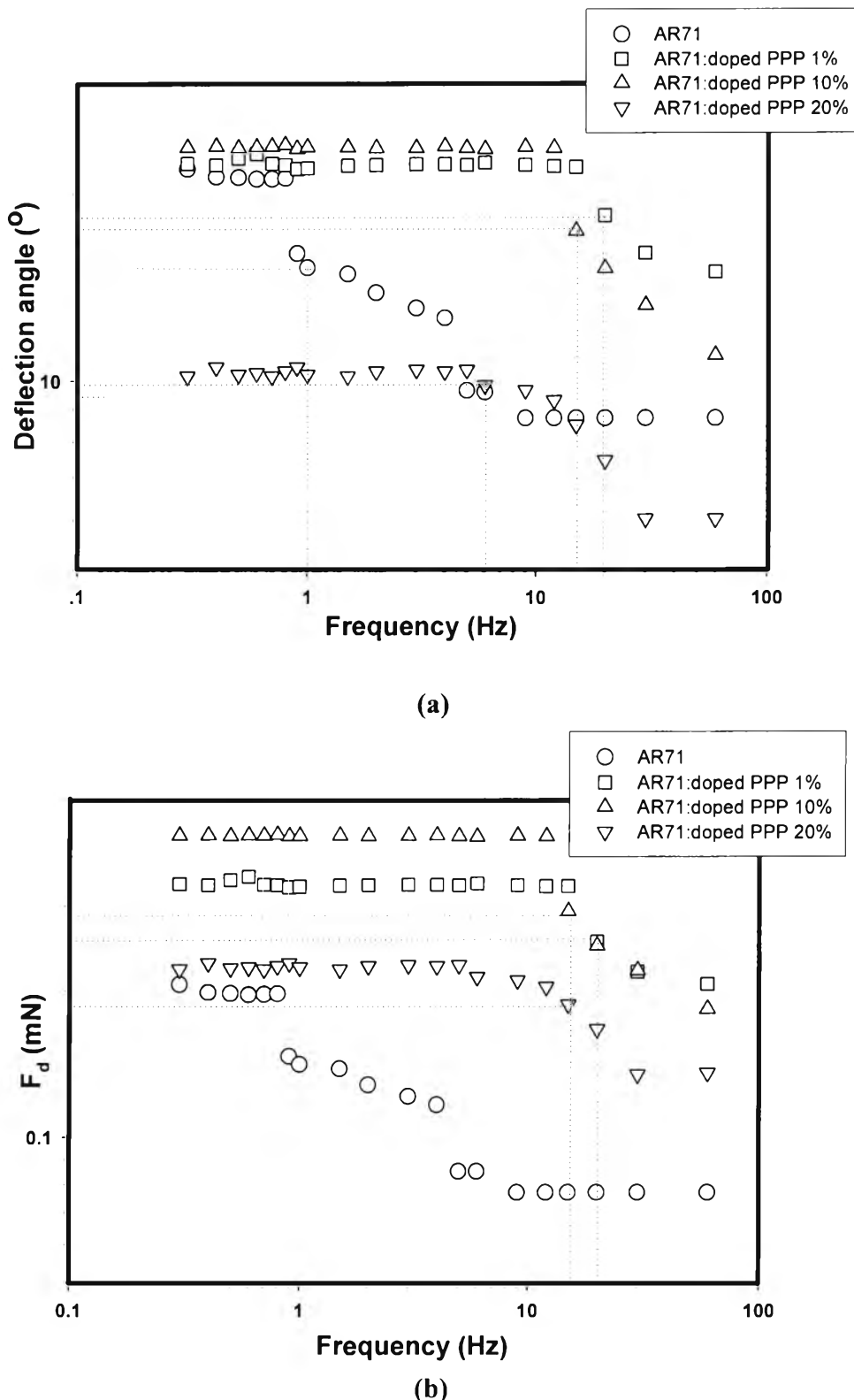


**Figure S4** Electromechanical responses of AR71:doped PPP (mol acid:mol PPP ratio = 100:1) at various poly(p-phenylene) concentrations under AC field  $E = 800$  V/mm, thickness  $\sim 0.20\text{--}0.30$  mm, (a) deflection angles; (b) dielectrophoresis forces ( $F_d$ ).

## CURRICULUM VITAE

**Name:** Mr. Ruksapong Kunanuruksapong

**Date of Birth:** May 3<sup>th</sup>, 1982

**Nationality:** Thai

**University Education:**

2000-2004 Bachelor Degree of Science in Polymeric Material, Faculty of Science, Chulalongkorn University.

**Work Experience:**

2007-2008 Position: Teaching Assistant in Polymer Physics Course  
Institute: The Petroleum and Petrochemical College,  
Chulalongkorn University, Bangkok, Thailand.

**Publications:**

1. Kunanuruksapong, R., Sirivat, A. (2007) Poly(p-phenylene) and acrylic elastomer blends for electroactive application, Materials Science and Engineering A, 454-455, 453-460.
2. Kunanuruksapong, R., Sirivat, A. (2008) Electrical Properties and Electromechanical Responses of Acrylic Elastomers and Styrene Copolymers: Effect of Temperature, Applied Physic A, 92, 313-320.
3. Kunanuruksapong, R., Sirivat, A. Effect of Dielectric Constant and Electric Field Strength on Dielectrophoresis Force of Acrylic Elastomers and Styrene Copolymers, submit to Current Applied Physics.
4. Puvanatvattana, T., Chotpattananont, D., Hiamtup, P., Niamlang, S., Kunanuruksapong, R., Sirivat, A., Jamieson, A.M. (2008) Electric field induced stress moduli of polythiophene/polyisoprene suspensions: Effects of particle conductivity and concentration, Materials Science and Engineering C, 28, 1, 119-128.
5. Thipdech, P., Kunanuruksapong, R., Sirivat, A., (2008) Electromechanical Responses of Poly(3-thiopheneacetic acid)/acrylonitrile-butadiene rubbers, eXPress Polymers Letters, 2, 12, 866-877.



6. Tangboriboon, N., Sirivat, A., Kunanuruksapong, R., Wongkasemjit, S., (2009) Electrorheological properties of novel piezoelectric lead zirconate titanate  $Pb(Zr_{0.5},Ti_{0.5})O_3$ -acrylic rubber composites, Materials Science and Engineering C, 29 (6), 1913-1918.
7. Thongsak, K., Kunanuruksapong, R., Sirivat, A., Lerdwijitjarud, W. Electroactive styrene-isoprene-styrene triblock copolymer: Effects of morphology and electric field, Materials Science and Engineering A, Article in Press
8. Thongchai, N., Kunanuruksapong, R., Niamlang, S., Wannatong, L., Sirivat A., and Wongkasemjit, S. (2009) Interactions between CO and Poly(p-phenylene vinylene) as Induced by Ion-Exchanged Zeolites, Materials, 2(4), 2259-2275.
9. Tangboriboon, N., Uttanawanit, N., Longtong, M., Wongpinthong, P., Sirivat, A., and Kunanuruksapong, R. (2010) Electrical and Electrorheological Properties of Alumina/Natural Rubber (STR XL) Composites, Materials, 3(1), 656-671, 2010.

### **Proceedings:**

1. Kunanuruksapong, R., Sirivat, A., (2007, August 2-5) The Effect of Temperature and Dielectricpermittivity on Electrorheological Properties of Elastomers, The 7<sup>th</sup> IEEE International Conference on Nanotechnology (IEEE-Nano 2007), Hong Kong.
2. Kunanuruksapong, R., Sirivat, A., (2006, December 6-8) Effect of Temperature on Electromechanical Properties of Elastomers, Asian Workshop on Polymer Processing (AWPP-2006), Rama Gardens Hotel, Bangkok, Thailand.
3. Kunanuruksapong, R., Sirivat, A., (2008, June 8-13) Dielectrophoresis force and the electromechanical responses of elastomers, 3rd International Conference Smart Materials Structures Systems. Acireale, Sicily, Italy.
4. Kunanuruksapong, R., Sirivat, A., (2009, March 9-12) A study of the dielectrophoresis force of elastomeric materials for artificial muscle applications, 16<sup>th</sup> Smart Structures and Materials & Nondestructive Evaluation and Health Monitoring, San Diego, California, USA.

**Presentations:**

1. Kunanuruksapong, R., Sirivat, A. (2006, 28 May – 1 June) Development of polymer blend of PPP and Acrylic elastomers for electroactive applications, MAM-06: Practical Nano-Chemistry and Novel Approaches, Tokyo, Japan.
2. Kunanuruksapong, R., Sirivat, A. (2006, December 6-8) Effect of temperature on electromechanical properties of elastomers, AWPP 2006, Bangkok, Thailand.
3. Kunanuruksapong, R., Sirivat, A. (2008, April 22-25) The effect of electric field strength on the dielectrophoretic force of elastomers, SmartMat 2008, Chiang Mai.
4. Kunanuruksapong, R., Sirivat, A. (2007, August 2-5) The Effect of Temperature and Dielectricpermittivity on Electrorheological Properties of Elastomers, The 7<sup>th</sup> IEEE International Conference on Nanotechnology (IEEE-Nano 2007), Hong Kong.
5. Kunanuruksapong, R., Sirivat, A. (2008, June 8-13) Dielectrophoresis force and the electromechanical responses of elastomers, 3rd International Conference Smart Materials Structures Systems. Acireale, Sicily, Italy.
6. Kunanuruksapong, R., Sirivat, A. (2008, August 19-20) The Effect of Elastomers Type on the Electromechanical Responses and Dielectrophoresis Force, Thai-Japan Joint Symposium on Advances in Materials Science and Enviromental Technology. Bangkok, Thailand.
7. Kunanuruksapong, R., Sirivat, A. (2008, April 3-5) Poly (p-phenylene) and Acrylic Elastomers Blend for Electroactive Applications, RGJ Ph.D. Congress IX, Pattaya, Thailand.
8. Kunanuruksapong, R., Sirivat, A. (2008, June 8-13) Dielectrophoresis force and the electromechanical responses of elastomers, 3rd International Conference Smart Materials Structures Systems. Acireale, Sicily, Italy.
9. Kunanuruksapong, R., Sirivat, A. (2009, June 7-9) Dielectrophoresis Force and Actuation Performance of Acrylic Elastomers and Styrene Copolymers for Artificial Muscle Applications, Frontiers in Polymers Science 2009. Mainz, Germany.

10. Kunanuruksapong, R., Sirivat, A. (2009, August 7) A Study of the Dielectrophoresis Force of Elastomeric Materials for Artificial Muscle Applications, RGJ Seminar Series LXII[Advanced Materials]. Bangkok, Thailand.